Re-Tightening the Large Anchor Bolts of Support Structures for Signs and Luminaries: Phase II

Brent M. Phares, Principal Investigator
Bridge Engineering Center
Iowa State University

OCTOBER 2021

Research Report
Final Report 2021-23

Technical Report Documentation Page

1. Report No. MN 2021-23	2.	3. Recipients Accession No.	
4. Title and Subtitle Re-Tightening the Large Anchor Bolts of Support Structures for Signs and Luminaires: Phase II		5. Report Date October 2021	
		6.	
7. Author(s) Zachary Dietrich, Brent M. Phares, and Zhengyu Liu		8. Performing Organization Report No.	
9. Performing Organization Name and Address Bridge Engineering Center Iowa State University 2711 S. Loop Drive, Suite 4700 Ames, IA 50010		10. Project/Task/Work Unit No.	
		11. Contract (C) or Grant (G) No. (c) 1033985	
12. Sponsoring Organization Name and Address Minnesota Department of Transportation Office of Research & Innovation 395 John Ireland Boulevard, MS 330 St. Paul, MN 55155-1899		13. Type of Report and Period Covered Final Report	
		14. Sponsoring Agency Code	
15. Supplementary Notes https://www.mndot.gov/research/reports/2021/202123.pdf			

16. Abstract (Limit: 250 words)

The Minnesota Department of Transportation (MnDOT) funded two projects in an effort to mitigate anchor bolt connection loosening and develop improved pre-tensioning steps for its sign, luminaire, and traffic signal (SLTS) structures. The Phase I study proposed new pre-tensioning procedures, completed laboratory testing, did an in-depth literature review, and set up instrumentation. The next part of the work started by implementing the proposed procedures in the field and suggesting revisions to be investigated further in Phase II. Through this work, the structural monitoring objective was to better understand field fatigue forces on the anchor rods and develop a testing procedure to replicate field stresses accurately in the laboratory.

In the Phase II project, lessons learned from both the field results and additional literature review were tested in the laboratory to balance the efficiency and efficacy of the revised pre-tensioning procedures. Feedback from stakeholders and experience from in-field inspections were considered for the revised procedures. Testing methods and conclusions were validated with finite element models and structural health monitoring.

This final report brings all aspects of the work together and recommends improved procedures and additional studies.

| 17. Document Analysis/Descriptors
Anchor bolts, Fatigue (Mechanics), Pretensioning, Laboratory tests, Structural supports | | 18. Availability Statement
No restrictions. Document available from:
National Technical Information Services,
Alexandria, Virginia 22312 | |
| 19. Security Class (this report)
Unclassified | 20. Security Class (this page)
Unclassified | 21. No. of Pages
107 | 22. Price |

Re-Tightening the Large Anchor Rods of Support Structures for Signs and Luminaires: Phase II

FINAL REPORT

Prepared by:

Zachary Dietrich
Brent M. Phares
Zhengyu Liu
Bridge Engineering Center
Iowa State University

October 2021

ACKNOWLEDGMENTS

TABLE OF CONTENTS

LIST OF FIGURES

LIST OF TABLES

EXECUTIVE SUMMARY

Throughout Minnesota and the United States, anchor rods for sign, luminaire, and traffic signal (SLTS) structures are coming loose at concerning rates. Anchor rods fasten SLTS structures to their foundations, so failure of these connections can result in collapse. The Minnesota Department of Transportation (MnDOT) has funded two projects in an effort to mitigate anchor rod connection loosening and develop improved pre-tensioning steps for its SLTS structures.

The Phase I study proposed new pre-tensioning procedures, completed laboratory testing, did an in-depth literature review, and set up instrumentation. The next part of the work started by implementing the proposed procedures in the field and suggesting revisions to be investigated further in Phase II. Through this work, the structural monitoring objective was to better understand field fatigue forces on the anchor rods and to develop a testing procedure to replicate field stresses accurately in the laboratory.

In the Phase II project, lessons learned from both the field results and additional literature review were tested in the laboratory to balance the efficiency and efficacy of the revised pre-tensioning procedures. Feedback from stakeholders and experience from in-field inspections were used to consider the revised procedures. Testing methods and conclusions were validated with finite element models and structural health monitoring.

This final report brings all aspects of the work together and recommends improved procedures and additional studies.

CHAPTER 1: **BACKGROUND**

1.1 INTRODUCTION

Over the past decade, loose anchor rod nuts have proven to be a drain on resources and present a potential danger to the public not only for Minnesota but also the nation. Connections tightened with the current pre-tensioning specifications were found to have loosened within a year after installation and some within months. Even posts retightened by MnDOT's maintenance department lost adequate pre-tension within two years. Therefore, the overall goal of this project was to develop effective and implementable anchor rod pretenstioning procedures for the installation and maintenance of MnDOT's structures for overhead signs, luminaries, and traffic signals (SLTS).

Two MnDOT funded projects proceeded this report, Phase I and the implementation phase for the overall *Re-Tightening the Large Anchor Rods of Support Structures for Signs and Luminaires* project. In Phase I, new procedures were developed through a thorough literature review, site visits, and laboratory testing. Procedures developed in Phase I were then iteratively tested in the field during the implementation stage of testing to check for constructability.

In the Phase II project, lessons learned in the implementation phase from both the field experience and additional literature review were tested in the laboratory to balance the efficiency and efficacy of the revised pre-tensioning procedures. Feedback from stakeholders and experience from in-field inspections were used in consideration of the revised procedures. Testing methods and conclusions were validated with finite element models and structural health monitoring.

1.2 REPORT ORGANIZATION

This report consists of multiple chapters, each focusing on a different aspect of the overall project. The basic content of each chapter is as follows:

- Chapter 1 presents background information regarding connection geometry and the procedures proposed in the Phase I project.
- Chapter 2 includes Interviews with stakeholders and site inspections of structures installed with the procedures from Phase I in the previous year.
- Chapter 3 contains the laboratory testing results for different tested tightening aspects deemed important during the implementation phase.
- Chapter 4 investigates anchor rod behavior further with finite element models for both individual anchor rods and the laboratory post structure as a whole.
- Chapter 5 summarizes the results of monitoring data from a cantilevered sign structure in Minneapolis, Minnesota, and validates variables used during testing.
- Chapter 6 brings all aspects of the project together, recommending improved procedures.

1.3 BACKGROUND OF MNDOT TYPICAL ANCHOR ROD CONNECTIONS

To transfer forces on its SLTS structures to foundation bases, MnDOT employs double nut connections on anchor rods cast into a concrete foundation (Figure 1.1).
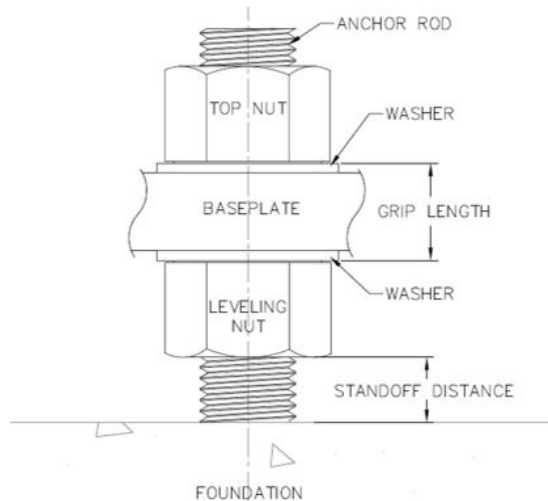
Figure 1.1. Typical double nut anchor rod connection

The connection is comprised of an anchor rod that clamps the baseplate of a structure with two nuts—commonly referred to as top and leveling. The leveling nut (on the bottom) is for leveling the structure before installation, and the top nuts are generally for tightening. Clamping force generated by tightening the top nut secures the baseplate of the structure in place. The thickness of the baseplate plus both top and bottom washers is referred to as the grip length, which is the length that the anchor bolt carries tension resulting from tightening to resist external loads (dead load, wind load, etc.) during service.

1.3.1 Geometry

Typical anchor rod dimensions and materials are covered before going over procedures proposed from Phase I. In the United States, the typical anchor rods used for SLTS structures adhere to the ASTM F1554-20 specification (ASTM 2020). Note that this specification differs from ASTM 325 and 490 for structural steel bolts. Anchor rods can be specified in three different yield grades: 36, 55, and 105 ksi. Of these, grades 55 and 105 are most frequently used by MnDOT. Threads are cut or rolled according to ANSI/ASME B 1.1 Class 2A, as outlined in Figure 1. 2.

Root to clear 0.125P width, may be flat or rounded

Will not assemble with UNJ external thread

0.625H

P (pitch)

0.125P

0.25P

0.125P

0.25P

0.125P

0.125P

0.125P

0.25P

0.75H

rad. = 0.10826P

H (fundamental triangle)

rad. = 0.14434P

0.75H

Nominal minor diam.

Will assemble with UN or UNJ internal

Nominal minor diam.

Will assemble with UN or UNJ internal

UN External Thread   **UNR External Thread**
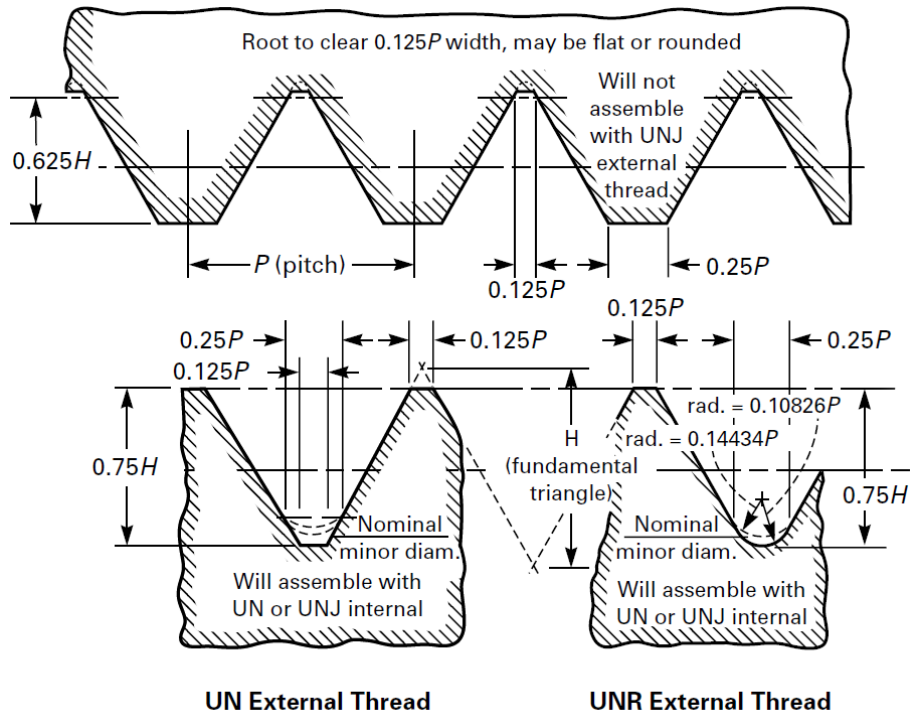
ASME 2005

Figure 1.2. Typical anchor rod dimensions, UN threads

In addition, grade identification is required on the ends of the anchor rods that project from the concrete to help facilitate easy identification in the field. As shown in Figure 1.3, marking can be completed with color coding or the ASTM F1554 supplementary requirement S3 for permanent marking. MnDOT requires both color coding and permanent marking.

AB36 PB — Grade 36   AB55 PB — Grade 55   AB105 PB — Grade 105
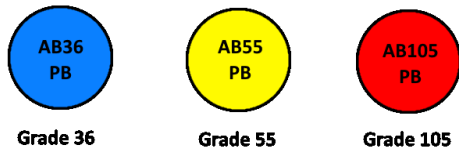
Figure 1.3. Typical anchor rod top coloring or stamped markings

As of 2018 construction specifications, MnDOT requires permanent markings (MnDOT 2018). Typical nuts are ASTM A563 grade DH or A194 grade 2H heavy hex, which follows the dimensions of ANSI B1.1 Class 2B, as shown in Figure 1.4.

3
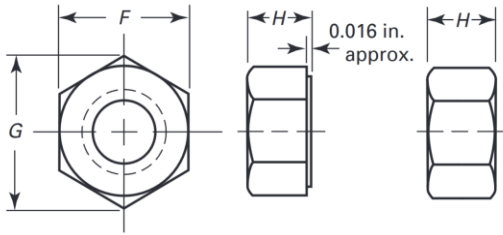
ASME 2010

Figure 1.4. Typical heavy hex nut dimension variables

Nuts have a proof load stress of 150 ksi (ASTM 2015 and 2017, ASME 2010). Finally, washers are specified to ASTM F436-19 (ASTM 2019).

1.4 SPECIFICATIONS FROM PREVIOUS RESEARCH PROJECT

Procedures tested in this project are based on those developed in a previous study titled *Re-Tightening the Large Anchor Bolts of Support Structures for Signs and Luminaires* (Chen et al. 2018). The previous project tested anchor rod tightening properties in the laboratory, instrumented an overhead sign for field monitoring, developed finite element models (FEMs) for numerical analysis, and developed new tightening specifications based on the American Association of State Highway and Transportation Officials (AASHTO) Load and Resistance Factor Design (LRFD) Specifications for Structural Supports for Highway Signs, Luminaires, and Traffic Signals (LRFD–SLTS) 5.17.5.2 (AASHTO 2015).

The new specifications developed through the previous project were primarily based on AASHTO LRFD–SLTS 5.17.5.2, but with primary changes to torque, in addition to turn-of-nut verification, defining snug tight, and taking into account grip length. All three changes were a direct result of laboratory testing and literature review. By adding these three items, the new specifications aimed to reduce inconsistency and better verify correct installation. The new specifications included an eight-step verification sheet, a table with the corresponding installation information (Table 1.1) and a table with wrench lengths for bringing nuts to snug tight.

Table 1.1. Example of torque turn specification sheet with OH sign anchor bolts and grip lengths

Pole Type	Anchor Bolt Ø	Bolt Type (Galvanized to Spec. 3392)	Baseplate Thickness	Snug Torque (ft-lbs)	Rotation Beyond Snug	Verification Torque, T_v (ft-lbs)	Re-Tightening Torque, T_r 48 Hours After Tightening
Type 5-7 Sign Truss	2-1/2 in.	Type B Grade 55 Spec. 3385.2B	2 in.	550	1/12	3,300	3,630

The eight steps are as follows:

1. Verify F1554 anchor bolt grade as specified for the project. Verify nuts are ASTM A563 heavy hex and washers are F436.
2. Verify anchor bolts are clean and not damaged and plumb, not more than 1:40 slope or 1/4 in. in 10 in. (If bolts are out of plumb or damaged, contact project engineer.)

4

3. Lubricate anchor bolts with MnDOT-specified bridge grease (within 24 hours of tensioning) and turn nut down to foundation. Lubricate bearing surfaces of leveling nut and top nut prior to tightening.
4. Level leveling nuts: make sure nuts are less than one anchor bolt diameter from the foundation but not less than 1-1/4 in. for overhead (OH) signs.
5. Install structure with an F436 washer below and above baseplate and snug top nuts. When snugging, use snugging torque or maximum open-end wrench length on both the top nut and the leveling nut following the star pattern. Two cycles of snugging shall be performed prior to Step 6.
6. Perform turn-of-nut tightening. Mark the nuts and adjacent baseplate and turn the minimum required turn per appendix, but do not exceed the verification torque.
7. Confirm verification torque was achieved or continue to turn nut until verification torque is achieved.
8. 48 hours after initial tightening, apply re-tightening torque. The re-tightening torque is 110% of the verification torque ($1.1 \times T_v$).

Table 1.1 is a shortened example of the new table provided for MnDOT specifications from the previous project. In the full table, there are 17 different types of structures and 22 different overall installation types. The full Table 1.1 that was provided to MnDOT is intended for contractors as a reference to find the correct values for a particular installation and to work through the eight steps defined above.

The previous project also completed a thorough literature review of current tightening practices along with a survey of various states' tightening procedures (Chen et al. 2018). Based on the prior study, 88% of states with tightening specifications used some form of turn of nut, with eight states lacking any specifications for tightening. Many states used multi-step specifications such as AASHTO LRFD–SLTS 5.17.5.2, going through lubrication, snug tight, and specified turns.

While states may not have common tightening procedures, one thing they did have in common was loose anchor rod nuts. Of 29 states, 80% reported having loose nuts on 1% to 90% of their structures, with many states reporting that the deficiencies were due to contractor error and inconsistent practices. For the four states in the survey that reported no loose nuts on their structures, their procedures were different; however, two of them had fairly rigorous contractor verification and inspection to ensure proper . Other states that reported loose nuts and subsequently implemented more rigid specifications experienced a decrease in loosening of the anchor rod connections but noted that the specifications were costly and time intensive to implement.

CHAPTER 2: **INTERVIEWS AND SITE INSPECTIONS**

2.1 OVERVIEW

Before testing occurred in the current phase, stakeholders were interviewed to guide research activities toward the most critical concerns. At this point in the study, it was also possible to investigate structures installed with the procedures proposed in Phase I to check the effectiveness of the previously proposed procedures.

2.2 INTERVIEWS

2.2.1 MnDOT Structure Maintenance Workers (Overhead Signs)

To investigate maintenance on overhead sign structures, workers from the MnDOT structure maintenance section were interviewed about their experiences retightening anchor bolts on both cantilever and bridge truss structures. Pat O'Brien and his crew gave feedback on the maintenance procedure experienced the previous summer, stating that it was fairly straight forward and not too burdensome, even though the nuts had to be removed and replaced from the structure.

Before the new procedures, the crew generally didn't use any methodology and went around tightening loose nuts with a TorcUp hydraulic wrench. When asked about difficulties implementing new procedures, the primary issue was the applicability to all structures. By O'Brien's estimation, the maintenance procedure could not be completed on about a third to half of the existing structures in the MnDOT metro district due to the condition of the rods. In their experience, the bridge maintenance crew stated that they had broken off a couple of studs due to the nut being rusted in place.

To address this issue, they requested that a max loosening torque for structures be calculated and recorded, to avoid breaking off studs during maintenance. Finally, the crew commented that checking and servicing the leveling nuts on many structures is not possible due to debris, clearance, and wire mesh rodent guards.

2.2.2 MnDOT Metro District Traffic Office Lighting Operations – Lighting Construction Inspectors

Metro District Lighting Operations lighting construction inspectors were interviewed for high mast light towers (HMLTs), light poles, and traffic signals. Given the installation procedures were still being developed during the interviews, no specific feedback was provided on the specified steps. Although the specifications were still being developed, the lighting construction inspectors still had feedback on the current procedures.

The inspectors asserted that using the turn-of-nut method inside the pole bases is impractical because it is very difficult to fully access the top nuts with the full sized manual type wrenches necessary to make the required turns and to see the required turns. This difficulty is especially true once the pole wiring is in place.

Much like the overhead signs, leveling nuts are also difficult to access on lighting poles. Figure 2.1 shows a sample stainless steel light pole base brought in to demonstrate the clearance issues.

Figure 2.1. Exterior of light pole base (left) and Interior of base (right)

Figure 2.1 makes it clear that the exterior overhang makes the observation of leveling washers under the structure difficult. Figure 2.1 also shows the 12 in. long offset flat specialty wrench made by the pole manufacturer that is used to snug tighten the leveling nuts of stainless steel light poles because of the baseplate overhang that covers the leveling nuts.

The specialty wrench is a stamped wrench, cold-punched from sheet metal. Because the wrenches are not forged or heat treated, the open ends will spread easily under forces greater than the snug-tight condition. The hydraulic wrench is shown for reference in Figure 2.1 (left). In the inspectors' experience, the specialty wrench tends to bend under repeated uses when used in conjunction with a pipe extension and is not designed to use for the final turn of nut. The pole manufacturer's instructions state to use the specialty wrench for snug-tight condition only. The consensus among the Metro District construction lighting inspectors was that the base design, in Figure 2.1, for standard stainless steel light poles is less than ideal for anchor rod tightening.

For inspections, it was brought up that having the contractor fill out a form for every light pole and HMLT installed is not feasible with the personnel available. Building on this fact, in the inspectors' experience, they are not always informed when pole installations are taking place on the project. To

alleviate the workload, lighting construction inspectors requested that a method for inspecting structures after installation be developed and a consolidated form created.

Finally, it was pointed out that the anchor rod tightening specification based on the AASHTO LRFD specifications needs to be simplified since contractors tend to get discouraged and ignore it if parts of the specification are difficult or not possible to complete. However, with the new anchor rod tightening specifications, this should no longer be an issue.

2.2.3 MnDOT Bridge Asset Management (Overhead Signs)

Bridge asset management performs the majority of inspections and cataloging of overhead signs in the MnDOT metro district. For this interview, Michael Cremin was available, and Douglas Maki submitted a filled out questionnaire. Cremin stated that MnDOT inspects and catalogs about 500 structures annually, with about 2,500 total structures in the Metro District. With the age range of structures, Cremin noted that inspectors have difficulty identifying the grade of anchor rods, since many are rusted, were installed with old specifications, and are often not marked on the top.

When asked about previous practices, it was indicated that contractors would often "put a little extra" torque than what was specified, thinking that it would help the connection. This indicates that it needs to be made clear to the contractor that exceeding the specification is just as damaging, if not more damaging, than under tightening.

Oftentimes during inspections, Cremin experienced anchor rods with more than 1/8 in. gap between some leveling washers and the baseplate. In his notes, Maki indicated that the old maintenance operations were "not a permanent fix" and that the old specification was written assuming all of the nuts were grade 36. No turn-of-nut procedure was used and the AASHTO procedures were not followed before the new procedures.

Much like comments from the Electrical Services Section (ESS) workers, both Cremin and Maki indicated that the inspection resources for structures maintenance are "spread thin" and that the field installation sheet is too cumbersome. During installation of a new sign truss structure on I-94, it was observed that the procedures were pretty quick to follow with the hydraulic wrench, and the contractor was able to reopen the road in a timely manner. However, it was also observed that, with the sign trusses, one side often has to be adjusted to affix the sign truss to the pole/s, possibly bringing the final installation out of plumb. Finally, Maki said that it would be nice to have some alternatives to the approved lubricant, since contractors often do not carry it with them.

2.2.4 Hydraulic Wrench Manufacturer

Along with MnDOT personnel, Glenn Lickness, a representative for a manufacturer of hydraulic wrenches, also participated in the interviews and offered feedback on the specifications. One of the important aspects that Lickness touched on was the obscurity of the term snug tight. He asserted that, in manufacturing, snug tight is generally connoted as hand tight. The Metro District lighting construction inspectors and structure maintenance inspectors agreed that this terminology was confusing to

contractors, and, even among themselves. they had different definitions. Lickness recommended that the snug-tight value be referred to as a "proof" or "initial" torque to avoid confusion.

Lickness also recommended that the specification table be ordered in the sequence of steps, since there was some confusion on when to perform the steps by the contractors that he observed.

Along with feedback on the specifications, Lickness provided information on the capabilities of the HyTorc hydraulic wrench system. He covered the fact that the pump is sensitive to the cold, and it's important to have the correct type of oil in it for the season. Lickness also brought up that the HyTorc washer could help with the fatigue loosening and would be safer than normal wrench operation, since a reaction bar is not used. The HyTorc washer helping with fatigue would match up with the literature and other proprietary non-slip washers, since the angle of the interaction of the HyTorc washer is greater than the thread pitch angle, helping to avoid rotation and loss of pre-tension in the bolt.

2.2.5 Interview Results Summary and Possible Solutions: Inspection Times and Verification

One of the common themes from all of the interviewed parties was to make the installation form more streamlined for both verification and the reference chart. In the reference chart, it would likely be beneficial to order it to follow the operation sequence. The turns or torques could also be included for each step, instead of having the contractor go back and forth in it, trying to find half turns or half torques.

Along with the changes to the chart, many of the MnDOT inspectors desired a more broad verification form that could be utilized for many structures. A range of structure options could be added on the form, and only the MnDOT inspector be needed to sign off on it when completed to help with efficiency.

The checklist for plumb installation and lubrication could be converted to smaller checkboxes to tick off in the form. Depending on the amount of detail desired, separate verification forms could also be created for traffic signal and lighting construction inspectors, and for structures.

In addition to streamlining the verification form, inspectors from both structures and lighting construction indicated that the inspection process for each individual structure is fairly burdensome and likely not possible for every structure installed each year with the personnel available. To this point, the inspectors wondered if there was a suitable method for inspection after installation, so one could sign off on the installation record without being tied to a contractor's schedule.

The two likely ways a post installation verification could take place is with a direct tensile indicator (DTI)/squirter washer specification or with an inspection torque. The downside to any post installation inspection is that the full process, and the star pattern and tightening steps in particular, may not be observed, and any mistakes may lead to a need for washers to be reinstalled.

A DTI/squirter washer specification would likely be the most efficient and accurate way to inspect installations for bolt pre-tension accuracy post construction. DTIs indicate the tension in a bolt using basic material properties; as more force clamps the washer, the dimples on the washer plastically

deform. As deformation occurs, greater area on the dimples needs to be crushed, requiring more force. With a normal DTI washer, the inspector could slide a feeler gauge between the base plate and the top washer to ensure correct pre-tension was reached. However, the designs of the bases that house the top nuts limit access, making this practice difficult if not impossible. Furthermore, like the inspection forms, having to use a feeler gauge on each anchor rod will be a burdensome task.

Some lighting projects have more than 50 light poles. Taking the DTI concept a step further, if a squirter type DTI washer is used, the inspector can look into the base to check if the squirter DTI had been activated by visually seeing the grease or other material from the dimples around it. A DTI specification may need to be fatigue tested before recommendation though. The lowered surface area between the dimples and the baseplate may result in less friction holding the nut from turning off.

If a DTI specification is not desirable, an inspection torque could present another option for post construction inspection. Inspectors could apply a determined torque amount with either a hydraulic or calibrated wrench in the counter-clockwise direction in an attempt to loosen the nut. The major benefit to a reverse torque based inspection is that it would not require training on DTI washers or changing the specification for DTI washers. However, a torque based post installation inspection procedure may not directly indicate the tension in the final installation due to lubrication conditions or steps taken.

2.2.6 Metro Lighting Operations: Lighting Construction Inspections

The procedures for installation on lighting structures, as of late October 2019, were still in development, so feedback from lighting construction inspectors was important to help develop a useful and accurate specification. There were many concerns with using turn of nut, especially in poles that have high or transformer bases. For poles with high or transformer bases, the turn-of-nut method would likely not be possible on the top nuts, since the bases do not allow enough space for full sized manual type wrenches. Furthermore, turning the leveling nuts on these same bases is not always practical either, especially with the stainless steel light pole bases and overhangs. The wrench could be used as a turn reference, but wrenches will often slip slightly and may not provide an accurate turn indication.

For light poles, the best maintenance operation may be to take off the top nuts with a manual wrench, one at a time, and re-lubricate, like the in the overhead sign procedure. If a usable socket is found for the hydraulic wrench, this maintenance operation may be completed with the hydraulic wrench; however, the relatively low torques required for light poles may lead to inaccurate final pre-tensions.

Many of the inspectors felt that it may be beneficial to improve the lighting base design, such as making the taper start later, allowing for more space inside the base, and/or moving the bolts to the outside of the base. However, these options had been looked at and suggested to the pole manufacturer in 2015 by the MnDOT Office of Traffic Engineering (OTE). It was also pointed out during the meeting and should be mentioned that any changes made to the design of the base would require the manufacturer to resubmit their product for crash worthiness of breakaway under the new Manual for Assessing Safety Hardware (MASH) criteria. Both would be a significant investment for the manufacturer.

2.2.7 Field Determination of Anchor Rod Grade

Determining steel grade in the field is an issue according to both construction lighting inspectors and structure maintenance workers. In the field, there are two primary ways that the grade of an anchor rod can be determined. For both of the field methods, the surface of the anchor rod would first need to be cleaned with a grinding wheel to get down to bare metal and to avoid testing any corrosion or rust on the surface of the anchor rod. On any galvanized structures, grinding the top of the anchor rod may not be safe due to the coating.

The first field identification option could be achieved with a handheld x-ray florescent (XRF) spectrometer. An XRF spectrometer could directly determine the amount of each element in the anchor rod, which would directly indicate the grade of the rod by the elements it is comprised of. However, an XRF spectrometer starts at approximately $5,000 for a used device, and workers would need to be trained on what element peaks to look for when using it.

For a less expensive and also less accurate field measurement of anchor bolt grades, a set of hardness files could be used. These files come in varying degrees of hardness and are used to scratch the metal to test for hardness. Depending on which files scratch the metal, the approximate hardness of the metal can be determined, after which the hardness can be correlated with a metal grade.

Finally, for a desk option, a historical specification and plan review could be completed to approximate which anchor rods are generally installed with which base plate designs. These could then put into a reference table for maintenance personnel in the field.

2.2.8 Specification Clarity and Simplicity

Regarding the specification itself, there were a couple areas for improvement from the interviews. Generally, all the feedback was to increase the clarity of the specification and to simplify it for installation.

The format and order of the reference table/chart was one issue brought up by a few different interviewees. It was determined that each step would be included in the installation reference chart, in the order that they should be performed. Ordering the chart with all the steps will likely make construction easier, since it eliminates the need to be flipping between the checklist sheet and the reference chart during installation.

Lubrication was another aspect of the current specification that could be improved. Currently, only MnDOT bridge grease is the approved lubricant for tightening, which has proved to be slightly restrictive for contractors. In the inspectors' experiences, contractors generally do not use the specified lubricant. Generally, contractors use a copper based lubricant sometimes in a spray form. While copper lubricants have a nut factor close to the specified grease, they are not quite the same, so pre-tension accuracy is likely impacted by deviation from the specification.

In future research phases, this issue can be approached in two ways: either research the error from using different lubricants and determine a range of lubricants that contractors can use, or enforce the

lubrication specification. Determining a range of lubricants may make it easier for contractors during installation, since there would be one less step in the specification.

However, it may be difficult for inspectors to verify that the type of lubricant used falls under the approved types, especially if the inspection takes place post installation. Additionally, there will be more error in final preload values with a broad specification for lubricant, since each lubricant will have a slightly different nut factor. The error caused by different lubricants could be alleviated with a DTI specification, as the pre-tension would be directly indicated by the washer. Stricter enforcement of the lubrication specification would require more initial work by MnDOT inspectors, but, after contractors have purchased the lubricant and use it, enforcement of the specification will likely be easier. By using the same standard lubricant, a DTI specification may not need to be implemented if fairly accurate pre-tensions can be achieved using the standard lubricant.

During the interviews, MnDOT personnel and the hydraulic wrench representative agreed that the term snug tight is misleading. While in academic studies, snug tight is generally defined where the torque-tension relationship starts to behave linearly, in the field, this terminology has different and varying connotations that may lead to confusion during installation. To increase the clarity of the specification, it was recommended that a term like "proof" or "initial" torque be used. This terminology would make it clear to contractors that the first step is not hand tight, and there is a particular and specific torque value that needs to be met. Another benefit of using an "initial" torque instead of the traditional snug-tight terminology is that the initial torque could be set at 20% yield, instead of the lower snug-tight values, often at 10% yield. This serves the dual purpose of ensuring that the high capacity hydraulic wrenches can accurately reach the lower torque values. With a higher "initial torque," the anchor rod will be more likely to start in the linear portion of tightening, resulting in more accurate turn-of-nut pre-tensions, if used.

2.3 SITE VISITS

2.3.1 New Procedures

Along with structures tightened with the old procedures, newly installed structures, tightened with the new procedures, were also inspected. Table 2.1 outlines the structures inspected, the year installed, and any notes on the inspection.

Table 2.1. New procedure installation inspection summary

Structure	Structure Type	Month/Year Installed	Inspection Date	Inspection Notes
OH MN36-090	OH Cantilever	X/2019	10/2019	No Loose Nuts
OH I94-688	OH Cantilever	10/2018	10/2019	No Loose Nuts
OH I94-689	OH Sign Truss	10/2018	7/2019	No Loose Nuts
OH I35-318	OH Sign Truss	X/2019	10/2019	No Loose Nuts, #5 not plumb
OH280-023	OH Cantilever	10/2018	7/2019	No Loose Nuts, #8 not plumb
OH MN51-013	OH Cantilever	8/2017	7/2019	No Loose Nuts

Of the six structures investigated in Table 2.1, none had loose top nuts, and the only defects were out of plumb anchor rods on two of the structures. The time between installation and inspection ranged from two years to around 4 months. The monitoring structure, OH MN51-013, was the oldest installed with the new procedures, and it is still performing well and without any loose nuts. OH I35-318 and OH MN36-090 were installed in early 2019, according to MnDOT, and show that the contractors are learning and implementing the new procedures well.

Nine months after installation, during July 2019, both of the overhead sign structures in the installation videos were checked to ensure that no nuts had come loose with the new procedures. The full-span truss sign OH I94-689 (Figure 2.2) was found to have no loose nuts after checking both the top and leveling nuts. It was, however, missing the MnDOT-specified rodent guard along the base.

Figure 2.2. Inspection of full truss OH I94-689 sign

On the cantilever sign, OH 280-023, all of the top nuts were tight, but, when the leveling nuts were inspected, it was found that nut 8 was slightly angled, with the rod itself out of plumb (Figure 2.3), likely causing the issue.

Figure 2.3. Rod 8 out of plumb

When further investigated, it was discovered that the leveling of this particular installation took about 30 minutes, and the final installation was slightly out of level (Figure 2.4).

Figure 2.4. Final installation of OH 280-023 out of level

The decreased clamping force in connection of rod 8 of this structure may cause additional stresses in the surrounding anchor rods and could be inspected on an increased schedule as a case study.

The monitoring structure, OH MN51-013, was also checked in July 2019 for nut looseness. This was completed to observe the performance of the specification along with ensuring that the strain measurements in the bolts were correctly reading. All of the nuts were found to be tight and all anchor rods were plumb.

In October 2018, three more overhead signs installed with the new procedures were inspected. While more signs were installed than inspected, these three were visited based on accessibility. All three of the signs had no loose nuts, but rod 5 on OH I35-318 was slightly out of plumb. In Figure 2.5 left, the leveling

washer of rod 5 has a space between it and the baseplate when compared to Figure 2.5 right, which is rod 8 on the same structure.

Figure 2.5. Rod 5 (left) and Rod 8 (right) on OH I35-31

Although one anchor rod was tilted, the remainder of the installations were in good condition. As an example of an ideal structure, OH I94-688 was installed exactly to specification, even with the turn-of-nut marks still visible on the nuts (Figures 2.6 left and right).

Figure 2.6. Turn-of-nut marks on nut (left) and baseplate of OH I94-688 (right)

2.4 CONCLUDING REMARKS

To reduce inspection time and resources, a DTI specification may be beneficial, and the verification form could be modified for post installation inspection. Since concerns were raised for inspector availability and coordination with contractors, an effective method for post inspection installation may be DTI washers, given they directly indicate the tension developed in the anchor rod; the inspector could then check the installation on their own schedule for better resource management.

The ESS slug wrench could be a solution to the maintenance on existing HMLT anchor rods. If the stack socket for the hydraulic wrench does not work on some existing HMLT structures, the slug wrench may be a good backup option for maintenance. If slug wrench maintenance is pursued though, more research into the maximum energy it can transfer to bolted connections needs to be completed and possibly a better designed wrench found, since the current wrench is unwieldy.

The lubrication specification can either be broadened or more strictly enforced. The current lubrication specification is generally not followed well, which could result in increased pre-tension scatter. If the specification is broadened, it may be beneficial to use DTIs to ensure correct pre-tension is reached. If the current lubrication specification is enforced, providing contractors with the lubricant could possibly help ensure the installations are lubricated correctly.

Because the term snug tight has different connotations, it may be beneficial to use an "initial torque" terminology instead. The "initial" torque could either be set at 10% or 20% yield depending on results from Phase II research on the snug-tight conditions. If the initial torque started a little higher, it would also make any turn-of-nut procedure more accurate, since the connection would be more likely to start in the linear range.

Sign posts installed with the new specification are still tight after up to 2 years. Comparing to the field monitoring data and the old procedure inspections, sign posts tightened with the new procedures are performing well and have not showed any signs of loosening since installation.

CHAPTER 3: **LABORATORY TESTING**

3.1 OVERVIEW

From the implementation study and stakeholder feedback, several improvements to the proposed procedures were determined for greater installation efficiency. However, increased efficiency could lead to decreased compliance with adequate pre-tension force. For this reason, the proposed improvements for increased lubrication flexibility, removal of the 48-hour retightening torque, and a turn-of-nut investigation were pursued in the laboratory testing. Connections were also fatigue tested on a full scale overhead sign base to investigate loosening over the lifespan of a structure and compare the results to field monitoring results.

3.2 LABORATORY FULL-SCALE SIGN POST TESTING

3.2.1 Methodology

3.2.1.1 Procedures

For the fatigue testing conducted as part of this project, the primary goal was to investigate the impact that fatigue loading has on the anchor rod connections using field monitoring data to provide the loading inputs. Two fatigue tests were completed with one replicating two years of in-field loads and another to relate known AASHTO constant amplitude fatigue life (CAFL) curves to pre-tension loss of anchor rods. Derivations of both procedures are presented after the static testing results in this chapter.

For both fatigue tests, the anchor rods were ed using an approach similar to that observed from field observations. First, the pole was checked for level, and the top nuts were brought to hand-tight. Leveling nuts were then tightened with a strap wrench to approximately 50 ft-lbs given a large enough open-ended wrench was not available. Using a TorcUp hydraulic wrench, the top nuts were tightened to 20%, 60%, and 100% increments of the verification torque, which is 3,300 ft-lbs. A 48-hour retightening torque was not applied to investigate the impact of relaxation on the rods without retightening.

3.2.1.2 Fatigue Test Setup

Figure 3.1 outlines the base and anchor rod instrumentation.
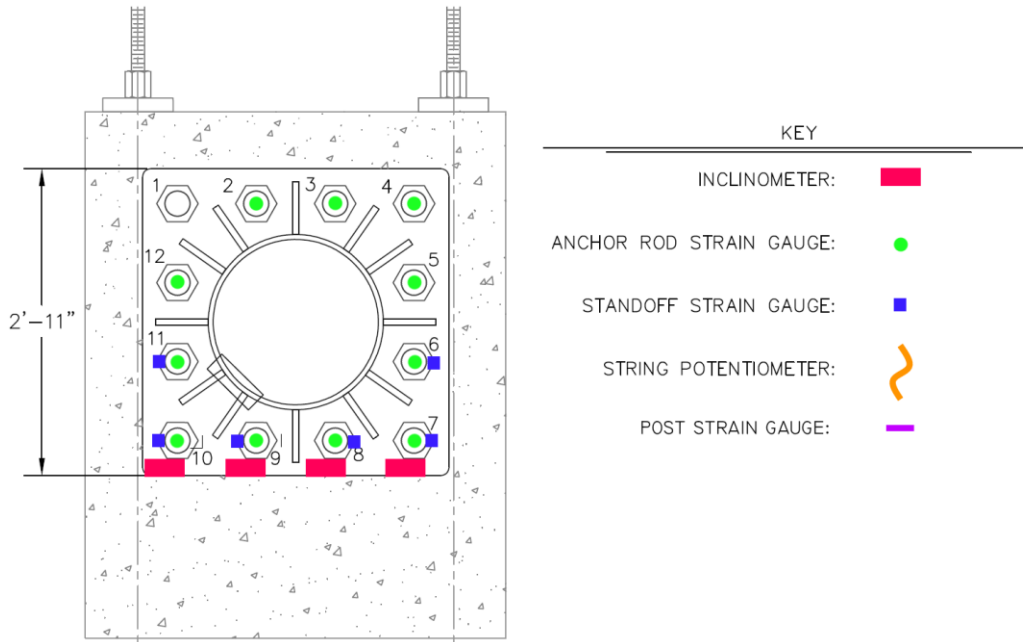
Figure 3.1. Base instrumentation

Figure 3.2 illustrates the sign-post instrumentation and overall test setup.
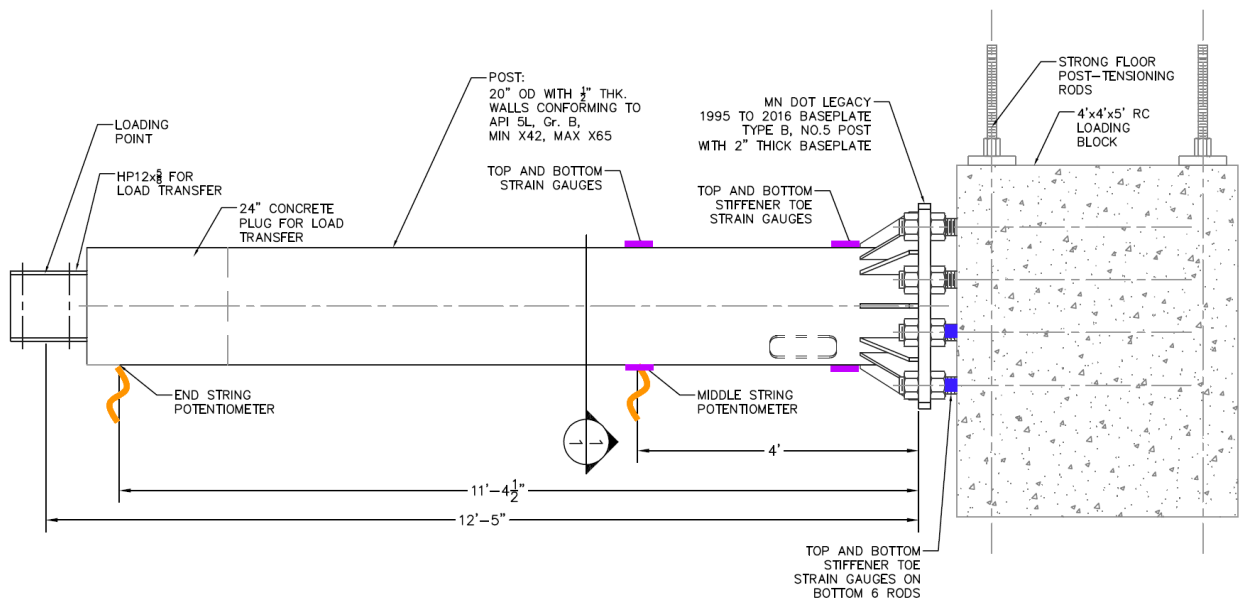
Figure 3.2. Sign-post instrumentation and test setup

For further details on the loading block and sign post, see Schaeffer 2018. Numbering for the anchor rods starts in the upper left corner and moves clockwise around the post following conventional identification procedures. Strain measurements were acquired from three-wire, quarter-bridge resistance strain gauges from Tokyo Measuring Instruments Laboratory Co, Ltd., and 6 mm gauges were used on the post and standoff. Strain gauges on the standoff and stiffener toe were applied after the first, field-replicated fatigue test. The anchor rod strain gauges were BTM series gauges from the same

manufacturer. They were epoxied into the anchor rods in the grip length. Middle strain gauges on the posts were affixed at the same distance from the base as those on the field monitoring structure. Figure 3.3 shows the standoff strain gauges and the top of the anchor rod strain gauges.

Figure 3.3. Lower sign-post instrumentation

The standoff gauges were located on the sides of the anchor rods to minimize strain readings from moment forces and measure axial forces. Schaevitz AccuStar inclinometers were used to monitor any nut turns on the lower four nuts. The inclinometers were mounted on timber boards, as shown in Figure 3.3, to avoid damaging the instruments during attachment to the nuts. The inclinometers measure around the center of the instrument, which, from geometry, would be equivalent to any nut turns observed. For turn verification, all nuts were also marked with turn lines after ing on the top nut (Figure 3.4 left) and the leveling nut (Figure 3.4 right).

Figure 3.4. Turn marks after tightening on top (left) and on leveling nuts (right)

The sign post was tested with a MnDOT legacy Interim Design B used from 1995 through 2019. The post was a Type 5 design on a Type B baseplate (MnDOT 2015). An exact steel strength was not specified, but it can range from 42 ksi to 65 ksi per MnDOT specifications. Anchor rods were F1554 2½ in. diameter, grade 55, which presented a limiting case given less available force to be developed than with grade 105 rods.

The anchor rods were cast into a reinforced concrete loading block during previous research activities. The loading block was post tensioned to the strong laboratory floor with 100 kips on each post-tensioning rod to provide an approximate fixed condition. Loading was applied with an MTS Systems Corporation hydraulic actuator (Figure 3.5 left) to a HP 12x74 steel section that was cast with concrete into the end of the post.

Figure 3.5. Hydraulic actuator (left) and data acquisition system and loading frame (right)

The MTS actuator was attached to a hollow structural section (HSS) steel frame post tensioned to the strong laboratory floor, as shown in Figures 3.5 (right). A VTI Instruments Corporation EX1629A data collection system was used to collect both voltage and strain data, while a VTI EX10SC was used to collect temperature data.

3.2.2 Static Testing

Before fatigue testing, the baseline relationship between the hydraulic actuator and the test sample response was acquired through static loading cycles. Note that, in the following plots, only the lower six anchor rods are shown for clarity, and notation for the following sections is taken facing the laboratory structure as shown previously in Figure 3.2.

For direction definitions, tension was considered as positive strains or stresses. Negative displacements indicate downward displacement on the end of the post, theoretically putting the lower six anchor rods and bottom strain gauges into negative compression. The conversion from microstrain to ksi is $\mu\varepsilon\times0.029$ for all components of this structure, and the strain measured is engineering strain, as opposed to true strain.

Figure 3.6 shows the static response of the anchor rod-embedded strain gauges measuring the change in clamping force in the grip length, in microstrain.

Static Loading Cycles - Lower 6 Rod Embedded Strain Gauges
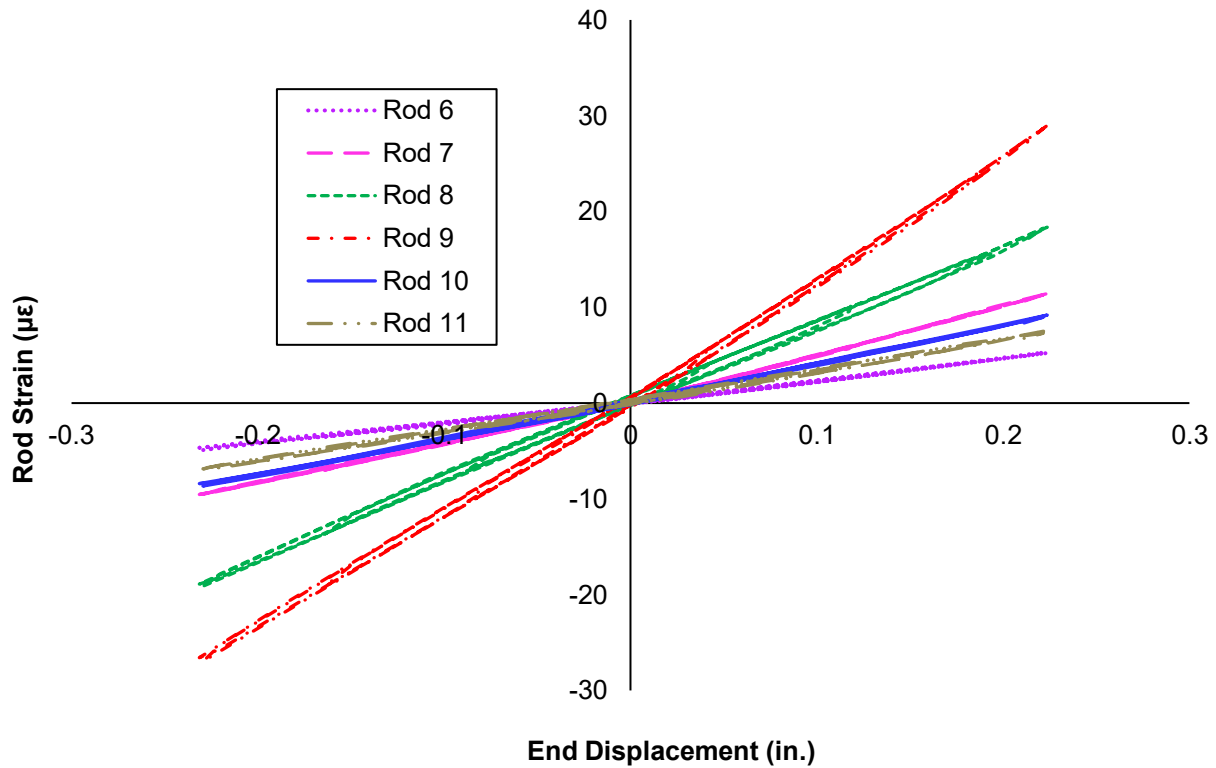
Figure 3.6. Anchor rod response to static loading

Note that these changes are in addition to any pre-strain in the anchor rods from tightening. Referring to Figure 3.6 and the previous Figure 3.1, the middle bottom rods, 8 and 9, experience the greatest strain at about +/- 19 με and +/- 28με, respectively. Next, the corner rods, 7 and 10, experience strains at about +/- 9με. Finally, rods 6 and 11 experience a differential of +/- 6με. All grip length strains exhibited a linear response to the loading.

Figure 3.7 illustrates the strains in the lower six rod standoffs.

Figure 3.7. Standoff strain response from static loading

The middle lower rods, 8 and 9, experience about five times the strain experienced by the corner or upper middle rods that are closer to the neutral axis of the post base. This strain increase is about double the differential observed in the grip lengths. The strains for SO11 and SO6 overlapped, which indicated the strain gauges were mounted fairly consistently between the two. Interestingly, the corner rods experienced an inverse force of what would be expected from the loading, and all the curves show some nonlinearity.

In addition to the recorded strains, theoretical strains for the anchor rods, calculated with the assumption of a uniform strain distribution, were plotted. The theoretical strain curves were based on the induced baseplate moment related to the displacement of the end of the laboratory test post.

Strains in the rod standoffs likely don't match the theoretical strains due to their non-uniform baseplate stiffness. Standoff distances in the lower middle anchor rods, which were the critical case, experienced approximately five times greater strains than the theoretical strain. The corner rods are farther out on the square baseplate and farther from the stiffeners, possibly causing a stiffness decrease, shifting the force transfer primarily to the middle anchor rods. Since the baseplate stiffness based on the distance from the edge of the post to the center of each anchor rod was not uniform, this may also explain the non-linearity of loading transferred to the foundation.

With regards to loosening from base shear forces, the square design may be beneficial since the corner rods would prevent the structure from slipping, with the middle rods taking the majority of the axial forces. Design of a square base may need to be reevaluated, though, as the current practice derived with a linear strain distribution does not accurately represent applied forces on the anchor rods. That guideline is from the American Institute for Steel Construction (AISC) Design Guide 1 (Fisher and Kloiber 2006), which is also the AASHTO recomendation for design.

The stiffness ratio (ratio of rod stiffness to connection stiffness), C, of the connections in the laboratory ranged from 0.20 to 0.54 and averaged out to 0.38. The stiffness ratio was much greater than the theoretical stiffness, which was calculated as 0.26, and may indicate that a greater than expected amount of stress is being transferred to the anchor rod grip lengths than anticipated.

Much like that seen from the embedded anchor rod strain gauges, there also may be some degree of scatter with the strain data from the standoff due to gauge mounting differences. Combined with the error from the anchor rod gauges, this may also explain the greater than anticipated stiffness ratios. The standoff strains on average, exhibiting greater and more uniform strains than the standoff distances, suggest that the sign post is acting composite with the pre-tensioned structural connections.

Figure 3.8 shows the sign-post strain response under static loading.
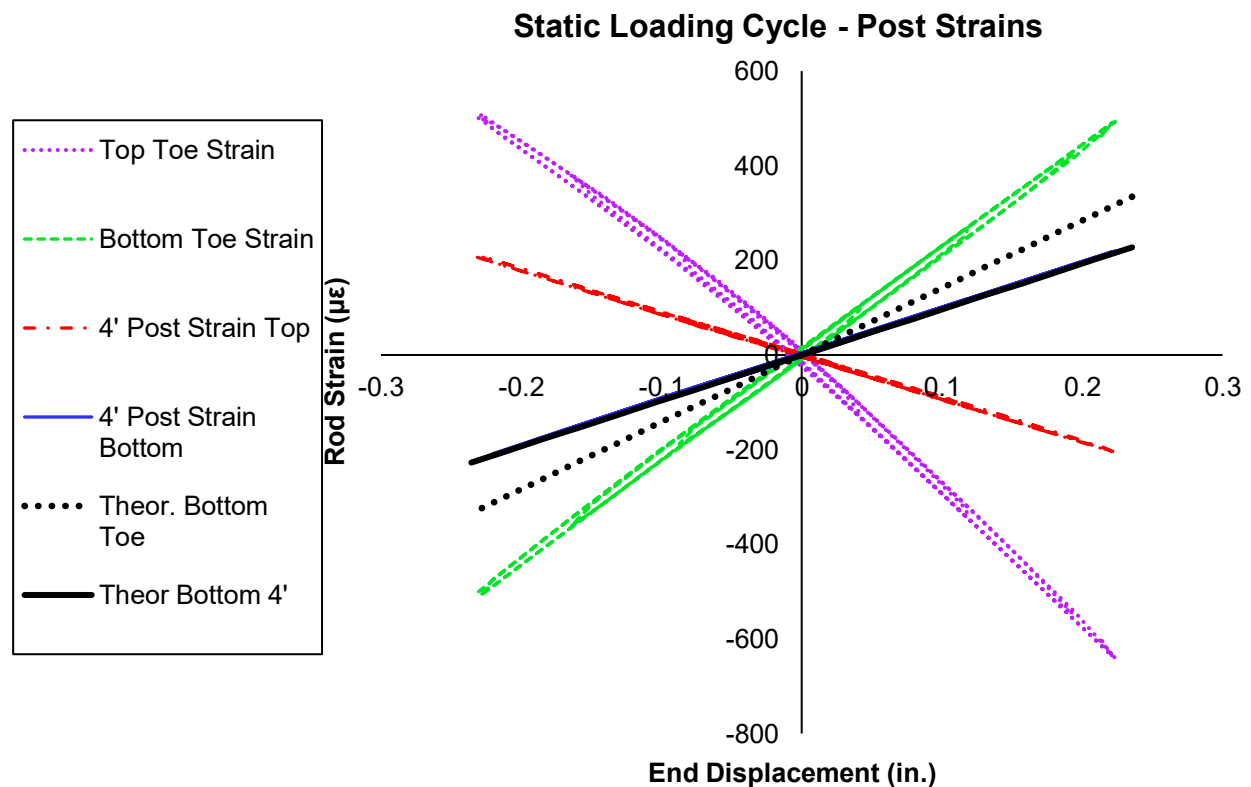
Figure 3.8. Sign-post strain response from static loading

24

Figure 3.8 shows the results for both the gauges mounted at the stiffener toes and at 4 ft above the baseplate. Note that the strains at the stiffener toes presented the limiting condition for the sign post, reaching a maximum of 640 με, or six times greater than the maximum strain experienced by the standoff rods and 20 times greater than the maximum strain in the anchor rods. These results align with James et al.'s testing in 1996, where the base-to-post weld connection failed multiple times and had to be repaired with welds throughout the testing (James et al. 1997).

The previous Figure 3.8 shows both the top and bottom gauges, so, unlike the previous Figures 3.6 and 3.7, inverse behavior is expected when comparing the values from the top and bottom gauges. Theoretical values are also plotted for the bottom gauges but are not shown for the top gauges due to redundancy. The theoretical values were calculated using a traditional mechanics approach.

For the middle 4-ft gauges, the theoretical values match experimental measurements relatively well, while the stiffener toe strain values are about 1.5 times the theoretical value due to the presence of stress concentrations. The discrepancy approximately matches the design assumptions in AASHTO and other research findings for stress concentrations around weld toes (Lassen and Recho 2006). From Figures 3.7 and 3.8, it is likely that the sign-post stresses at the weld details will generally govern for overhead signs when compared to those for the anchor rods, even when base stiffness is considered.

3.2.3 Field-Replicated Fatigue Testing

3.2.3.1 Derivation and Methodology

As discussed in the field monitoring sections of the companion report to this one from the implementation phase of this project, an equivalent stress range for anchor rod pre-tension loss cannot be developed with the assumptions in the current stress (S) against the number of cycles to failure (N), S-N practices, for traditional fatigue testing, since a damage fraction for pre-tension loss has not been derived. Due to the equivalent stress range limitations, a laboratory testing procedure that approximately replicated the field loading conditions was derived from the in-field rainflow counting results.

Field stresses from gauges mounted on the sign post were used to approximate the loading on the anchor rods due to uncertainties in the field-measured rod strain values and because of different baseplate designs. The field stresses were replicated with an approximate summation procedure, setting pre-determined strains to induce with the MTS hydraulic actuator, and then finding how many cycles in the field occurred in the strain ranges to program the tests accordingly.

In the summation procedure, counts under 4 με (0.116 ksi) were disregarded considering noise in the strain gauges and because it was hypothesized that the significantly lower stress ranges would not have a major impact on loosening the connections. Also, the counts for lower strain ranges would have required about a month to replicate at low stresses. The following equation outlines the summation procedure used for each laboratory testing bin.

$$\sum_{\varepsilon_i}^{\varepsilon_{2i}} n = N_{t\varepsilon i}$$

When compared to the next equation, which was based on Miner (1945) and is covered in the companion Phase I final report (Chen et al. 2018) for this project, the summation equation for laboratory testing cycles is similar but without the number of defined cycles to failure, and the result is not a damage fraction, but a true count of cycles within each predetermined bin.

$$\sum_{i=1}^{k} \frac{n_i}{N_i} = C$$

Figure 3.9 outlines the laboratory testing cycles compared to the summed stress range cycles.
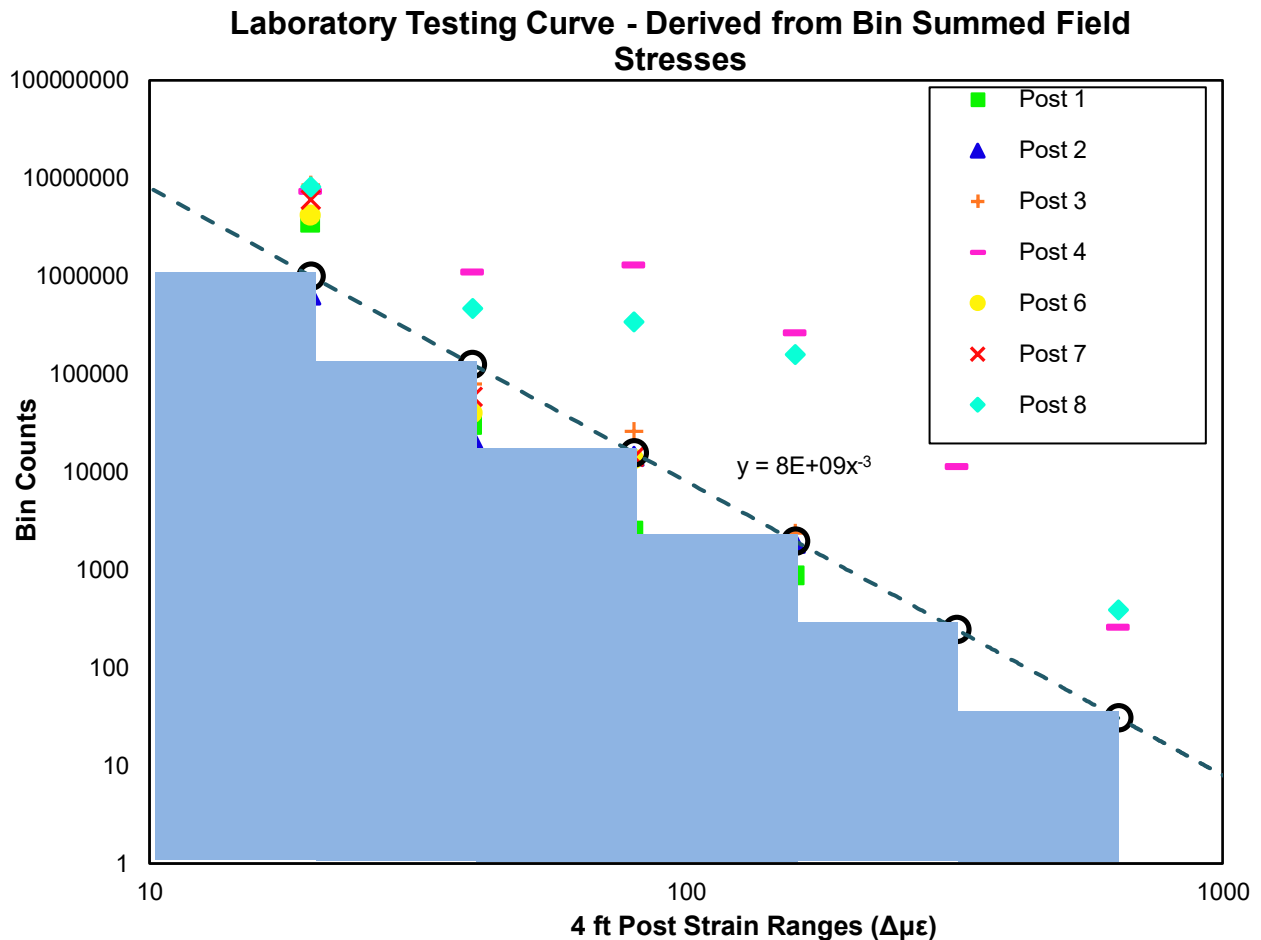
Figure 3.9. Field-derived laboratory testing curve

After summing the strain range bin counts for each sign-post gauge, an average of the fitted exponential curves was taken to derive a laboratory testing curve. After deriving the field curve, it was normalized for the total number of days recorded in the year and broken into individual cycles by the greatest stress

range. The actuator was then programmed with the respective number of cycles in each loop. Table 3.1 outlines the final laboratory testing cycles used from the field stress results.

Table 3.1. Field-derived laboratory testing cycles

Desired Test Stress Range (*ue*)	Field Curve Cycles (using *c*=E8×ε⁻³)	Yearly Cycle Correction (193/365 days recorded)	Single Laboratory Test Loop Cycle Count	Cycles to Replicate # Years = 2	Stroke +	Stroke -	+/- Load (kips)	Loading Rate (Hz)
20	1,000,000.00	1,689,815	**32,497**	3,379,688	0.013	-0.013	0.323	5
40	125,000.00	211,227	**4,063**	422,552	0.026	-0.026	0.646	3
80	15,625.00	26,404	**508**	52,832	0.051	-0.051	1.293	2
160	1,953.13	3,301	**64**	6,656	0.103	-0.103	2.585	1.5
320	244.14	413	**8**	832	0.205	-0.205	5.170	1.25
640	30.52	52	**1**	104	0.410	-0.410	10.340	1

Total Cycles = 3,862,664 and Loops to Test = 104

Although the laboratory testing curve appears to not be conservative for sign-post gauges 4 and 8, all of the field cycles that fell into the bins were tested in a higher bin range. For example, if the field sign post experienced 50 counts of 321 Δμɛ stress reversals, the 50 counts would be tested at 640 μɛ in the laboratory, since 321 Δμɛ is in the next higher bin. Approximating from traditional fatigue testing, damage fractions tended to increase exponentially, so, while the summed counts for sign post gauges 4 and 8 were greater, it is likely that the pre-tension loss "damage" was adequately accounted for using the prescribed method.

3.2.3.2 Results

Table 3.2 shows the results of the field-replicated fatigue loading test.

Table 3.2. Field-replicated fatigue results

Measurement	Rod 2	Rod 3	Rod 4	Rod 5	Rod 6	Rod 7	Rod 8	Rod 9	Rod 10	Rod 11	Rod 12
Initial pre-tension (μɛ)	720	7	989	74	820	648	688	914	468	580	520
48 hr relax (μɛ)	687	-8	959	39	783	606	662	892	467	519	511
% Change of initial pre-tension	-5%	-222%	-3%	-47%	-5%	-6%	-4%	-2%	0%	-11%	-2%
Strain after fatigue test (μɛ)	689	-20	846	39	777	597	669	853	481	488	514
% Change of initial pre-tension	-4%	-394%	-14%	-47%	-5%	-8%	-3%	-7%	3%	-16%	-1%
Immediate loosening (μɛ)	614	22	913	8	1,214	505	633	896	445	466	344
% Change of initial pre-tension	-15%	223%	-8%	-89%	48%	-22%	-8%	-2%	-5%	-20%	-34%
% Relaxation losses	31%	-99%	39%	53%	-10%	29%	47%	127%	2%	53%	5%

Table 3.3 shows the averages and standard deviations with rods 3 and 5 excluded.

Table 3.3. Field-replicated fatigue summary

Summary Result	Avg.	Std Dev.
% Total test losses	-6.2%	6%
% Direct loosening	-14%	23%
% Loss from relaxation	36%	40%

In Table 3.2, the strains after initial pre-tension, 48-hour relaxation, fatigue testing, and immediate losses (when the nut was removed) are illustrated for a full overview of the strain losses in the sign post. The absolute pre-tension losses in the anchor rods were recorded during nut removal to validate losses recorded at the end of fatigue testing.

The results in Table 3.2 show a fair amount of variability in the individual rod results in all regards. Due to the strain variability, each anchor rod's performance was compared relative to itself in terms of percent losses. In addition, rods 3 and 5 were not considered due to sensitivity issues and given the gauge for rod 4 was broken off while repositioning the wrench to remove nut 3, while it still returned loosening data.

After the 48-hour relaxation, the average loss from the initial pre-strain was -4.1%. Note that the 48-hour losses were recorded after tightening, so the "initial pre-strain" does not account for the immediate losses after tightening. Immediate losses in conjunction with the 48-hour losses are discussed further in a following section.

After the fatigue test, the average overall loss, including the relaxation, was -6.2% for the anchor rods, with rod 12 having the greatest overall losses of -16% of the initial strain. When directly loosened, the total average losses amounted to -14% of the initial pre-strain. The immediate loosening value was taken as more reliable than the final fatigue value, because the absolute strain loss could be immediately measured practically without temperature and strain drift impacts. Taking the immediate loosening values was also more conservative, as the average recorded losses were approximately double that of the ones recorded at the end of the fatigue test. The researchers suspected that the wiring for rod 6 was not completely secure; while loosening, the value increased nearly 400 $\mu\varepsilon$ from the initial value, and those results were disregarded from the averages.

All inclinometers indicated negligible turns after the fatigue test, with a maximum change of 0.025 degrees (1/14,500 of a turn), which is within the error range for the inclinometers. These minimal turns indicate that transverse loading is likely not a primary loosening mechanism, which matched expectations from the literature (Bickford 1995).

Considering the immediate loosening, an average of 36% of all losses came from losses recorded 48 hours after the initial pre-tensioning. If the ends of the fatigue losses are considered, initial relaxation was 74% of all losses. However, the fatigue test was started five days after the initial pre-tensioning, so it is likely there was additional minor, unrecorded relaxation before commencing fatigue testing.

Finally, the replicated two years of fatigue loss was far less than the strain drop observed on the field-monitoring sign post. This may indicate that a majority of the perceived strain losses in the field is due to drift of the strain gauges and not actual loss; considering the strain drift observed in the laboratory, this

would be fairly reasonable. If anchor rods are properly pre-tensioned, it is likely that relaxation and temperature have a far greater impact on pre-tension loss than fatigue loading. Finally, much like traditional fatigue testing, it is likely that the lower strain ranges have little impact on anchor rod pre-tension loss.

3.2.4 AASHTO Reference Service Life Replicated Fatigue Testing

3.2.4.1 Derivation and Methodology

After observing that the field-derived fatigue testing had little impact on the pre-tension loss in the anchor rods, it was decided that fatigue testing of the anchor rods would be related back to a typical AASHTO CAFL curve of a known detail. This approach was conceptualized for a few reasons.

First, the time required to replicate the field stresses on the sign post using the prior procedures takes about a week per year replicated, and it was not feasible to replicate a full 25-year or longer design life. Second, testing at a known AASHTO CAFL could give a reference benchmark for loosening that could be related back to accepted standards. Third, the applied fatigue stress will be greater, hopefully resulting in definitive, quantifiable, fatigue-induced pre-tension loss in the anchor rods.

The standoff anchor rods acted as the baseline AASHTO CAFL. However, they were not stressed to their full CAFL since the sign-post stresses controlled the loading. Using the equations and procedures from AASHTO, the post at the stiffener toe has a finite life constant, A, of 11×10^8 ksi^3, and a threshold, ΔF, of 7 ksi. The anchor rods have a threshold of 7 ksi. Both of the details are for AASHTO fatigue curve D (AASHTO 2015).

Referring to the static testing, the anchor rod standoff distances could not be brought to their threshold stress, or CAFL, due to concerns about prematurely failing the post, as with James et al.'s research (1997). The middle lower rod standoffs (for rods 8 and 9) were the controlling anchor-rod stresses. The lower two anchor rod standoff distances were stressed to an average of 166 $\Delta\mu\varepsilon$ (4.8 ksi), which aimed for the AASHTO fatigue curve CAFL E and corresponded to 1,088 $\Delta\mu\varepsilon$ (31.6 ksi) at the weld toes of the structure and 51 $\Delta\mu\varepsilon$ (1.5 ksi) in the anchor rod grip lengths of rods 8 and 9.

Equation 11.9.3-2 from AASHTO (2015) was then used to find the theoretical cycles to failure for the post in a finite life, since the 32 ksi stress reversal is greater than the AASHTO CAFL for the details of 7 ksi. With a 32 ksi stress reversal, AASHTO allows for 33,600 cycles until failure, which was deemed overly conservative due to the stress concentration factor included in the recorded laboratory sample strains. Therefore, a theoretical stiffener toe stress was calculated as 666 $\Delta\mu\varepsilon$ (20 ksi) and used. This was deemed valid because the AASHTO fatigue stress concentration factor, Kf, from Table 11.9.3.1-1, for the detail was calculated at 2.28, which allows for the calculated stress to be used.

Using the pure AASHTO calculation procedure, the finite lifespan of the sign post was found to be 137,500 cycles at 20 ksi stress reversals at the top and bottom stiffener toes. After derivation, the sample was tested using a displacement-controlled sinusoidal loading with an MTS actuator stroke amplitude of 0.28 in. (static loading of +/- 6.9 kips) at a frequency of 1 Hz. A major crack or failure was

not discovered after 800,000 cycles (nine straight days of testing) of the loading outlined above, or about six times the AASHTO design life.

Given that no cracks were discovered, it was decided to load the standoff strains to their full AASHTO CAFL of 7 ksi. In this fatigue test, the critical anchor rod standoffs were strained at 250 Δμε (7.25 ksi), which corresponds to sign post-stiffener toe strains of 1,500 Δμε (43.5 ksi) and anchor rod grip length strains of 75 Δμε (2.2 ksi). In addition, the loading was changed from displacement to load-controlled to account for any softening of the details from fatigue.

The loading was applied using the MTS actuator in a sinusoidal pattern with an amplitude of 11.5 kips (0.46 in. under static loading) at 1 Hz. This test ran for 9,450 cycles before failing the top cross beam of the testing frame in fatigue. It is likely that the fatigue crack in the frame had initiated during the previous fatigue test and was brought to failure by the higher number of loading cycles.

Overall, the final cycles brought the total AASHTO design life to 6.2 times longer than allowed in the sign-post detail specifications. To check for micro cracking, dye penetrant testing was utilized, but observations were inconclusive due to the rough surface on the post and possible crack locations being longitudinal to welds, which made proper cleaning difficult.

3.2.4.2 Results

A summary of the final fatigue test losses is presented in Table 3.4.

Table 3.4. AASHTO reference detail replicated fatigue pre-tension loss results

Measurement	Rod 2	Rod 3	Rod 5	Rod 6	Rod 7	Rod 8	Rod 9	Rod 10	Rod 11	Rod 12
Initial Pre-tension (με)	798	-5	50	1,011	261	791	1,088	857	529	276
48 hr relax (με)	775	-2	73	954	265	789	1,008	832	504	251
% Change of initial pre-tension	-3%	-53%	47%	-6%	2%	0%	-7%	-3%	-5%	-9%
Strain After Fatigue Test (με)	768	9	73	987	263	747	999	829	523	167
% Change of initial pre-tension	-4%	-267%	47%	-2%	1%	-6%	-8%	-3%	-1%	-40%
Immediate Loosening (με)	676	25	8	950	242	721	986	810	402	131
% Change of initial pre-tension	-15%	-568%	-84%	-6%	-7%	-9%	-9%	-5%	-24%	-52%
% Relaxation losses to fatigue losses	19%	9%	-56%	95%	-23%	2%	79%	54%	20%	17%

Table 3.5 shows the averages and standard deviations with rods 3 and 5 excluded.

Table 3.5. AASHTO reference detail replicated fatigue pre-tension loss summary

Summary Result	Avg.	Std Dev.
% Total test losses	-7.9%	24%
% Direct loosening	-16.1%	16%
% Loss from Relaxation	14.0%	42%

Much like the field-replicated fatigue loading, a strain-time plot is not presented.

Pre-tension loss, on average, in the anchor rods was similar to the field-replicated fatigue, only differing by 2% for both the total recorded test losses and the immediate loosening recorded losses. In the second fatigue test, there appeared to be lower pre-tension losses from initial relaxation. However, the AASHTO-replicated fatigue was started a day after the 48-hour relaxation, so some of the losses could be from relaxation and creep as opposed to the field-replicated fatigue test that was started a week after the initial pre-tensioning.

It is likely that fatigue loading does not have a significant impact on connection loosening if the anchor rods are properly pre-tensioned. Comparable fatigue loading in the Phase I study (Schaeffer 2018) resulted in anchor rod loosening after 6,000 cycles when the anchor rods were pre-tensioned with MnDOT's old specification of 480 ft-lbs or 14% of the AASHTO-recommended verification torque.

3.2.5 Sign-post Response to Anchor Rod Pre-Tensioning

Direct torque tension curves are not presented for the strain gauges inside the anchor rods due to their variability and error concerns. As in the previous fatigue testing results, only the relative results are primarily the ones presented.

3.2.5.1 Standoff Distances

The baseplate stiffness impact that was observed in the static testing results was further observed during pre-tensioning of the anchor rods. Before pre-tensioning, the leveling nuts were torqued to approximately 50 ft-lbs. As shown in Figure 3.10, the standoff strains were fairly impacted by the pre-tensioning, especially for the corner rods that experienced an average of 1,050 $\mu\varepsilon$ (30.5 ksi tension).

Figure 3.10. Standoff strains during anchor rod pre-tensioning

The middle anchor rods experienced an average increase of -163 µε (4.7 ksi compression). The unexpected behavior of the standoff strains may be due to the baseplate stiffness, making the corner rods "pull" the sign base in and putting the middle rods into compression.

Most of the strain increase occurs during the 20% or approximately snug-tight phase of pre-tensioning. This behavior suggests that it is critical to properly tighten the leveling nuts. The rod standoffs may have experienced lower strain increase if the leveling nuts had been tightened against the baseplate to a greater degree but is unlikely, because the corner rods, further from the stiffeners, exhibited the greatest increase, while the increases in the other standoffs were approximately negligible. The non-uniform baseplate stiffness is likely influencing this behavior but would need further investigation.

3.2.5.2 Relative Relaxation

Experience in the field indicated that 48-hour retightening of anchor rods is fairly difficult and resource intensive, especially if the structure is mounted in the median of a highway. To investigate if the 48-hour retightening step can be skipped, relaxation of the anchor rods was recorded for the laboratory sign-post specimen. Relaxation was also investigated for Skidmore anchor rod pre-tensioning results; however, due to different connection stiffness properties, the results are not presented given the Skidmore tension tester relaxations would likely be less than actual connections would experience.

Note that the scope of the relaxation data is limited in regards to the anchor rod and base thickness of the laboratory structure and may not necessarily directly extrapolate to other base conditions. In addition, the anchor rods referred to as "retightened" were on the field-replicated sign post, and the "un-retightened" anchor rods were on the AASHTO-replicated post. The reasoning for this is that the original field-replicated fatigue test did not have strain gauges mounted for the standoff distances.

Before the field-replicated fatigue, the anchor rod locations had been previously pre-tensioned, but the data logger was improperly configured. After the field-replicated fatigue, the post was moved forward 2 in. on the anchor rods to allow for mounting of the standoff strain gauges, which moved the top and leveling nuts onto untightened areas of the anchor rods. There could also likely be error from reusing the nuts and washers, leading to greater relaxation in the field than that observed in the laboratory.

Figures 3.11 and 3.12 present the relative relaxation data for the initial 30 minutes after pre-tensioning for the tightened and retightened cases, respectively.

Immediate Anchor Rod Pre-tension Relaxation

$y = x^{-0.005}$

$y = 0.95x^{-0.025}$

Legend: Rod 2, Rod 7, Rod 8, Rod 10, Rod 11, Rod 12, Upper Limit, Lower Limit

X-axis: Time (s)
Y-axis: Percent of Original Immediate Pre-Tension
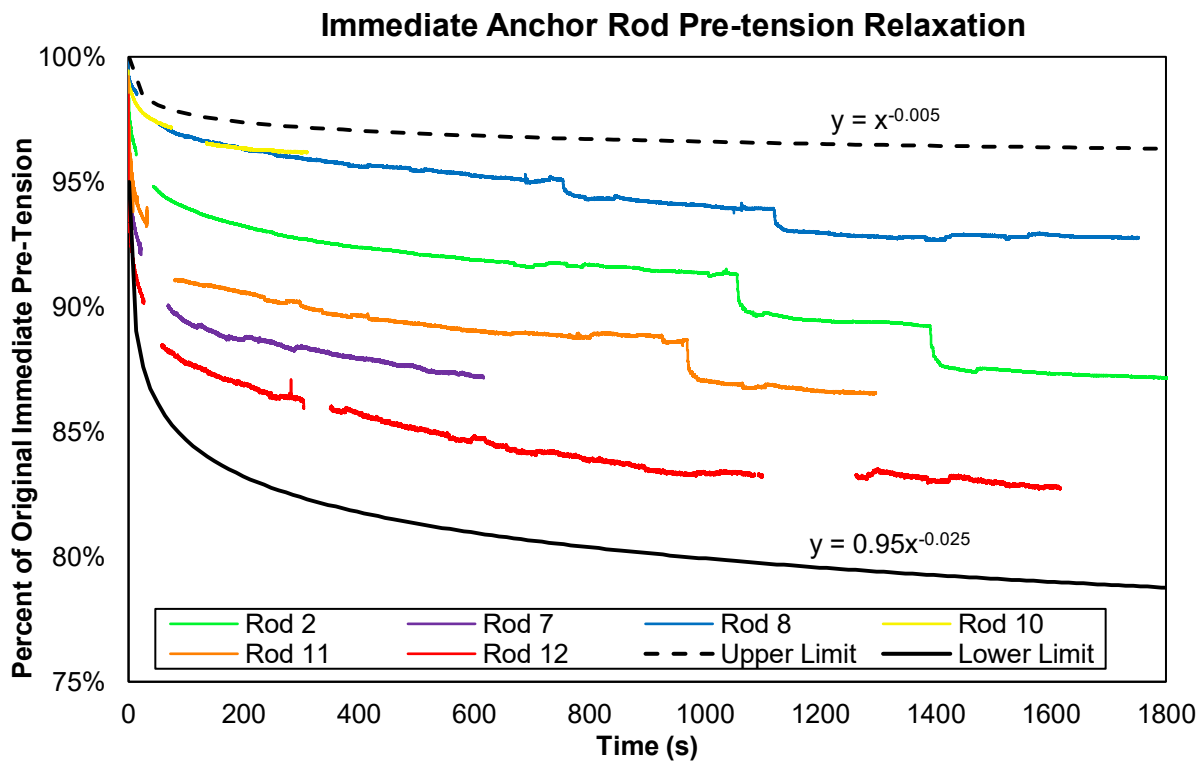
Figure 3.11. First 30-minute anchor rod pre-tension loss without retightening

Re-Tightening Immediate Anchor Rod Pre-tension Relaxation

Figure with axes: Y-axis "Percent of Original Immediate Pre-Tension" (75% to 100%), X-axis "Time (s)" (0 to 2000). Equations shown: $y = x^{-0.005}$ (upper limit) and $y = 0.95x^{-0.025}$ (lower limit). Legend: Rod 2, Rod 7, Rod 8, Rod 10, Rod 11, Rod 12, Upper Limit, Lower Limit.
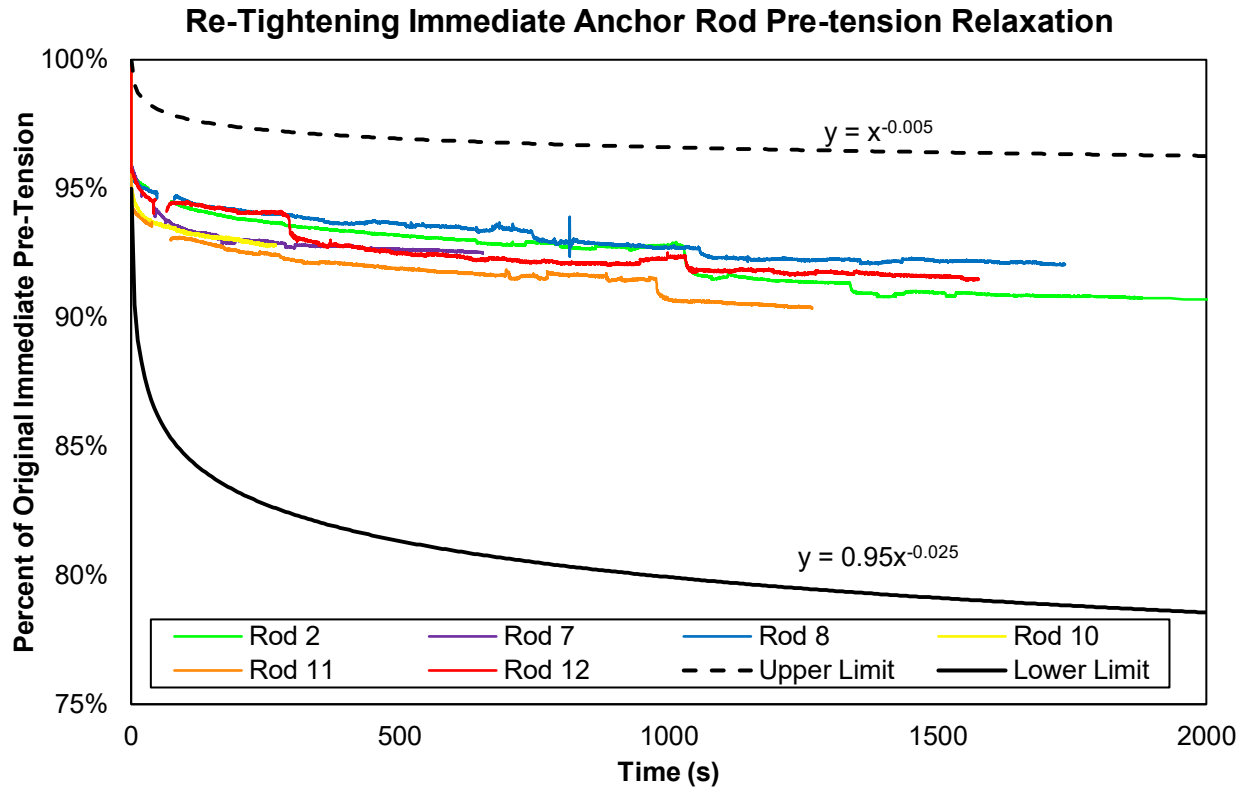
Figure 3.12. First 30-minute anchor rod pre-tension losses after retightening

Spaces in these data are for clarity and occurred when the strain gauges were disconnected to put the hydraulic wrench on or when work around the sign post disturbed the gauge. Quick drops in the strains may have either been due to disturbances or impacted by tightening of the other anchor rods, but the data were included for the sake of completeness. Data ends at different points for each of the anchor rods due to the tightening order. Finally, not all rods were included due to strain sensitivity causing excessive noise in the data for rods 5, 6, and 9.

All of the relative losses in the previous Figure 3.11, which shows the un-retightening relaxation, exhibit a power distribution. All of the losses are fairly widely scattered between the two approximate upper and lower loss limits. The loss limits were approximated from previous literature along with these data (Yang and Dewolf 1999, Nijgh 2016). Both the power pattern and the losses match up fairly well with previous research.

If a 50-year lifespan is considered for the upper limit relaxation, the anchor rods would lose 10% of the original pre-tension; with the lower limit of relaxation, an anchor rod might experience 45% total lifespan losses from relaxation. Due to the power distribution, the majority of the losses take place within the first week after tightening. Although results from tightening suggest that AASHTO and AISC guidelines are generally correct in recommending that connections are retightened after 48 hours, the previous Figure 3.12 illustrates that the timeframe is likely much shorter than 48 hours.

In Figure 3.12, showing the relaxation losses after the retightened case with the anchor rods, immediate relaxation exhibits greater consistency, and lifetime relaxation is limited to approximately 25% over the

rod lifespan. This suggests that, if the anchor rods are retightened at any point, relaxation should be of a lesser degree and of greater uniformity.

These observations are confirmed by Nijgh (2016) from research at the Delft University of Technology, where the relaxation of European structural bolt connections with different coating types was investigated. Nijgh found that galvanized structural bolts relaxed approximately half as much with a greater uniformity when they were retightened after 40 minutes. This behavior was observed without taking the bolts off, helping to validate results for the field.

Figure 3.13 presents the combined initial and 48-hour relaxation data for the tightened case but with time on a log scale.

Immediate to 48hr % Anchor Rod Pre-tension Relaxation
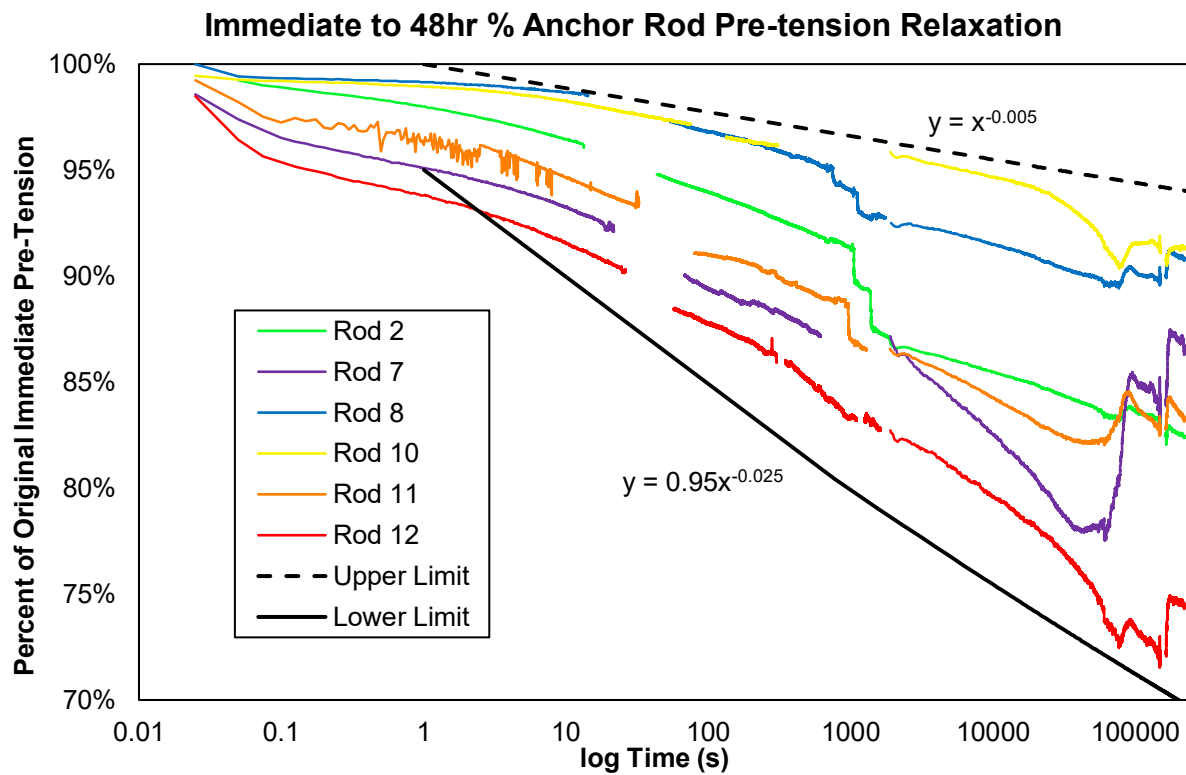
Figure 3.13. Combined initial and 48-hour anchor rod pre-tension relaxation on a log scale

Note that the relaxation values in this plot will be greater than the 48-hour relaxation presented in Table 3.4. The recorded data for Table 3.4 was taken after the initial 30-minute tightening and not immediately after the applied pre-tensioning torque is removed as with Figure 3.13. During the 48-hour relaxation, temperatures in the laboratory varied by about 4 degrees Celsius because the laboratory was opened to allow for other operations. The temperature differential caused strain increases at the end of the 48 hours.

Only data from the non-retightened test is presented, because data from the field-replicated fatigue test were only collected at 10 Hz, which was not sufficient resolution to observe the initial relaxation within 0.1 of a second. Looking into the first minute, Figure 3.13 shows that the relative strains exhibited an

initial decrease of about 5% in the first 0.1 to 0.5 of a second after removal of the torque. After that, the connections took about 60 seconds to 10 minutes to start exhibiting a power-log relationship, as modeled in previous literature. The exact mechanism behind this behavior may be a combination of localized plastic yielding, zinc flow from the galvanizing, and creep in the steel itself, combined with many other factors that could be contributing.

Figures 3.14 presents roughness that leads to some degree of anchor rod relaxation.
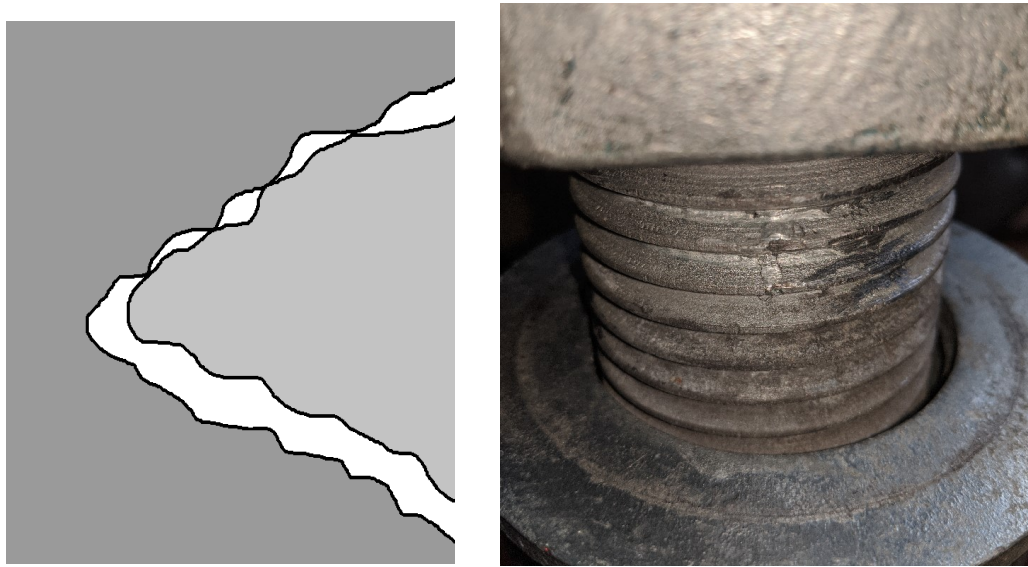
After Bickford 1995 (left)

Figure 3.14. Thread roughness (left) and roughness on rod 12 galvanizing (right)

If the initial minute to 10 minutes of relaxation is alleviated by retightening, the connections likely will perform at a fairly uniform distribution, having about 5% initial losses. Recorded losses also align approximately with the observations from directly loosening anchor rods, as shown in the previous Table 3.4, validating the relaxation approximations. Finally, the 48-hour values in the previous Tables 3.2 and 3.4 match up approximately, suggesting that, after the initial relaxations, pre-tension loss is fairly uniform, since the pre-tension directly after tightening was not considered as "initial" for the 48-hour losses. Overall, the 48-hour AASHTO retightening torque could likely be deleted from the specification and replaced with a 10-minute retightening torque to minimize pre-tension loss and maximize labor efficiency.

3.3 TIGHTENING PROPERTIES

3.3.1 Methodology

Tightening tests focused on torque-controlled pre-tensioning on three different anchor rod diameters with five different lubricants. Each lubricant and rod combination was tested five times. Three different wrenches were utilized due to various limitations and to ensure that different torque measurement methods provided consistent results. The first wrench was a HYTORC Stealth 4 with a Vector pump, as shown in Figure 3.15 (left).
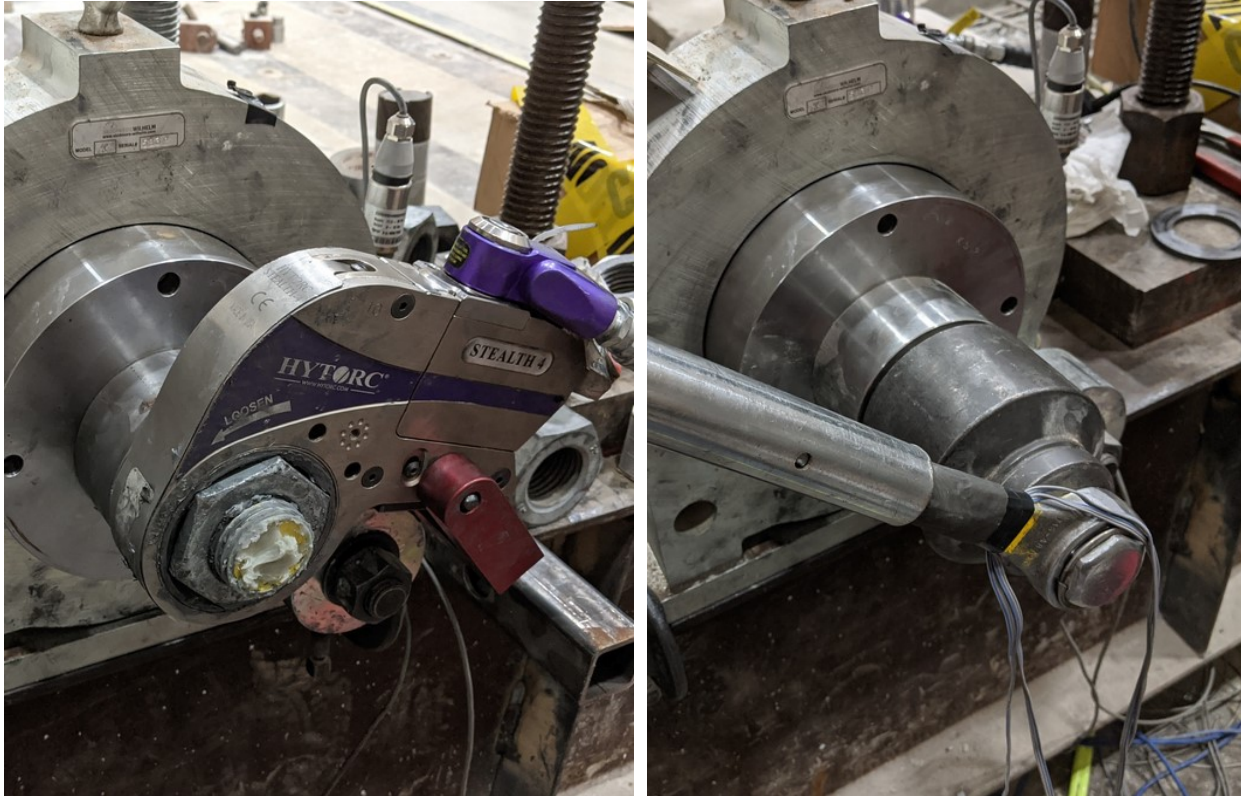
Figure 3.15. Skidmore Model K pre-tensioning with hydraulic wrench (left) and calibrated strain wrench (right)

Pressure was measured with a Schaevitz 10,000 psi hydraulic pressure transducer that could be correlated to torque through a calibration curve. The second wrench, shown in Figure 3.15 (right), had a fixed-end socket with four foil strain gauges mounted near the base to measure torque indirectly. The calibration curve for this wrench was developed with basic mechanics equations and verified using the other two torque wrenches. Finally, for lower torque measurement, a 100 ft-lb torque transducer was used (Figure 3.16).
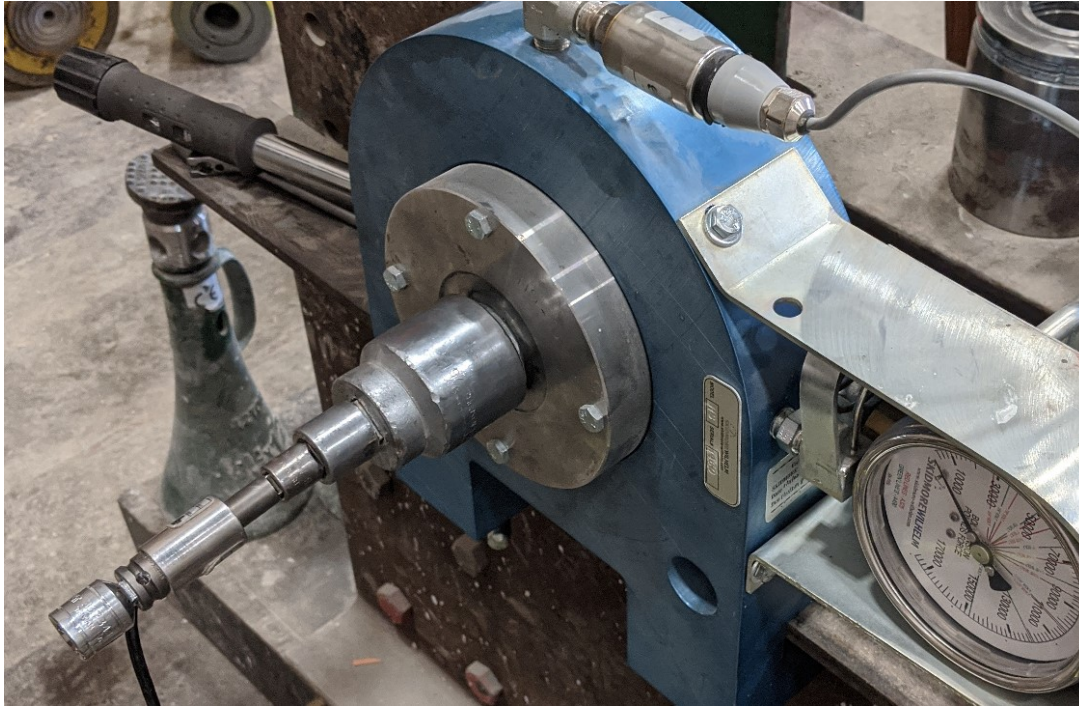
Figure 3.16. Pre-tension testing with Skidmore Model MK and torque transducer

Larger diameter anchor rods, more than 1.25 in. diameter, were tested using a Skidmore-Wilhem Model K bolt tension tester, while smaller anchor rods were tested using a Skidmore-Wilhelm Model MK. A VTI Instruments EX1629A data collector. Data were collected at a sampling rate of 200 Hz with all instruments.

3.3.2 Lubrication

The results from the laboratory testing lubrication results are presented in Table 3.6 (and Figure 3.17 and 3.18 shown later in this discussion).

Table 3.6. Summary of tightening/loosening aspects and statistics

Lubricant	Laboratory K	% K uncertainty	Clamp Force Std. Error (kips)	R^2	Laboratory Loosen -K	% K uncertainty	Clamp Force Std. Error (kips)	R^2	Ratio of Loosen to Tighten
Dry*	0.270	0.265%	1.27	0.939	-0.207	-0.389%	-1.85	0.993	-0.766
WD 40**	0.212	0.080%	0.14	0.995	-0.163	-0.212%	-0.18	0.972	-0.765
Never Seez	0.120	0.131%	2.49	0.966	-0.097	-0.287%	-5.42	0.946	-0.809
Copper Spray	0.115	0.129%	2.28	0.972	-0.091	-0.324%	-4.52	0.951	-0.795
Wax	0.106	0.105%	2.14	0.984	-0.081	-0.225%	-4.21	0.965	-0.764
Combined	0.113	0.009%	2.39	0.971	-0.090	-0.197%	3.99	0.966	-0.792

*Did not test on 1.5 in. due to torsional damage concerns with the Skidmore tension tester
**Only tested on the 1 in. diameter rod due to torsional damage concerns with the Skidmore tension tester

The lubrication impact was tested both for tightening and loosening anchor rods to investigate the possibility of an inspection torque that could be utilized after installation to ease labor concerns. This section refers to the equation below for torque controlled pre-tensioning, where T is the torque required to be applied to the connection, F is the final clamp or pre-tension force, D is the diameter of the anchor rod, and K is referred to as the nut constant.

$$F = \frac{T}{KD}$$

These tightening data mainly illustrate that the current AASHTO-recommended nut factor of 0.12 is likely sufficient for the anti-seize type lubricants on galvanized ASTM F1554 anchor rods. If any of these factors are changed, it would impact the final nut factor and therefore the pre-tension. In fact, when testing lighter lubricants, like WD-40 and non-lubricated rods, the testing was limited due to the torsional capacities of the Skidmore-Wilhelm tension tester and the double locked nut connection in the back.

All of the anti-seize lubricants that were observed in the field or used by other DOTs preformed approximately the same, averaging out to a nut factor of 0.11 using three different types of wrenches for pre-tensioning. The 95% confidence interval for these laboratory data would result in an error of +/- 4.7 kips of final clamping force using the nut factor of 0.113. Although 0.113 is 8% less than the current specification nut factor, it is recommended that the 0.12 factor is still used. Unlike all prior studies, this nut factor is directly correlated to the instruments and not manually read, which is impacted by the immediate relaxation.

All of the nut factors are laboratory derived, with lubrication thoroughly applied and no environmental variables. Also, as experienced on site, ideal conditions will often not be the case, generally resulting in an increased nut factor. Figure 3.17 shows the scatter of these tightening data along with reference nut factors.
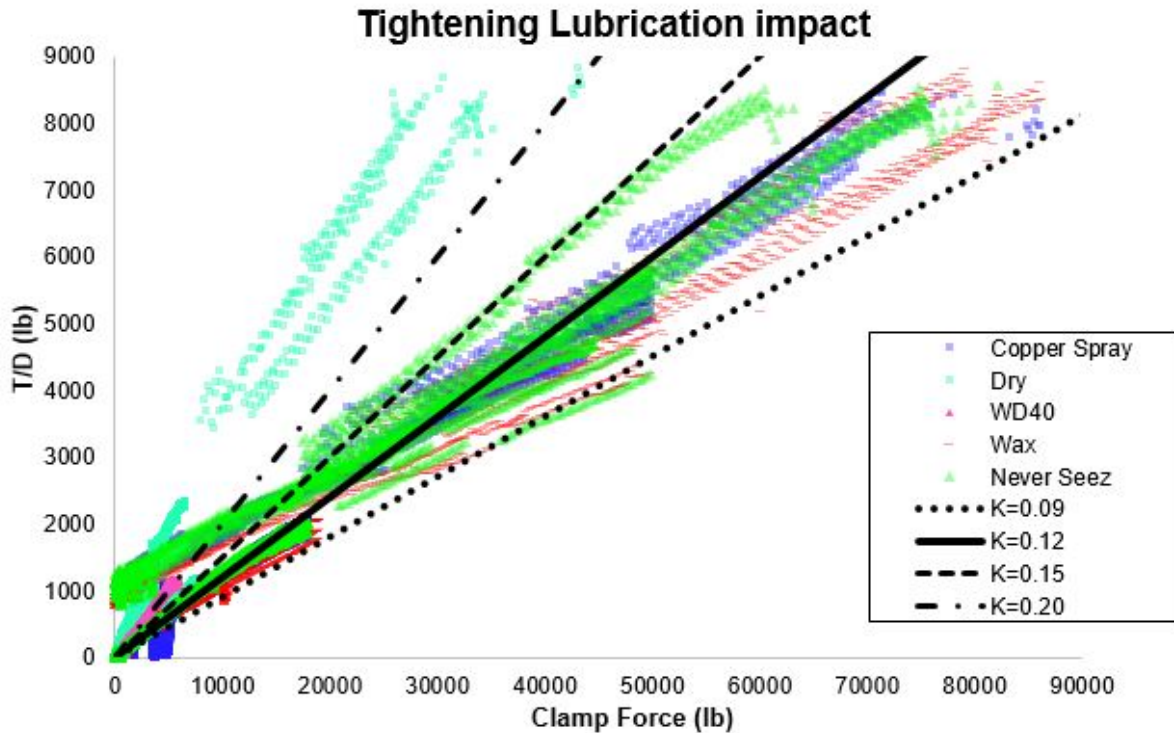
Figure 3.17. Tightening laboratory tested properties

Note that the axis in both this figure and Figure 3.18 (shown later in this discussion) are in lbs. The x axis is clamp force and the y axis is applied torque divided by the diameter of the tested rod. These data were plotted in this manner so the slope of the trend line would be the nut factor and statistics could be directly performed on the slope.

The nut factors on the graph are purely for reference and are not statistical in nature. Because the hydraulic wrench has a minimum operating pressure, there is an apparent skew at the lower end of the pre-tensioning data. This was investigated with the other two wrenches at lower torques, and, as the torque equation suggests, is due to the operating pressure of the wrench. While this may add uncertainty to the data, it was not removed for transparency and to indicate there will be greater error when the hydraulic wrench is used at lower torques.

The loosening data resulted in about 80% of the tightening nut factor and generally had a greater standard error, which aligns with the available literature (Bickford 1995). For the combined anti-seize lubricants, a loosening *k* of -0.09 was observed with a 95% confidence interval of +/- 7.8 kips of clamping force. In addition, the starting point of all of the loosening torques would be impacted by the immediate relaxation of the anchor rods. Figure 3.18 shows the distribution of the loosening data points with reference negative nut factors.
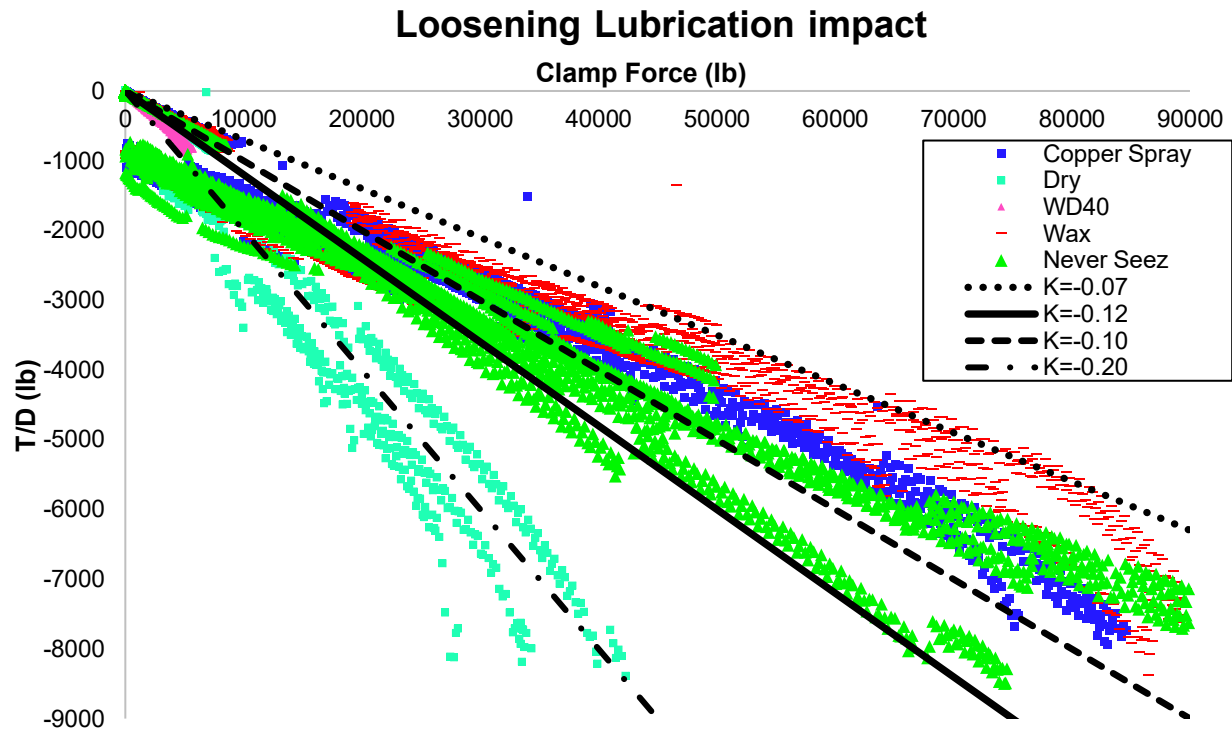
Figure 3.18. Loosening laboratory tested properties

The lower skew in the tightening data was the same for lower torques when using a hydraulic wrench for pre-tensioning. Also note that some lubricants, like the wax, have a certain amount of non-linearity at the beginning of the loosening curve. This is likely due to the lubrication properties and the wrench having to overcome the static friction of the connection before loosening.

For an inspection torque, the error and relaxation losses are a crucial factor to ensure that the inspection procedures verify adequate pre-tension for the connection but not return excessive false positives. Another important distinction to make is that the inspection torque could only tell how much torque was originally applied to the connection; lubrication must also be verified during inspection, for an approximation of the final pre-tension force.

3.3.2.1 Parametric Turn Study

Throughout the course of the study, it became clear that a parametric investigation of anchor-rod turn properties would likely have greater efficiency than directly testing the turns in the laboratory. Literature indicates that joint stiffness is highly dependent on the baseplate and the composition of it (Bickford 1995, Kulak et al. 2001). A turn and grip length study cannot be accurately replicated with a load cell or bolt tension calibrator because the stiffness distribution of the joint will be in a cylindrical, not frusta shape.

To accurately model turn properties for the baseplates on MnDOT structures, multiple individual plates of galvanized steel at the same thickness of the baseplates would need to be used. A minimum of three anchor rods of each size would need to be instrumented with a bolt strain gauge, calibrated and fixed on

one end, possibly in concrete. For measurements, the turn would need to be continuously measured with inclinometers, string potentiometers, or digital image correlation due to torsional relaxation. Considering the experiences in implementation that turn-controlled pre-tensioning is not ideal for many structures due to clearance issues and that there is a significant amount literature available for turn-controlled pre-tensioning, a parametric approach was used for the best value for MnDOT.

Recalling the previous equation from the review of anchor rod tightening properties, where F is the final pre-tension or clamp force, L is the length of the bolt in the grip length, C is a ratio of bolt stiffness to connection stiffness, E is Young's modulus, P_i is the pitch (distances between threads, i.e., a UNC 6 rod would be 1/6), and A is the tensile area of the fastener, α is the nut turn angle in a full-turn ratio (i.e., 1 is a full turn and 1/6 turn is 0.1667).

$$F = \frac{C\alpha P_i AE}{L}$$

Theoretically, from the equation, as L approaches 0, F should approach infinity; and as L approaches infinity, F should approach 0, following a power pattern with L^{-1}. Naturally, this behavior is critical for SLTS baseplate connections, which are generally ¼ to 3 in. thick. At these typical thicknesses, the connections are highly sensitive to turn angle and connection stiffness. Additionally, turns in the field can only be accurate to about 1/12 of a turn, which even then is difficult to accurately achieve for smaller diameter rods.

The equation can be rearranged to the following, which is strain based for turn-angle approximation and used to derive the values in Table 3.7 that follows.

$$\alpha = \frac{\varepsilon L}{P_i C}$$

Table 3.7. Approximate turns required for anchor rod grades (not recommended for use)

L/D	Turn required for *0.6 Fy after 0.1 Fy Snug Tight		
	Gr. 36	Gr. 55	Gr. 105
≤1	**	**	1/12
1 to ≤ 2.5	**	1/12	1/6
2.5 to ≤ 5	1/12	1/6	1/4
5 to ≤ 8	1/6	1/4	1/3
8 to ≤ 11	1/4	1/3	5/12
11 ≤	Determined by Calculation		

L = grip length and D = rod diameter
*Fy is the yield strength of F1554 anchor rods
**Displacement-controlled pre-tensioning not recommended; 400% error possible

Table 3.7 is similar to that from the Research Council on Structural Connections (RCSC 2015) and the Eurocode (CEN 2018), based on grip length (L), rod diameter (D), and anchor rod grade. However, what is shown in Table 3.7 is not recommended for use, since the error for the turn values is +100% and -50%.

The major limitations with SLTS anchor rods are that they are not tightened past yield, like structural steel bolts, and that there is a wide variation in structure base designs for SLTS structures. Inherently, turn-based pre-tensioning is a displacement-based method, which, with small grip lengths, requires a high degree of accuracy. In addition, snug-tight pre-tensions cannot be controlled by turns due to turn non-linearity before the snug-tight condition.

Since snug-tight is the initial condition for turn-based pre-tensioning and the rod is desired to stay in the elastic region, any error in the initial snug-tight condition is transferred to the turn-of-nut. Since the subsequent turn-of-nut procedure requires a calibrated torque wrench for the snug-tight and verification torque steps, it tends to be somewhat redundant for the desired elastic connections.

The high degree of accuracy in structural steel connections, as covered in various literature (Kulak 2002, RCSC 2015), is from the yielding of the bolt as outlined in Figure 3.19.

Theoretical Error Comparison Between Structural Steel Bolting and F1554 Anchor Rod Pretensioning Procedures
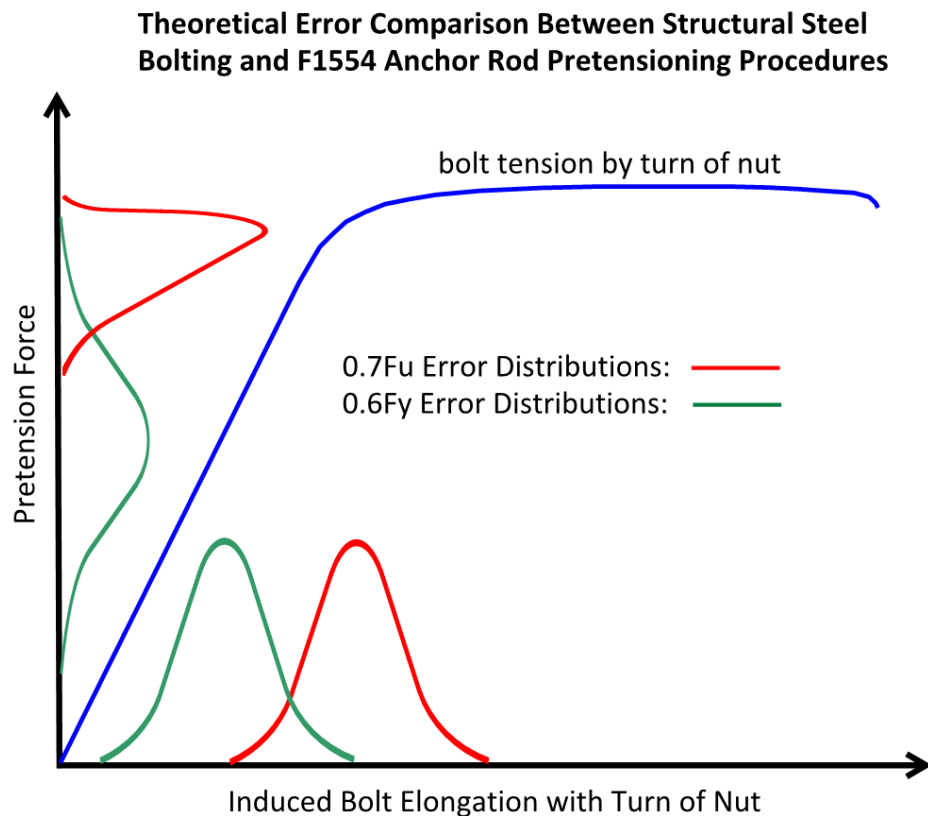
Figure 3.19. Final pre-tension error differences between structural steel bolts and anchor rods

The elongation procedure from turn-of-nut works well for structural steel because the bolts are displaced into the plastic region, where the tension-displacement curve flattens, as shown in Figure 3.19. The bolts being in the plastic region results in minimal final pre-tension error, because pre-tension changes minimally with increased turn. In addition, yielding of structural bolts does not significantly lower the connection pre-tension, which suggests that concerns about yielding anchor rods for loosening may be dubious. The importance of yielding structural steel connections can also be observed

in the allowable error in the RCSC procedures, which is +1/6 and -1/3 turn. This error range could represent the entire AASHTO pre-tensioning specification.

To further illustrate the current limitations of the AASHTO turn standard, two predicted pre-tensions for AASHTO base designs can be investigated, with both bases chosen from AASHTO 2015 Table C11.9.3.1-1. One base is stiffened with longitudinal attachments and a solid 2 in. thick baseplate, while the other base has 18 in. stool type stiffeners.

The following assumptions are considered: anchor rods are 1.5 in. diameter F1554 grade 55, the connection stiffnesses are approximately the same (0.2), and a 1/3 turn is used (AASHTO Table C15.6.3-1). The 2 in. baseplate would develop 3,100 $\mu\varepsilon$, 226 kips of pre-tension force (3.0 Fy, likely rupturing the anchor rod), and the 18 in. stool baseplate would develop 344 $\mu\varepsilon$, 25 kips (0.32 Fy) of pre-tension. This near 1,000 % difference makes sense because turn-controlled pre-tensioning is inherently a displacement-controlled method, requiring stiffness to be taken into account, which currently is not in the AASHTO specification. The possible yielding of anchor rods with the current AASHTO specification was also documented by Hoisington and Hamel (2014) in research on HMLT structures in Alaska.

Finally, from the National Cooperative Highway Research Program (NCHRP) Report 469 (Dexter and Ricker 2002), which first proposed the current procedures in AASHTO, torque was disregarded primarily based on structural steel connection research, along with the fact that James et al.'s 1996 study found torque measurements to be unreliable (James et al. 1997). The torque method that was used to assert that torque is unreliable was an un-calibrated 3 ft pipe wrench attached to a laboratory crane attached to a load cell. In addition, all of the research on the tightening properties currently in AASHTO were on flat baseplates and did not consider structures with large grip lengths, like with current stool-stiffened bases.

3.4 CONCLUDING POINTS

- **It is likely fatigue loading has relatively little impact on properly pre-tensioned anchor rods**. These findings match findings by previous researchers. Additionally, because the fatigue forces on the anchor rods is primarily axial, lock washers for the nut connections would not significantly decrease pre-tension loss from fatigue.

- **Anchor rods designed with the AASHTO procedure will likely not be the critical details in fatigue**. SLTS structures are usually governed by the post-to-baseplate connection as observed in testing and by other researchers.

- **For square anchor rod groups with more than four rods, the AASHTO-recommended AISC design practice of using a linear strain distribution to determine design forces is likely not valid**. Assuming a linear strain distribution may result in underestimations of the applied force to the middle anchor rods and underestimations for corner anchor rods. The observed behavior is likely due to non-uniform baseplate stiffness, resulting in a non-linear strain distribution to the anchor rods. MnDOT may want to reevaluate their design process for determining forces for square anchor rod groups.

- **Leveling nuts are likely to be more critical than the top nuts for loosening**. This is because the anchor rods are acting as a structural member and fastener instead of just a fastener like structural steel bolts. The increased forces on the grip lengths must be transferred through the leveling nut to the baseplate. There were also large strain increases in the standoff distances of the corner anchor rods when the leveling nuts were brought to a low level of snug-tight on the laboratory specimen sign post, suggesting that sufficiently tightening the leveling nuts is critical for installations.

- **Relaxation and creep appear to be the major sources of pre-tension loss in SLTS anchor rods, with possible losses up to 50% of the original pre-tension if the anchor rods are not retightened.** Retightened anchor rods appear to exhibit a maximum of 25% total lifespan losses. Ninjh's 2016 research in Europe on relaxation of structural steel bolts came to similar conclusions. Hoisington's and Hamel's 2014 research hypothesized that localized plastic yielding may be a source of pre-tension loss for HMLT anchor rod connections in Alaska. Finally, research suggests that gross yielding of the anchor rods during initial pre-tensioning does not cause significant pre-strain loss (Kulak 2002); therefore, time-dependent losses, like relaxation, may be more likely.

- **Retightening the anchor rods significantly decreases the relaxation losses**. In addition, retightening after about 10 minutes will exhibit the same improved relaxation performance as rods retightened 48 hours after installation. The time between initial and retightening should be at least 10 minutes if possible.

- **For tightening, the current AASHTO nut factor of 0.12 is sufficient and fairly accurate for most anti-seize lubricants**. The laboratory testing verified that the nut factor for a variety of anti-seize and wax lubricants matches the values found by Till and Lefke in 1994, off which the current AASHTO verification torque is based.

- **An installation inspection nut factor of -0.07 could be used to approximately check the pre-tension in a connection**. This factor would capture almost all error from relaxation and lubricant variation during the original installation.

- **Turn-based pre-tensioning is not recommended for connections that are desired to remain in their elastic range.** Accuracy of elastic turn-based pre-tensioning is predicated upon accurate snug-tight values, which can only be determined by torque; this is also noted by Hoisington and Hamel (2014) and Schaeffer (2018). Additionally, the nature of SLTS double nut connections, with large diameter rods and short grip lengths, makes the connections highly sensitive to small variations in turns, which are difficult to control in the field. Creating an elastic, accurate turn specification would also require significant effort, since each connection property and stiffness would need to be directly replicated. A load cell or tension calibrator would have limited use in determining connection stiffness, because they do not accurately represent the true connection stiffness.

CHAPTER 4: **ANALYTICAL MODELING**

4.1 OVERVIEW

The objective of the analytical work for Task 4 of this project was to simulate the anchor rod tightening and loosening process. The results from this work enhanced the understanding of the behavior of the anchor rod when it is subject to preload and cyclic loading. The analytical study was conducted in four phases: modeling of the Skidmore test; modeling of the laboratory tested specimen, modeling of a single rod, and a parametric study.

The modeling work with the Skidmore test provided an opportunity to study the rod-nut behavior during the tightening process. The model calibration work helped to determine the coefficient of friction (COF) for different lubrication methods. It also provided a validated modeling approach for the modeling work in the subsequent steps.

Considering the requirement of the fine mesh at the thread region and the need for highly nonlinear material properties and contact behavior, modeling of the whole laboratory-tested sign-post structure using commercially available finite element (FE) analysis software is impossible. After a preliminary study using the Skidmore test, it was decided to model the laboratory-tested specimen using a coarse mesh first. The results from this step helped to determine the critical rod that experienced the most strain changes when subjected to cyclic loading.

After that, the single-rod model was created and studied utilizing the modeling approach developed in the work on modeling using the Skidmore test. A parametric study was then performed on the single-rod model to study the influence from various parameters.

The modeling details and results from the Skidmore test, laboratory-tested specimen, and single rod are presented in sections 4.2, 4.3, and 4.4. The results from the parametric study are presented in section 4.5. A summary of findings is presented in section 4.6.

4.2 MODELING OF SKIDMORE TEST (SKIDMORE MODEL)

The objective of the Skidmore testing was to study the rod-nut behavior during the tightening process and provide a validated modeling approach for the analytical work in the subsequent steps. The model was created for the Skidmore test specimen completed in Task 2 of the project. During the Skidmore test, three rods with different diameters, 1.0 in., 1.5 in., and 2 in., were tested.

The rod in the laboratory-tested sign-post specimen had a diameter of 2.5 in. The analytical model in this step was created based on the 2 in. diameter Skidmore-tested rod, given this size is closest to the size of the rod on the laboratory-tested sign-post specimen.

4.2.1 FE Model Development

The model was developed with one 2 in. diameter anchor rod, two nuts (one near each end of the rod), a 2 in. thick plate (between the two nuts) that represents the load cell on the Skidmore machine, and two washers between the nuts and the plate. Figure 4.1 shows the geometry of the FEM for the Skidmore test.
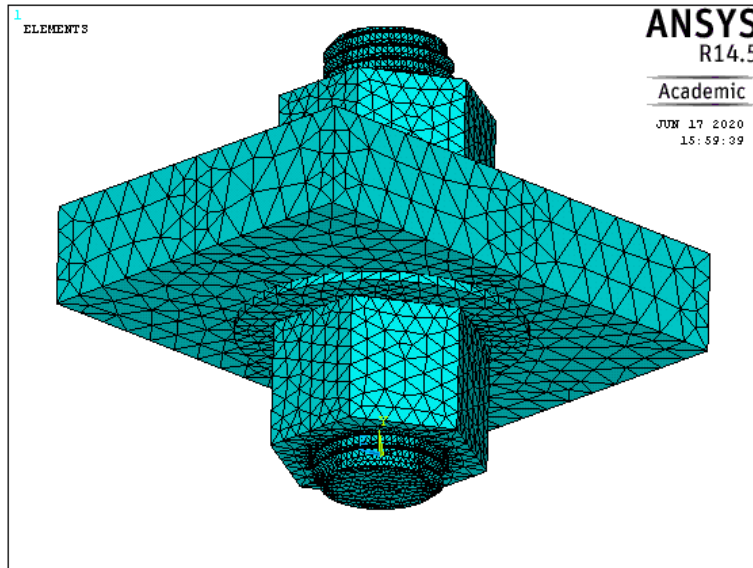

Figure 4.1. FE model for Skidmore-tested specimen developed during preliminary study

On the FEM, the upper level nut was restrained for rotation, and the lower level nut was loaded to create torque. Although during the laboratory tests, two nuts were used at one side of the load cell to provide sufficient restraints in order to lock the rod, the model was created with only one nut on each side, given the rotational restraints could easily be applied to the rod and nuts in the FEM.

Table 4.1 shows the element type, geometric dimensions, and material properties used on the Skidmore model.

Table 4.1. Skidmore model details

Component	Element type	Dimensions	Material characteristic	Material strength
Rod	Solid element	2 in. diameter	Elastic-plastic	$f_y = 55\ ksi, f_u = 75\ ksi$
Washer	Solid element	Standard 2 in.	Elastic-plastic	$f_y = 55\ ksi, f_u = 75\ ksi$
Nut	Solid element	2 in. diameter	Elastic-plastic	$f_y = 150\ ksi, f_u = 175\ ksi$
Plate	Solid element	2 in. thick	Elastic-plastic	$f_y = 55\ ksi, f_u = 75\ ksi$
Nut-washer interface	Contact element		Compression only	
Washer-plate interface	Contact element		Compression only	
Nut-rod interface	Contact element		Compression only	

All of the components, including two nuts, one plate, one rod, two washers, and thread details for the rod and nuts, were modeled utilizing three-dimensional (3D) solid elements. The interface at the nut-to-washer, washer-to-plate, plate-to-nut, and thread region were modeled using surface contact elements. These contact elements were defined to carry only compression and no tension.

The contact behavior generally follows the column friction model and a COF was defined and calibrated for the use of different lubrication methods. To obtain a deep understanding on the structural behavior (stress distribution) during tightening, a very fine mesh was used to simulate the thread for ultimate potential incorporation into a larger model. The preload was applied on the model by applying a torque on one of the nuts and restraining the rotation on the other nut.

The yield and ultimate strength of each component was determined based on the Skidmore-tested specimen (2 in.) as detailed. For example, the rod was defined with a yield strength of 55 ksi and ultimate strength of 75 ksi. The nuts were designed with a yield strength of 150 ksi and ultimate strength of 175 ksi. Given the local stress concentrations occurring on the threads may result in local stresses beyond the yield strength, and this stress concentration could cause permanent local damage and eventually affect the tightening/loosening behavior of the structure, the material properties were defined to be able to simulate this elastic-plastic behavior. Figure 4.2 shows the elastic-plastic stress-strain behavior for the two material types used in the FEM.
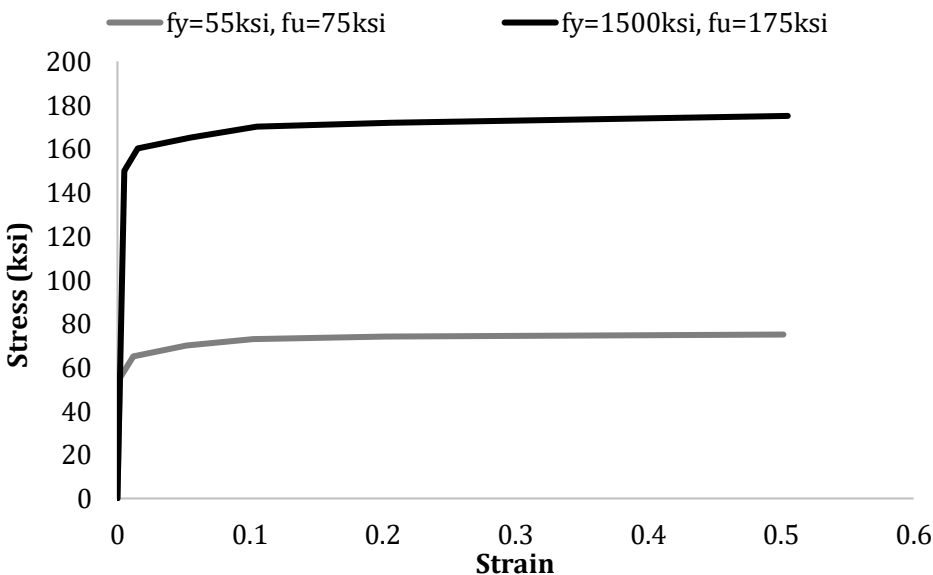

Figure 4.2. Material properties used

These stress-strain curves were reconstructed based on the yield and ultimate strength, and Young's modulus.

4.2.2 FE Model Calibration for COF

In this section, the model was calibrated to determine the COF for the various lubrication methods. To calibrate the model, the tension force generated in the rod was obtained by outputting the reaction

force between the nut and the plate and then used to compare with the clamping force measured during the test.

During the laboratory test, four lubrication methods were studied, and the clamping force vs. torque relation was captured. During the calibration of the FEM, the model was calibrated with the COF increment of 0.005 to 0.01 to look for the best COF that could represent the friction on the tested specimen. The torque and clamping force data were output from the models with a COF of 0.05, 0.07, 0.1, and 0.2, respectively. The results are shown in Figure 4.3.
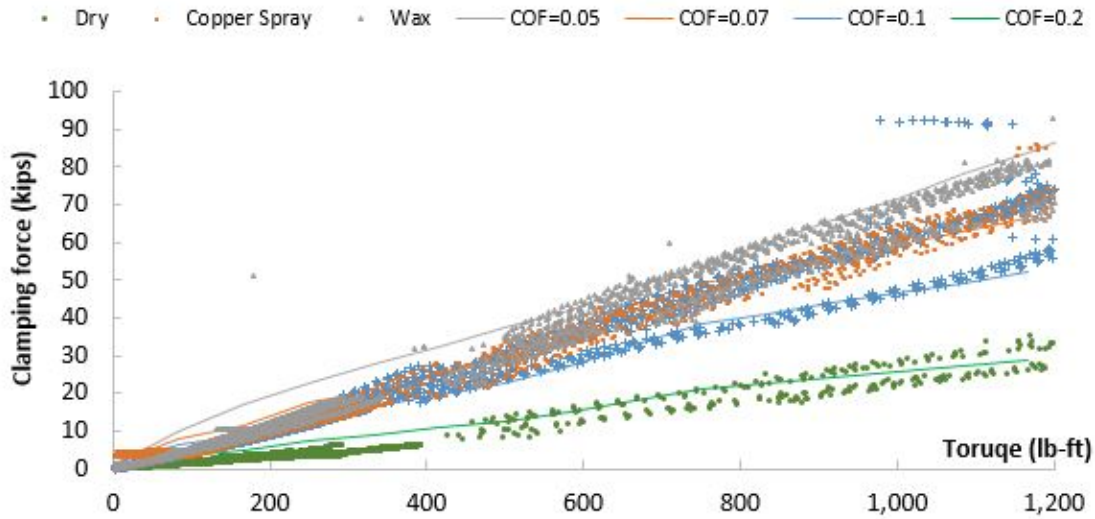
Figure 4.3. Model calibration for the friction coefficient

The results indicated that the data obtained from the dry condition, as shown in green, had the lowest slope between the torque and clamping force and could be fitted with the solid green line, which is output from the model with a COF of 0.2. Similarly, the data from the conditions of Never-Seez, copper spray, and wax could be fitted with the data output from the model with 0.1, 0.07, and 0.05, respectively.

Figure 4.4 shows the relationship between K and COF.
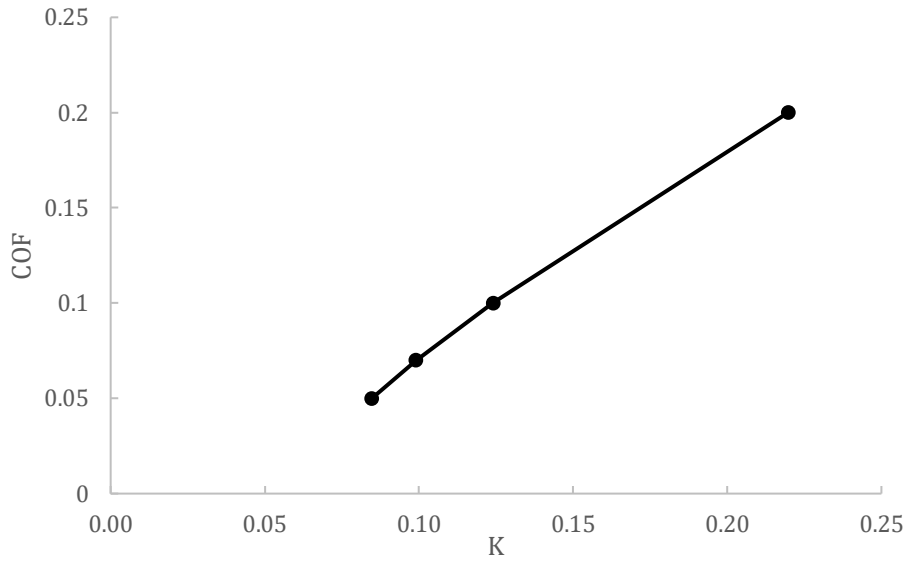
Figure 4.4. Relation between K and COF

The K is the torque-friction coefficient calculated based on the laboratory tests and the COF is the friction coefficient used on the FE model.

Although a small difference exists between the K and COF, the model still illustrates the relation between the clamping force and torque appropriately.

Figure 4.5 and Figure 4.6 show the von Mises stress distribution on the rod and nut, respectively.

Figure 4.5. Vertical stress distribution in the rod (Skidmore)

Figure 4.6. Von-mises distribution in the nut (Skidmore)

Figure 4.5 and Figure 4.6 show the stress when the torque is 1,200 lb-ft. The results indicated that the stress in the middle of the rod is about 37 ksi, and mainly in the vertical direction. Higher stresses do

occur near the roots of the thread. The results also indicated that high stress concentrations occur at the thread region of the rod and nuts.

4.3 CRITICAL ROD ON THE LABORATORY-TESTED SIGN-POST SPECIMEN
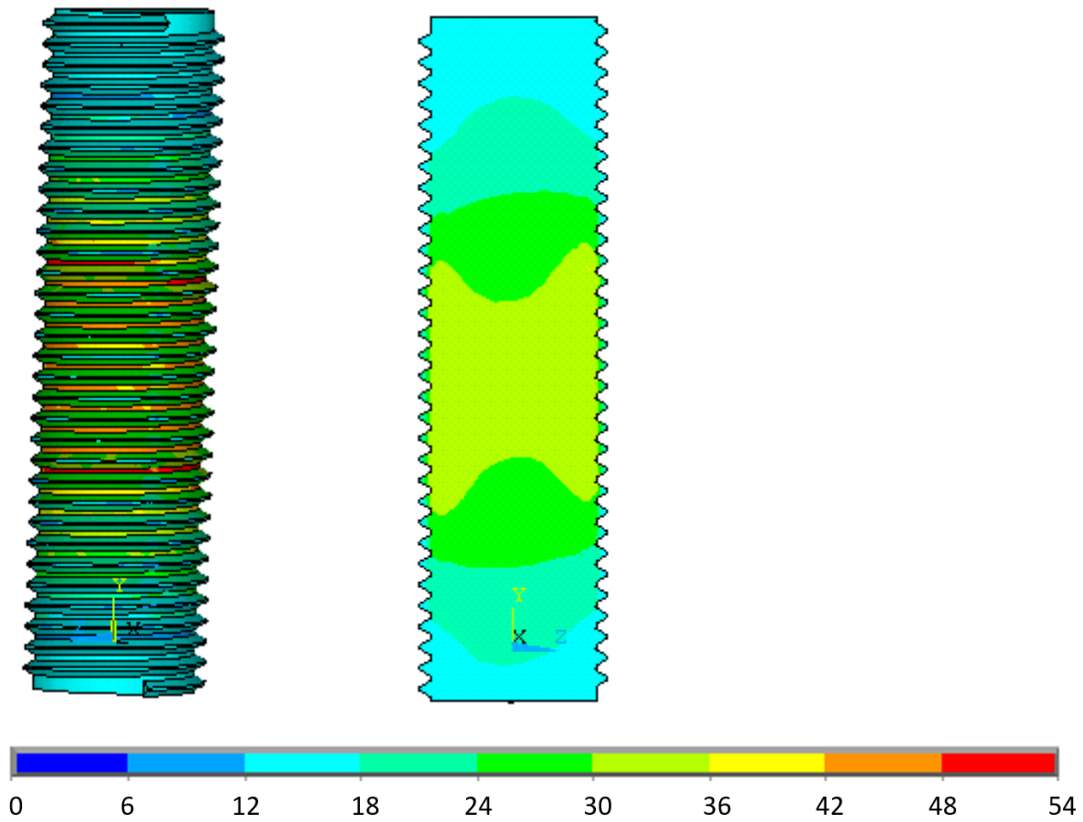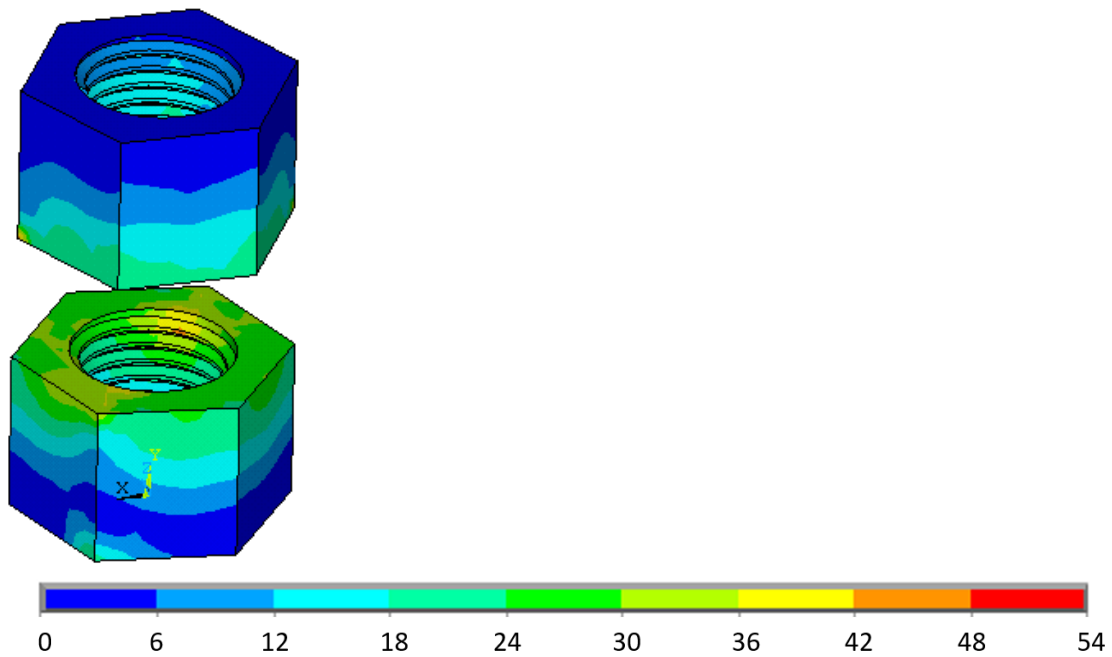
The objectives of this step were to find the critical anchor rod on the laboratory-tested specimen and determine the load protocol from the post acting on that rod. The load protocol that was determined would then be used in the next step. To achieve the objective, two approaches were utilized to perform the analytical analysis, as follows:

Approach I: Simple statics hand calculation. The hand calculation was performed first to estimate the load acting on each rod as produced by cyclic loading. This method was consistent with current MnDOT design procedures.

Approach II: FE model. Instead of generating a finite model with threads, the model in this step was used mainly to find and simulate the global behavior of the laboratory-tested sign-post specimen. Each rod was simply modeled with a few beam elements, and the load acting at the end of the beam element was output as the load acting on the rod.

To compare the results from hand calculations with those from the FEM, a 7 kips vertical load was assumed to be placed at the end of the post. Figure 4.7 (top) shows the load protocol and Figure 4.7 (bottom) shows the location and labeling for each rod.
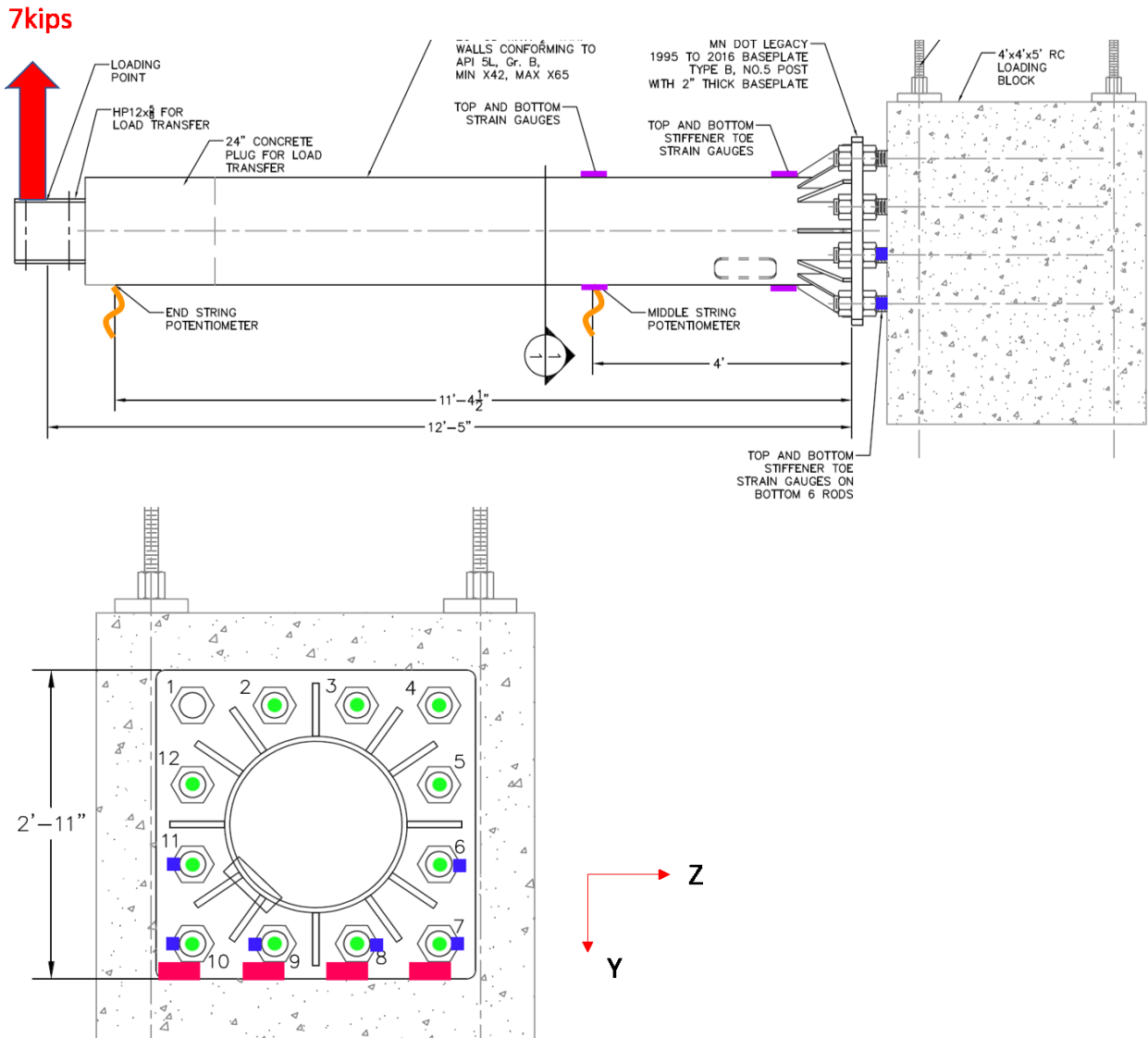
Figure 4.7. Static load protocol: elevation view (top) and front view (bottom)

4.3.1 Hand Calculation

The hand calculation was performed with four steps: (1) calculate the shear force acting on each rod,(2) calculate the moment generated by the external vertical load on the sign post, (3) calculate the moment of inertia on the group of rods, and (4) determine the axial force carried by each rod. The following equations were used to accomplish the hand calculation.

$$F_y = \frac{F}{n}$$

$$I = \sum A\,d^2$$

$$F_x = \frac{My}{I} \times A$$

Given the laboratory specimen was symmetrical, only the forces in rod 6, rod 7, and rod 8 were calculated and used as output for a comparison that follows.

4.3.2 FE Model Development

The model developed in this step consisted of the post, post toe stiffeners, baseplate, and rods. Figure 4.8 shows the FEM, and Table 4.2 shows the modeling details.

Figure 4.8. FE model for laboratory-tested specimen

Table 4.2. Sign-post model details

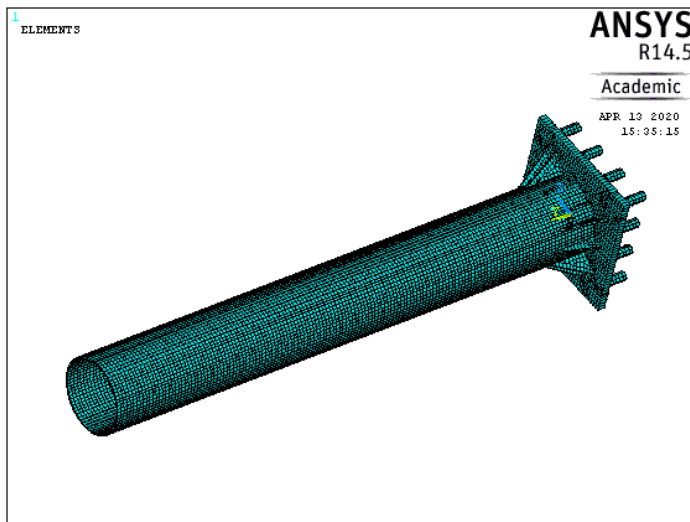| Component	Element type	Dimensions	Material character
Post	Shell element	2 ft diameter	Elastic
Post toe stiffeners	Shell element		Elastic
Base plate	Shell element	2 in. thick	Elastic
Rod	Beam element		Elastic

The post, post toe stiffeners, and base plate were modeled using 3D shell elements, and the rods were modeled using a beam element. The aspect ratio for all the elements on the model is less than 3. When the model is subject to the external load, the post, post toe stiffeners and base plate is generally subject to bending and shear. The 3D shell element, which accounts for bending, in-plane forces, and out-of-plane shear, were used in the model. The model was developed assuming all of the materials were in the elastic range and that no material nonlinearity occurs when the load increases from 0 to 7 kips. Hence, the material properties for all of the components were defined as elastic and assigned with a Young's modulus of 29,000 ksi. The project part of the anchor rods is modeled as beam elements in this analysis. The beam elements for the rod were connected to the shell elements for the base plate by sharing the same nodes. The nodes on both type of elements have six degrees of freedom and are capable to transfer the forces and moments in three Cartesian coordinates. Since all of the rods were embedded into the concrete block on the laboratory-tested specimen, a fixed condition was assumed in the FEM at the end of each rod.

4.3.3 FE Model Validation

To validate the sign-post model, the strain on the post and end displacement results were output and compared with the data captured during the laboratory test. Figure 4.9 and Figure 4.10 validate the model against the strain and displacement data.
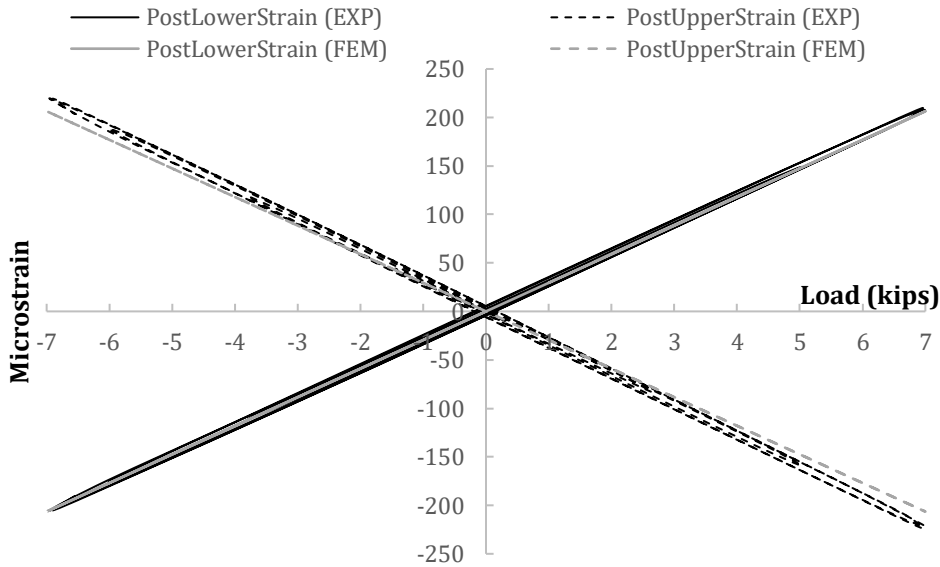
Figure 4.9. Model validation against the strain on post
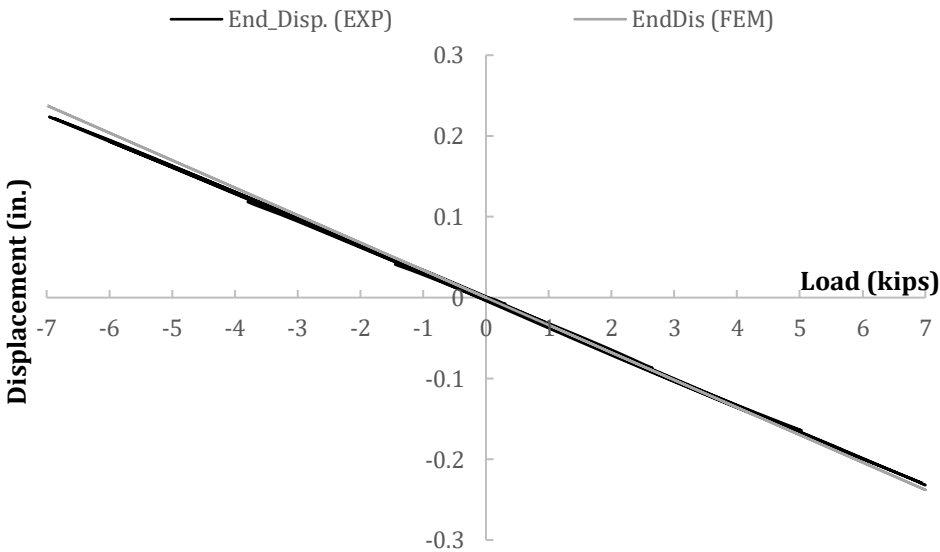
Figure 4.10. Model validation against post end displacement

Figure 4.9 indicates that, when the load increased from 0 to 7 kips upward, a positive moment was induced and the PostUpperStrain is negative and PostLowerStrain is positive. When the load reversed from 0 to 7 kips downward, the structural response reversed. Although Figure 4.9 and Figure 4.10 show a small difference between the FEM and field test results, it was decided that this difference is acceptable.

4.3.4 Determination of Critical Rod

The load carried by rod 6, 7, and 8 calculated by both hand calculation and the FEM are presented in Table 4.3.

Table 4.3. Results from hand calculation and FE model

Units	Rod 6					Rod 7					Rod 8				
	Fx (kips)	*Fy* (kips)	*Fz* (kips)	*My* (kips-in)	*Mz* (kips-in)	*Fx* (kips)	*Fy* (kips)	*Fz* (kips)	*My* (kips-in)	*Mz* (kips-in)	*Fx* (kips)	*Fy* (kips)	*Fz* (kips)	*My* (kips-in)	*Mz* (kips-in)
FEM	6.7	1.1	1.0	-2.7	1.91	1.7	-0.5	0.89	-2.11	-2.3	15.96	-2.31	0.75	-1.86	-7.18
Hand Calc.	3.5	0.58				11.2	-0.58				11.2	-0.58			

Unit designations shown in Figure 4.7 (bottom)

Comparing the results from the hand calculation and the FEM, the researchers found the hand calculation can only predict the shear force in the Y direction, while the FEM was able to predict the shear force in the Z direction and the moment in the Y and Z directions. The hand calculation assumes the shear was equally carried by each rod, but the FEM results indicated a difference exists. On the FEM, the moment exists, while the hand calculation assumes the end moment is carried by axial forces in each rod, and no moment is generated at the end of the rod.

For the axial forces, the hand calculation assumes that rod 7 and rod 8 carried the same amount of axial force (11.2 kips) to resist the external moment, since both of them have the same distance from the natural axis, while the FEM results indicate quite a difference in the axial force between rod 7 (1.7 kips) and rod 8 (15.98 kips).

Given that the results from the FEM show more comprehensive details on the loads experienced by each rod, the loads predicted by the FEM were used in the subsequent steps. Comparing the FE results for rods 6, 7, and 8, there is no doubt that rod 8 experienced a quite large axial force and moment in the Z direction. Hence, rod 8 was determined as the critical rod.

Figure 4.11 and Table 4.4 show the load experienced by rod 8 during one load cycle.
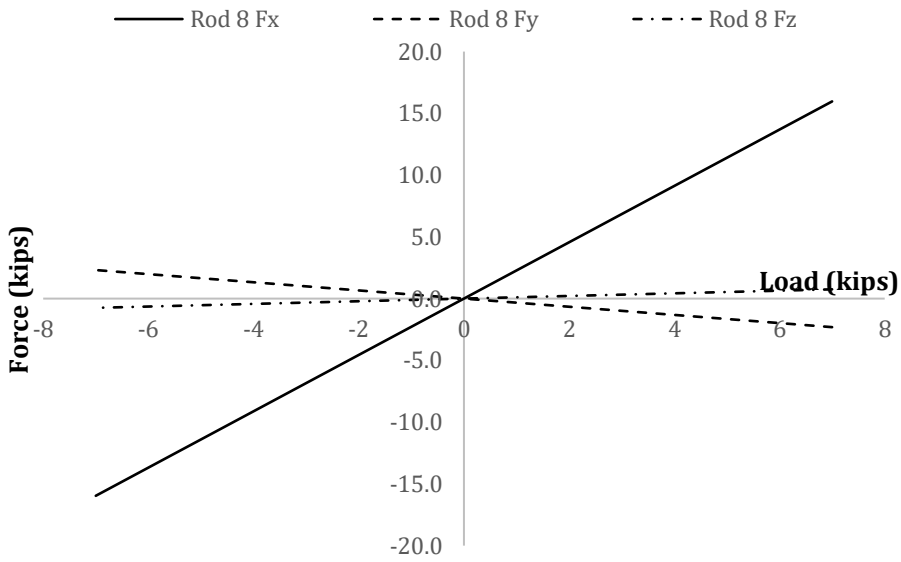
Fx, Fy, and Fz
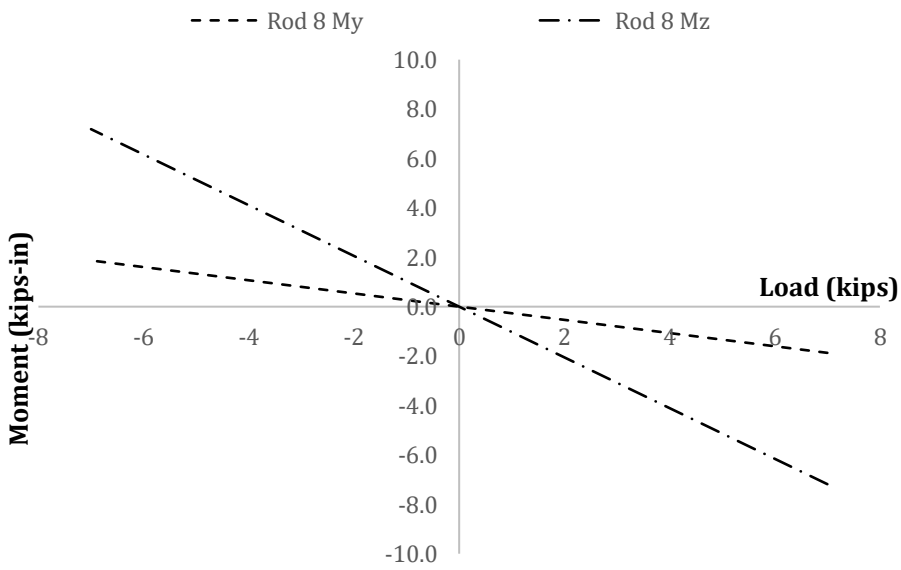
My and Mz

Figure 4.11. Load transferred to rod 8: Fx, Fy, and Fz (top) and My and Mz (bottom)

Table 4.4. Forces and moments on rod 8

Loading (kips)	Rod 8				
	Fx (kips)	Fy (kips)	Fz (kips)	My (kips-in)	Mz (kips-in)
1	2.3	-0.3	0.1	-0.3	-1.0
2	4.6	-0.7	0.2	-0.5	-2.1
3	6.8	-1.0	0.3	-0.8	-3.1
4	9.1	-1.3	0.4	-1.1	-4.1
5	11.4	-1.7	0.5	-1.3	-5.1
6	13.7	-2.0	0.6	-1.6	-6.2
7	16.0	-2.3	0.7	-1.9	-7.2
6	13.7	-2.0	0.6	-1.6	-6.2
5	11.4	-1.7	0.5	-1.3	-5.1
4	9.1	-1.3	0.4	-1.1	-4.1
3	6.8	-1.0	0.3	-0.8	-3.1
2	4.6	-0.7	0.2	-0.5	-2.1
1	2.3	-0.3	0.1	-0.3	-1.0
0	0.0	0.0	0.0	0.0	0.0
-1	-2.3	0.3	-0.1	0.3	1.0
-2	-4.6	0.7	-0.2	0.5	2.1
-3	-6.8	1.0	-0.3	0.8	3.1
-4	-9.1	1.3	-0.4	1.1	4.1
-5	-11.4	1.7	-0.5	1.3	5.1
-6	-13.7	2.0	-0.6	1.6	6.2
-7	-16.0	2.3	-0.7	1.9	7.2
-6	-13.7	2.0	-0.6	1.6	6.2
-5	-11.4	1.7	-0.5	1.3	5.1
-4	-9.1	1.3	-0.4	1.1	4.1
-3	-6.8	1.0	-0.3	0.8	3.1
-2	-4.6	0.7	-0.2	0.5	2.1
-1	-2.3	0.3	-0.1	0.3	1.0
0	0.0	0.0	0.0	0.0	0.0

4.4 MODELING OF SINGLE ROD ON THE LABORATORY-TESTED SPECIMEN

The objective of this step was to study the anchor rod behavior on the laboratory-tested sign-post specimen when subjected to the cyclic load protocol. The single-rod model was developed based on the geometry of the rod (2.5 in.) on the laboratory-tested sign-post specimen. The model was first loaded

with the preload and loaded with the load protocol previously determined to simulate the anchor rod behavior under cyclic loading. The model was then validated using the test data collected during the application of the preload and cyclic load data.

4.4.1 FE Model Development

The model consists of one rod, two nuts, two washers, and one plate. Figure 4.12 shows the single-rod FEM.
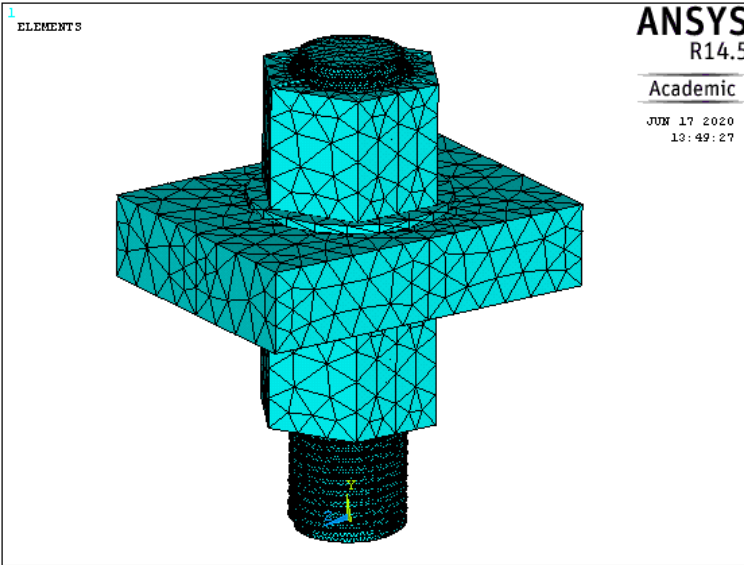

Figure 4.12. Single-rod FE model

The previous Table 4.1 lists the details for each component of the model. The elastic-plastic stress strain curve utilized was shown previously in Figure 4.2. The single-rod model was developed utilizing the modeling approach validated in section 4.2. The differences on the size of the rod, nuts, and washers were to accommodate a larger diameter rod of 2.5 in. During the test, each rod was lubricated using the MnDOT specification method. According to the results from section 4.2.2, a COF of 0.1 was assigned to the contact elements between the rod and nuts. The bottom of the rod, modeled right to the top of concrete, was fixed since the concrete encasement on the laboratory-tested specimen provides rigid restraint to the rod.

4.4.2 FE Model Validation by Preload

In this section, the model was validated against the strain data collected from the laboratory test. The strain collected from the strain gauge embedded in the rod at the baseplate level was used to accomplish the validation (see the previous Figure 4.7 for the gauge location). During the laboratory test, rod 8 was tightened to a torque of 3,300 lb-ft, which resulted in an axial strain of 770 microstrain. Figure 4.13 compares the strain collected from testing and output from the FEM.
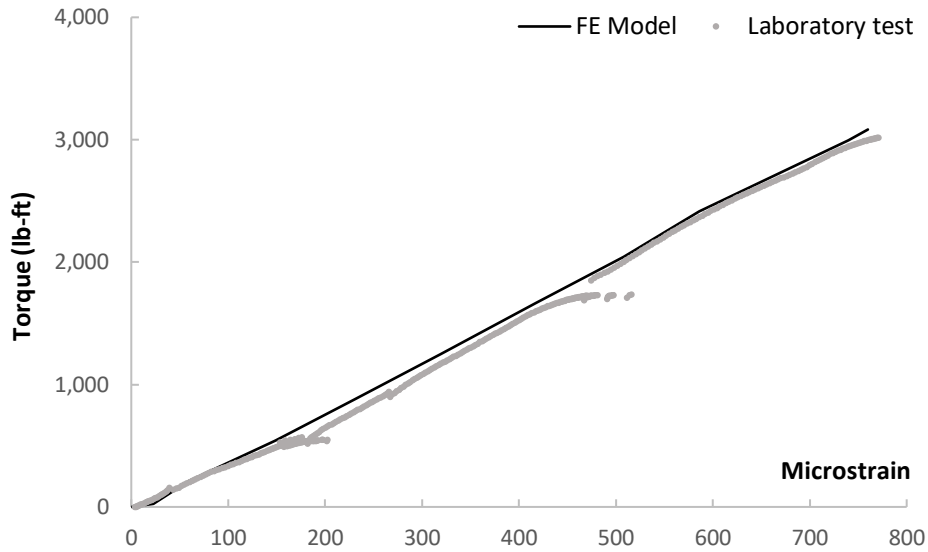
Figure 4.13. Model validation by rod strain at plate level (preload)

Good agreement existed between the analytical and experimental results.

Figure 4.14 shows the von Mises stress distribution in the rod and nuts.
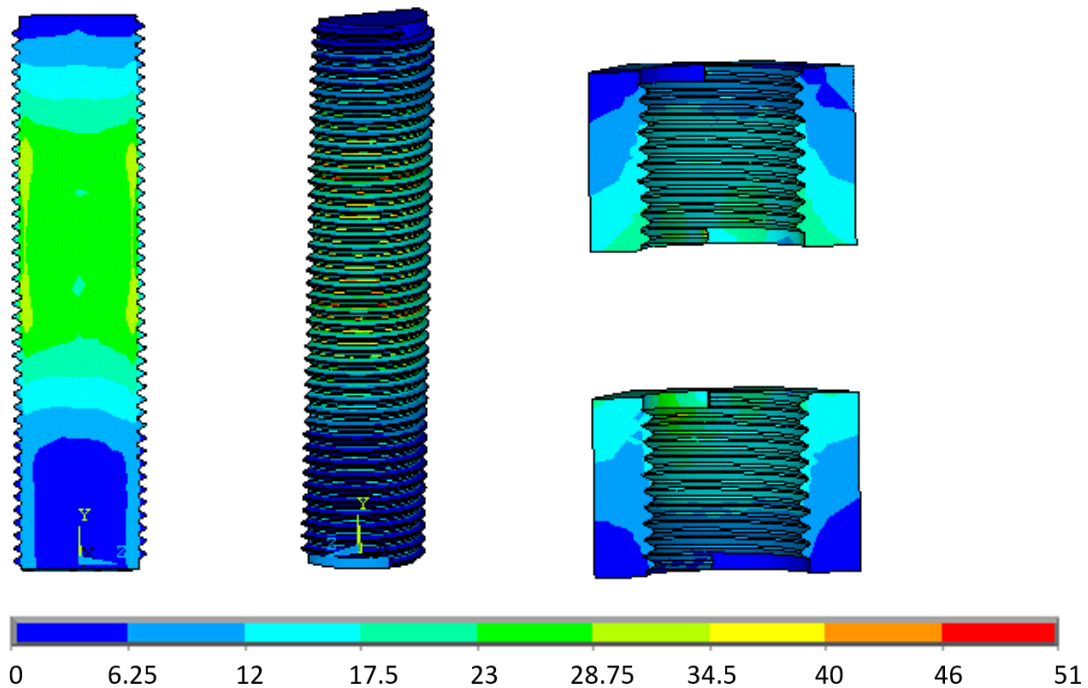
Figure 4.14. Von-mises distribution in the nut (preload)

The results indicated the stress concentration occurs near the thread root. This shows good agreement with the results from the work conducted by Fukuoka and Takaki (2003) that found stress concentration occurs at the thread root when subject to the tightening force. However, the stress magnitude at the

stress concentration was about 30 ksi, which is lower than the rod yield strength of 55 ksi. The stress in the middle of the rod was about 23 to 28.75 ksi. A detailed observation indicated that this stress is generally in the axial direction.

Stress concentration also existed on the thread between the rod and nuts. This stress concentration was about 51 ksi and very close to the yield strength of 55 ksi.

### 4.4.3 FE Model Validation by Cyclic Load

The model was then validated against the strain values collected during cyclic loading. During the test, nearly 100 cycles of a 7.5 kips load was applied at the end of the post. For a better comparison, the load acting on the rod calculated in section 4.3, based on a post end load of 7 kips, was amplified by 7.5/7 and applied on the FEM in sections 4.4 and 4.5. In this step, the resulting axial and shear forces and moments were applied on the plate of the FEM.

Figure 4.15 shows the clamping force (P) reduction with respect to the increase in load cycles.
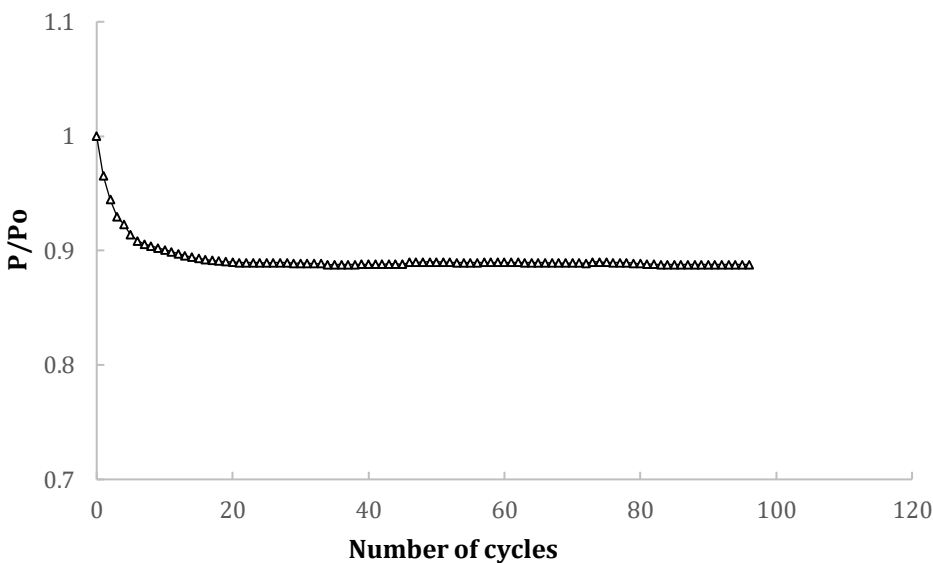
Figure 4.15. Clamping force reduction with respect to load cycles

The figure clearly shows that the clamping force experienced a significant reduction during the first few cycles, and this reduction bottoms out to minimum after application of about 20 cycles. During the experiments, this phenomenon was not measured since the application of these 100 cycles at 7.5 kips loading was not the first cyclic loading applied after tightening. However, these results are consistent with the work conducted by Jiang et al. (2003), Zhang et al. (2007), and Yokoyama et al. (2012).

Because of the preload reduction on the FEM in the first 20 cycles, the strain data used in the validation were output from the load cycles after the first 20. The strain from both the embedded gauge and the standoff gauge were utilized for the validation. Figure 4.16 shows the model validation by rod strain at the plate level.
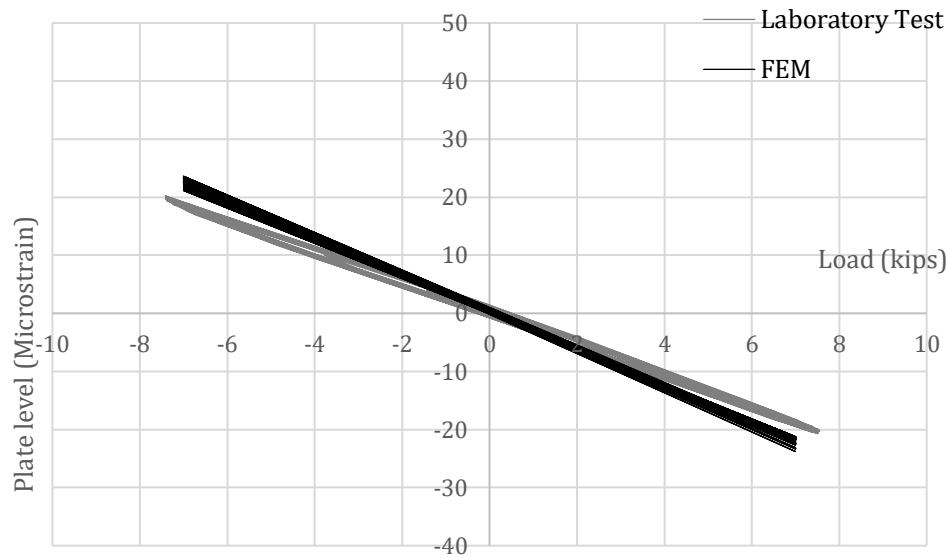
Figure 4.16. Model validation by rod strain at plate level (cyclic load)

Figure 4.17 shows the model validation by the strain from the standoff gauge.
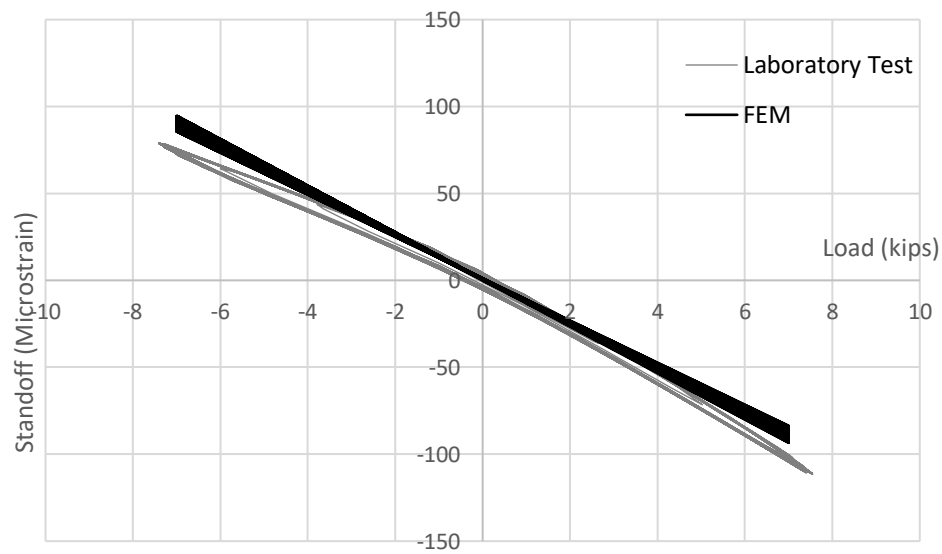
Figure 4.17. Model validation by strain from standoff strain gauge (cyclic load)

Both comparisons indicated that the analytical and experimental results show good agreement.

Figure 4.18 (left and right) show the stress distribution in the rod and nut, respectively, when the load was maximum.
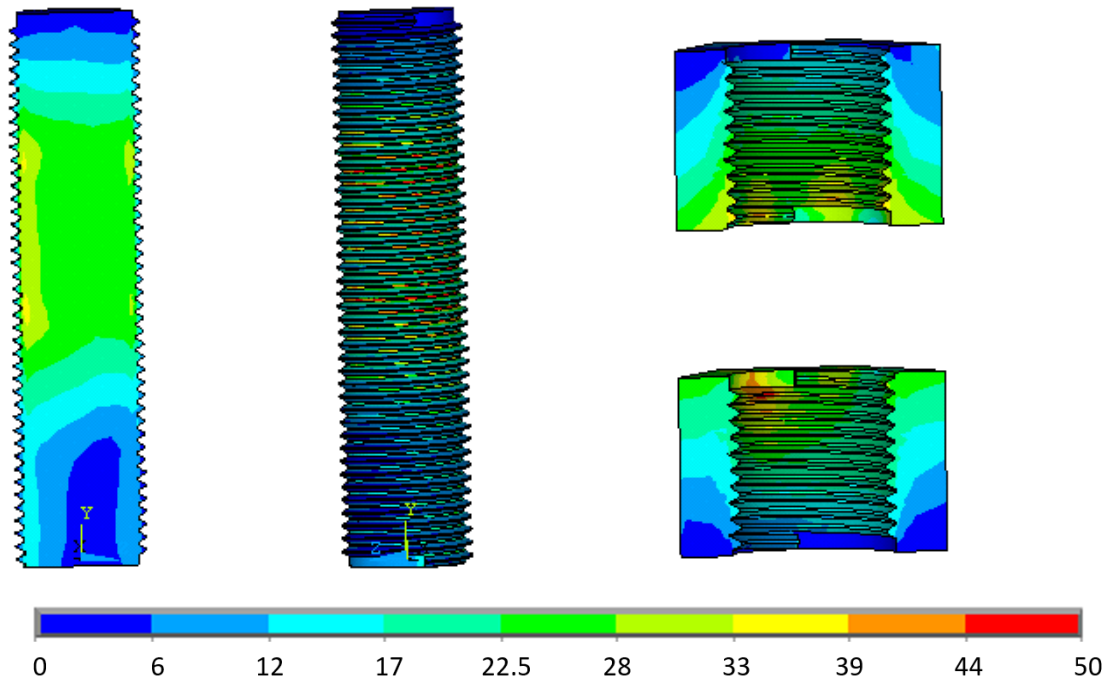
Figure 4.18. Von-mises distribution in the rod and nut (cyclic load)

The results indicated that, because of the bending moment induced by the post end loading, a high tensile stress in the vertical direction (about 33 ksi) occurs at one side of the rod near the thread roots.

4.5 PARAMETRIC STUDY

The objective of the parametric study was to study the parameters that may influence the rod tightening and loosening process. The parametric study was performed on the single-rod model created as described in section 4.4. The load protocol derived in section 4.3 was used to study the parameters, including the tightening preload level, variation of the preload level, washer size, grip length, etc. In addition, the load derived from the field data was also studied.

4.5.1 FE Model Development

Table 4.5 shows the details for each of the models used in this section.

Table 4.5. Parameters studied during parametric study

Model	Model No.	Tightening	Variation	Total	Washer Size (in.)	Grip Length	Cycles
Single-rod model (2.5 in. diameter)	1	60°	-22.5°	37.5°	2-1/2	2.375	100
	2	60°	0°	60°	2-1/2	2.375	100
	3	60°	+22.5°	82.5°	2-1/2	2.375	100
	4	90°	-30°	60°	2-1/2	2.375	100
	5	90°	0°	90°	2-1/2	2.375	100
	6	90°	+30°	120°	2-1/2	2.375	100
	7	180°	-45°	135°	2-1/2	2.375	100
	8	180°	0°	180°	2-1/2	2.375	100
	9	180°	+45°	225°	2-1/2	2.375	100
	10	100°	0°	100°	2-5/8	2.375	100
	11*	100°	0°	100°	2-1/2	2.375	478
	12	100°	0°	100°	2-1/2	4.375	100

* Cyclic load per field data as further described in the text that follows

Models 1 through 3 were tightened to 60° with a variation of -22.5°, 0°, and 22.5°, respectively. The final tightening rotations on Models 1 through 3 were 37.5°, 60°, and 82.5°, respectively. Using the same calculation method, the total nut rotations on Models 4 through 9 were 60°, 90°, 120°, 135°, 180°, and 225°, respectively. It should be noted that Model 2 and Model 4 had the same nut rotation of 60°, and only one of them was analyzed.

To study the effect of the washer size, Model 10 was analyzed with a larger sized washer (2-5/8 in.), while Models 1 through 9 were analyzed with the standard 2-1/2 in. washer. Models 1 through 10 were analyzed with the load derived in section 4.3 with an amplification factor of 7.5/7.0.

To investigate the model performance subject to field loading, Model 11 was calculated with the load derived from the field data: 832 times at 5.17 kips loading, 104 times at 10.34 kips loading, and millions of lower level loadings occurred. Considering the long computing time of each load cycle, a combination of 416 times of 5.17 kips loading and 52 times of 10.34 kips loading were applied to Model 11 to simulate the field loading in one year, and the lower level loadings were ignored. On Models 10 and 11, the nut was tightened to a rotation of 100° as used on the calibrated model.

The effect of the grip length was also studied on Model 12. The grip length is defined as the distance between the bottom surface of the upper nut and the top surface of the lower nut. It is equal to the sum of the thicknesses of two washers and the base plate. On Model 12, the grip was elongated to 4.37 in. and filled with two 2-1/2 in. washers and one 4 in. thick base plate. Except for the grip length and thickness of the base plate, the other parameters on Model 12 were the same as those for the calibrated model.

4.5.2 Parametric Study Results

Table 4.6 shows the clamping force reduction after the first 20 load cycles.

Table 4.6. Parametric study results

Model No.	Nut rotation	Torque (kips-ft)	Clamping force after preload application (kips)	Clamping force after 20 load cycles (kips)	Loss of clamping force after 20 load cycles (%)
1	37.5°	698	41	35	15
2	60°	1,368	63	55	13
3	82.5°	2,450	84	74	11.7
5	90°	2,817	91	81	11.5
Calibrated	100°	3,243	101	90	11
6	120°	4,331	121	109	10
7	135°	5,025	135	122	9.5
8	180°	7,230	175	162	7.5
9	225°	9,435	219	207	5.5
10	100°	3,235	101	90	11
11	100°	3,243	101	86.3	14.5
12	100°	2,500	85	73	14

All of the models studied during the parametric study showed a similar trend to the calibrated model, indicating that a significant reduction in the clamping force occurred after the application of the first 20 load cycles. Additional reduction tended to be minimal after the 20th load cycle.

Although all of the models showed a clamping force reduction, the researchers found a relationship between the magnitude of preload and the clamping force reduction. Figure 4.19 shows the percentage of the clamping force reduction versus the preload level.
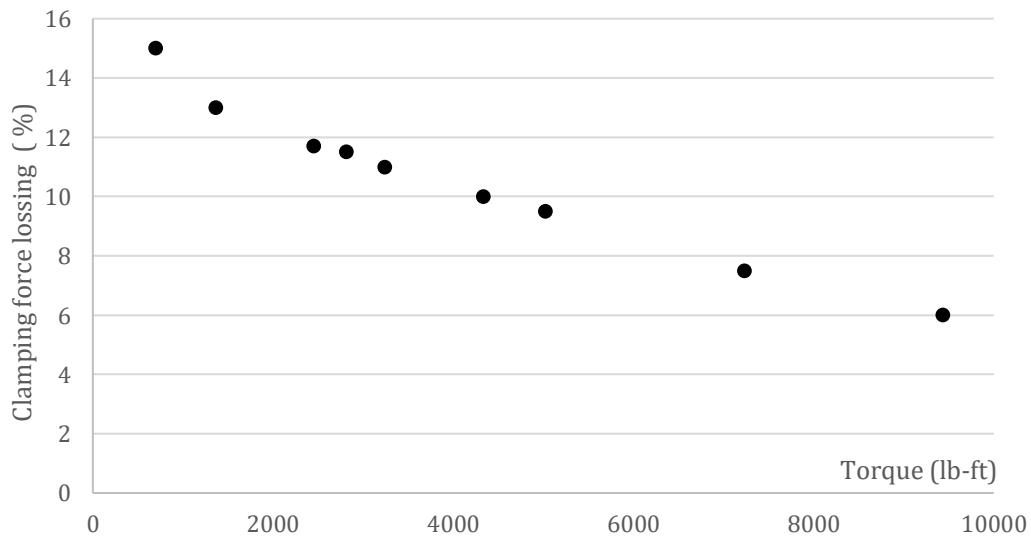
Figure 4.19. Stress loss after during first 20 load cycles (for Model 1 through Model 9 and calibrated model)

The researchers observed that, as the nut was tightened with a higher level of preload, the percentage of preload reduction after first 20 load cycles reduced. This showed an agreement with the work conducted by Jiang et al. (2003) and Zhang et al. (2007). However, it should be noted that, as the preload increased, more stress reduction concentration occurred at the thread region on the nut and

rod, which eventually resulted in a plastic deformation on the thread when the stress level exceeded the steel yield strength.

Comparing the results from Model 10 to that from the calibrated model, the researchers found that the size of the washer had no significant influence on the nut loosening. Model 11, loaded with a higher load level in the first 20 cycles, showed a higher clamping force reduction of 14.5% after the first 20 load cycles.

Comparing results from Model 12 and the calibrated model, it was found that the longer grip length resulted in a reduction on the clamping force. This is because, with a certain elongation induced by the nut rotation, the longer grip length results in lower stain and eventually lower clamping force. These results show an agreement with the results from Christopher's and Fisher's (1964) research.

4.6 SUMMARY AND CONCLUSIONS FROM ANALYTICAL STUDY

In this portion of the project, the anchor rod tightening and loosening process was simulated utilizing the FE method. An FEM was developed for a rod on the laboratory-tested sign-post structure and calibrated against the laboratory test data. The results indicated that stress concentration occurs near the thread root and on the thread after the application of the preload.

The current tightening approach generated a stress concentration in the rod of about 30 ksi, which is 55% of the rod yield strength of 55 ksi. The results also indicated that the clamping force experienced a significant reduction during the first few cycles and that further reduction is minimal after the application of about 20 cycles.

The model was then studied in a parametric study to investigate the effect from different variables including tightening preload level, variation of the preload level, and washer size. The researchers found that, when the nut was tightened with a higher level of preload, the percentage of preload reduction after first 20 load cycles was reduced.

The results indicated that the high preload can reduce the preload reduction due to nut backward rotation during the first few load cycles; however, it may induce plastic deformation on the thread and in the rod, and cyclic load will increase the stress level at these locations. The accumulation of this damage under cyclic loads may induce loss of clamping force after a significant number of load cycles. It appears that the choice of a preload level that ensures enough tightening and avoids the permanent damage on the rod is critical for preventing or reducing the nut loosening effect.

CHAPTER 5: CONTINUED OVERHEAD SIGN MONITORING RESULTS

5.1 OVERVIEW

5.1.1 Monitoring Objectives

In Phase I and the implementation parts of this overall effort, the primary goal of field monitoring was to derive laboratory testing procedures based on in-service loading conditions. Phase I focused on the instrumentation and preliminary data processing, and the implementation work in Phases I and II developed fatigue N-S curves along with a procedure for laboratory testing.

After completion of the laboratory testing, the next phase of monitoring focused on a review of the instrumentation for the post structure along with validation of both the procedures and results from laboratory testing. While the previous implementation report covered long-term temperature response trends, this chapter of this final report focuses on the structural response to wind loading and wind conditions at the site.

5.1.2 Instrumentation Details

The instrumented sign was a cantilevered overhead sign structure at the southbound ramp from Snelling Avenue to TH 36 westbound in Roseville, Minnesota (Figure 5.1).

Figure 5.1. Instrumented sign post (left) and data logger cabinet (right)

All of the figures in this chapter covering instrumentation were also in the previous Implementation of New Guidelines for Tightening Large Anchor Rods of Support Structures for Signs and Luminaires report (Phares et al. 2020) and are presented for completeness.

Installation of data acquisition hardware and associated instrumentation took place in August 2017 during the Phase I study. Instrumentation was designed to approximately replicate previous studies (AASHTO 2015, Hoisington and Hamel 2014, Hosch 2015).

For wind data, an R. M. Young Company Model 05103V wind monitor was fixed near the support of the structure at an elevation of 33 ft above the roadway to replicate the instrumentation used for development of the AASHTO wind fatigue design specifications. Placing the anemometer near the support post and above the sign area minimized the impact of truck gusts in the recording, so the wind distributions and speeds would have greater validity in the wind recordings. All wind directions were measured in azimuths with north as zero and wind speed measured in mph.

Strain measurement used two different types of gauges. On the post, eight 6 mm temperature-compensated foil strain gauges produced by Tokyo Measuring Instruments Laboratory Co., Ltd. were affixed following manufacturer specifications for surface preparation and adhesive choice for the environment. The anchor rods were bored 4½ in. down into the approximate grip length and instrumented with a bolt strain gauge series BTM 6 mm produced by the same company. Both strain gauges have a three-wire configuration in an effort to minimize temperature and wire resistance effects on the strain readings.

The structure being monitored was a cantilevered overhead sign structure with a sign area of 202 ft^2, cantilever length of 33 ft, and height above the roadway of approximately 19 ft 3 in. Figure 5.2 shows a simplified elevation view of the structure with dimensions and a section of the roadway as shown from the decreasing, southbound direction on the roadway.
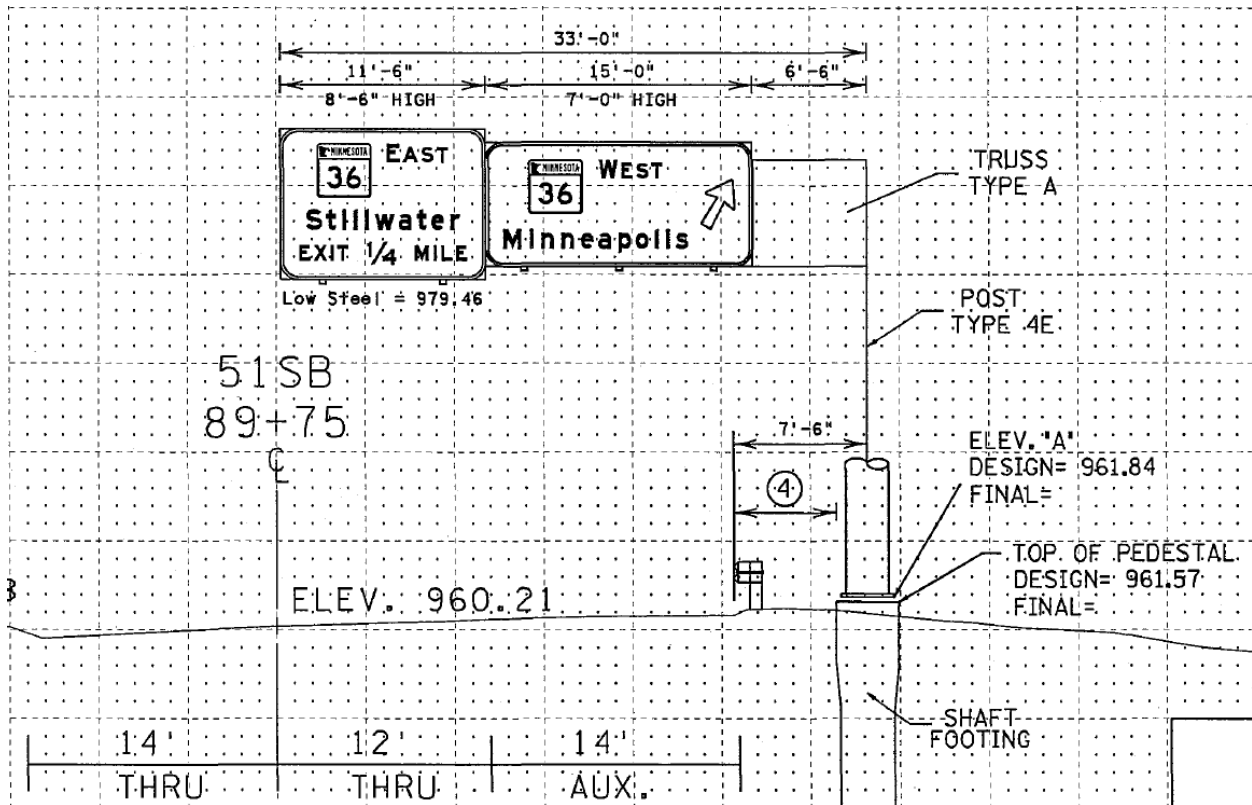
Figure 5.2. Elevation of sign structure from southbound travel

Anchor rods were F1554 Grade 55, 2¼ in. diameter, and the post was a MnDOT Type 4E with a Type A base (MnDOT 2019). For more information on the installation, see the previous Phase I study report (Chen et al. 2018).

Data collection was completed continuously throughout the year with a Campbell Scientific CR9000 data logger (previous Figure 5.1 right) The collection system also consisted of an internet modem/router and a central processing unit (CPU) for data transmittal and storage. The wireless connection enabled data to be continuously collected and transmitted to servers at Iowa State University's Bridge Engineering Center.

A sampling rate of 100 samples per second was used to effectively detect the resonant frequencies of the structure up to about 10 Hz. Data processing was primarily completed with python code in order to efficiently process the large data set collected over the past three years. As of June 2020, 7.3 billion data entries had been collected.

Figure 5.3 shows reference locations for all gauges with an elevation and plan view of the post base.
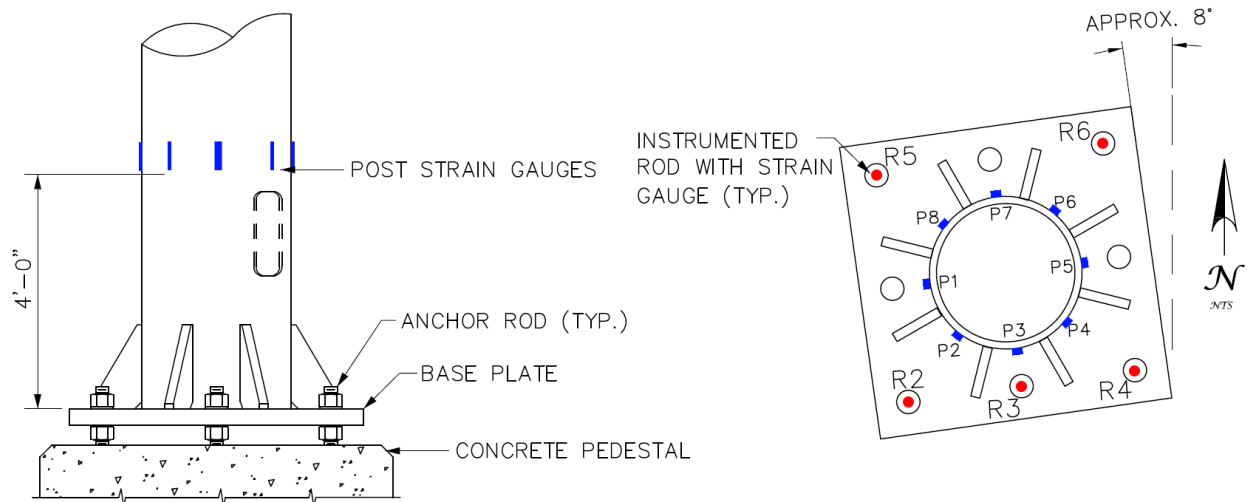
Figure 5.3. Lower post instrumentation elevation view (left) and post base instrumentation plan view (right)

For specific dimensions, see MnDOT Standard Plan 5-297.764 (MnDOT 2015).

5.1.3 Instrumentation Limitations

The instrumentation for the sign structure was originally designed for developing anchor rod fatigue stress ranges to replicate during laboratory testing. As the study progressed, the researchers found that many other aspects regarding the sign-post behavior could be derived from the data had the instrumentation been installed. Given the additional information from the instrumentation was above the original scope of the project, limitations had to be considered during data processing.

Since thermocouples or a method of temperature monitoring was not installed at the site, temperature monitoring limited the scope of the project. For long-term approximations that are broader and averaged daily, recorded temperatures from the Minneapolis-St. Paul International Airport were used in the previous phase reports to approximate temperature-induced strain changes. However, direct strain temperature compensation could not be effectively completed for the site on shorter timeframes due to regional temperature changes.

Acceleration values for the sign post were not measured. For wind- and vehicle-induced vibrations, not having acceleration values limits the dynamic analysis that could be completed on the structure.

Strain gauge placement also limited the force analysis, because the instrumentation design was originally planned to only measure axial and overturning moment forces induced along the post. Any torsional modes of vibration or force may go undetected or may need to be approximated numerically based on the measured axial strains.

Resistance strain gauges were utilized for all of the collected strain data. As originally intended, resistance strain gauges are generally used for short-term measurement. Over longer periods of time though, either vibrating wire or fiber optic gauges are better suited for stability concerns (Dally and Riley 2005). With the resistance strain gauges on site, the gauge factor could change with the temperature,

leading to increased uncertainty for long-term measurements. Additionally, measurements from resistance gauges have a tendency to drift over longer periods of time due to a variety of variables (Tokyo Measuring Instruments Laboratory Co., Ltd. 2020). All compiled data were analyzed over short timeframes that were no greater than one day to avoid the long-term sensitivity impacts on the strain gauges.

The embedded rod strain gauges have increased sensitivity and error compared to the post strain gauges. As discovered during laboratory testing and derivation of anchor rod properties, the clamped distance in the grip length experiences minimal force changes, so small disturbances to the instrumentation may lead to false readings.

Placement of the gauges also has some uncertainty. Gauges in the anchor rods are inserted blind and may not be perfectly parallel with the anchor rod, or not in the intended location.

Finally, snow being plowed into the lower rod gauges during the winter led to decreased stability and the failure of many of the rod gauges. During one inspection, it was found that the wires for one of the failed rod gauges was corroded, possibly due to chloride intrusion from deicing salts.

One additional note: given this is only one structure, data may not completely represent the behavior of all SLTS structures.

5.1.4 Data Collection History

Instrumentation was installed in August 2017 with the partial data from that year reported in the Phase I report (Chen et al. 2018). As of July 2018, only rods 2 and 3 were still transmitting data, likely due to intrusion of water or snow impacts during the winter and spring of 2017–2018. The gauges could not be replaced in the fall and winter due to weather constraints. In September and October of 2018, the data were corrupt due to an issue with the logger.

In mid-April through early May 2019, the data logger failed, leading to missed data for parts of those months. Finally, in July 2019, the broken strain gauges were replaced in the field (Figure 5.4 left and right); however, measurements for the rod 3 strain gauge began to drift after the other gauges were replaced, and the gauge stopped working completely in early August 2019.

Figure 5.4. Drilling out failed strain gauge (left) and replacing strain gauge and injecting epoxy (right)

During the July installation, unstrained gauges in separate ASTM A325 bolts placed under the structure were added on site in an effort to correct measurement drift or temperature compensation. After data collection, it was found that the unstrained bolt gauge measurements did not drift or respond to temperature consistently, which matched laboratory results, so the rod gauge strains could not be effectively normalized.

In late January 2020 through early February 2020, the power supply to the logger shorted out and three weeks of data were lost due to inaccessibility of the site.

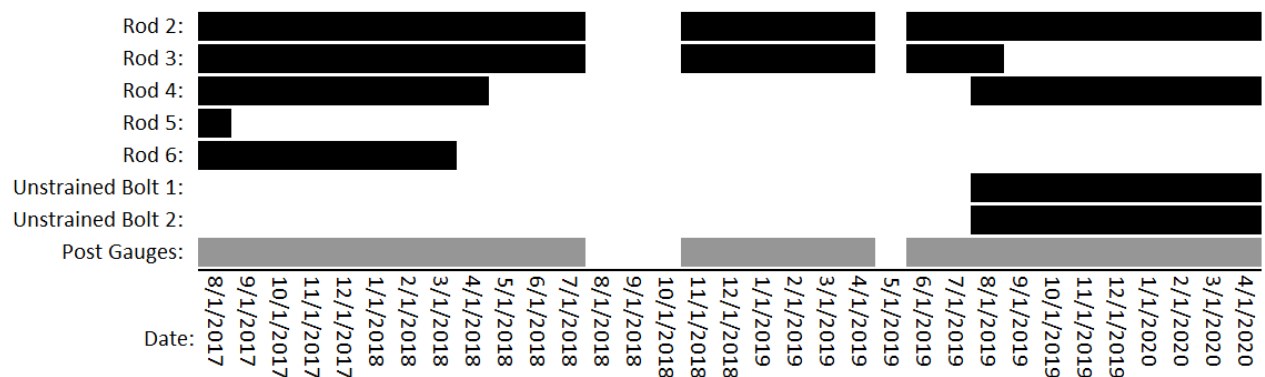Figure 5.5 illustrates the instrumentation and data collection history for the sign-post structure.

Figure 5.5. Instrumentation timeline

Note that, for the post gauges, the timeline excludes gauge 5, which was disconnected from August 2018 to June 2019. All other post gauges were transmitting during this time. This timeline is derived from the average daily values, so some of the rod gauges may have exhibited sensitivity errors on shorter timeframes that were not detectable when the daily average was calculated.

5.2 DATA

Data processing in this phase of the study focused on wind loading and the sign-post dynamic response in an effort to further validate the laboratory test results and procedures. The implementation report contains the rainflow counting and approximate temperature-induced forces. The laboratory testing chapter in that report contains the derivation of the laboratory testing procedure from the field N-S curves.

Wind-induced forces were investigated in three steps, which are covered in this section. First, the daily minimum, maximum, and wind speed/direction distributions were processed for the collected data. Second, the maximum daily strains and wind speed were investigated for a single day. Third, the dynamic properties were investigated over a long-term basis and for a short wind gust duration.

5.2.1 Overall Wind Speed and Direction Probability Density Distributions

Wind speed and direction were both measured at a sampling rate of 100 Hz for approximately continuous data records. Three aspects of wind loading were investigated over the entire recording period: wind speed, wind direction, and maximum daily wind speed. Due to the large number of total sample bins and for comparison to comparable studies, data are presented as probability density distributions. Figure 5.6 shows the probability density distribution of the overall wind speed distribution.
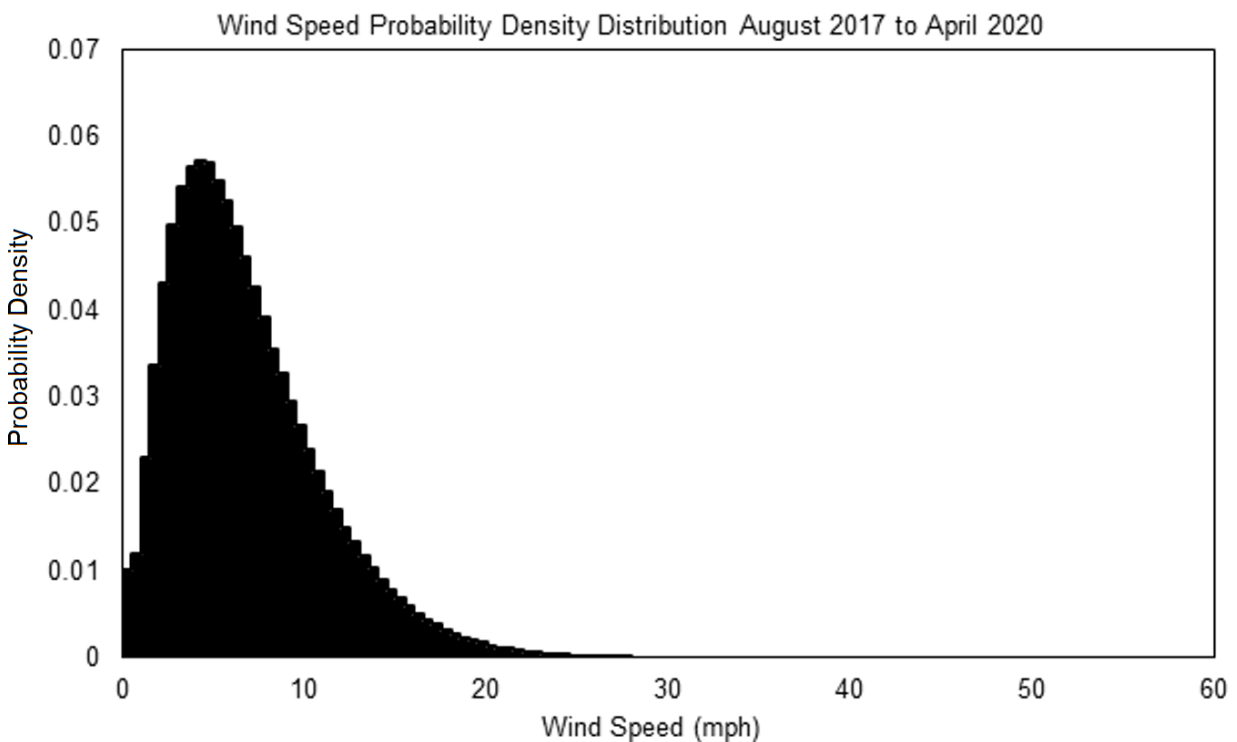

Figure 5.6. Overall wind speed probability density distribution

Wind speed for the monitoring period exhibits a fairly uniform Weibull-distributed pattern, which is expected from the literature (Harris 1996). The peak is in the 4 mph to 4.5 mph bin with a probability

73

density of 5.7%. During the monitoring period, the prevailing wind directions were from the northwest and southeast, which corresponded to azimuths of 310 and 140 degrees, respectively (Figure 5.7).
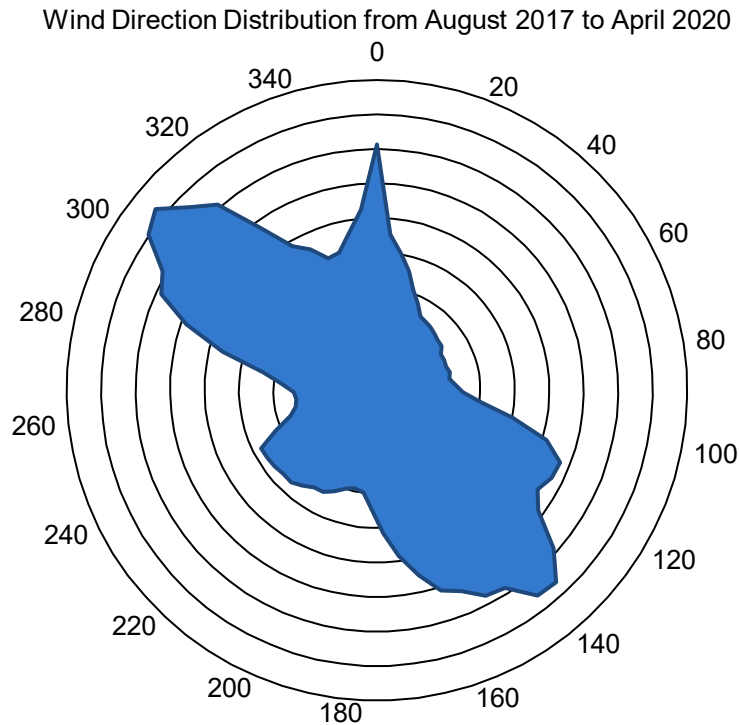

Figure 5.7. Overall wind direction distribution

There was also a secondary, concentrated peak at 0 degrees, or from the north, which was likely due to vehicle gusts. As discussed in the instrumentation subsection previous to this, the wind speed monitor was located above the post, which minimized vehicle gust measurements. Figure 5.8 shows a probability density distribution of the daily maximum wind speeds recorded during the monitoring period.
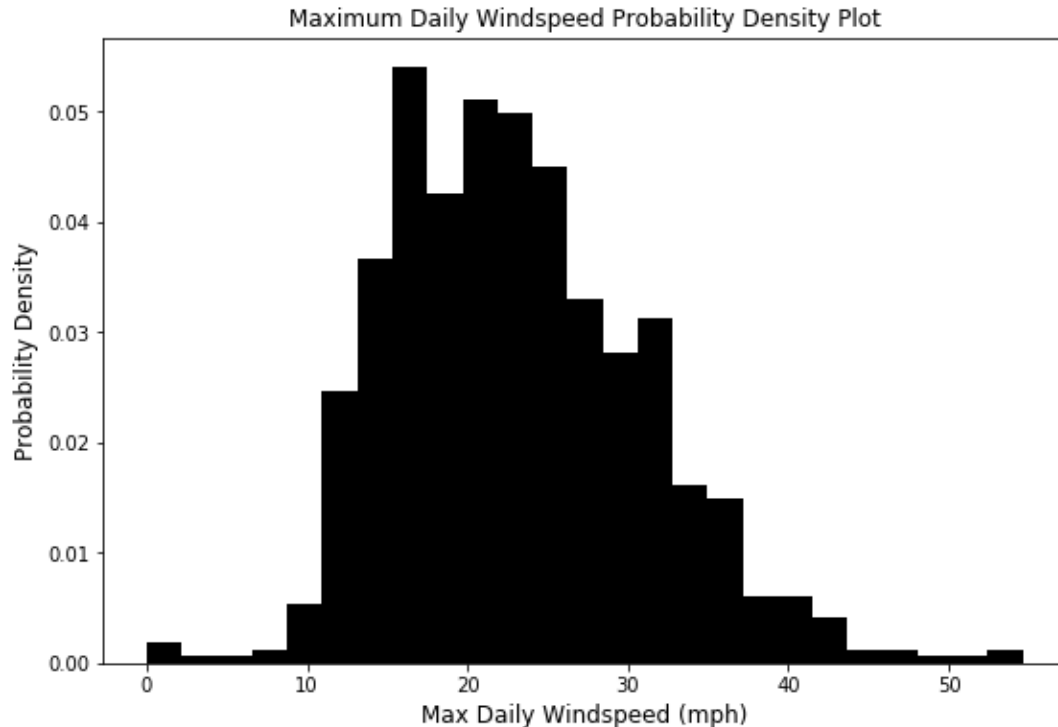
Figure 5.8. Maximum daily wind speed probability density distribution

The maximum recorded wind speed was 54.6 mph on July 15, 2019, and the distribution is a Weibull or inverse Weibull curve, although it has less uniformity than that shown in the previous Figure 5.6 due to fewer data points.

5.2.2 Daily Wind-Induced Forces and Distribution

The wind-induced forces on September 4, 2017 were the primary focus for the investigation on the impact of wind direction and speed on the anchor rods and post forces. Although the maximum wind speed on September 4 was not the greatest in the data set, an earlier data point when all of the anchor rod gauges were operational was desired. In addition, the wind speed was within the top 0.5% of the maximum recorded probable wind gusts and the top 0.00003% of probable recordings overall, so it was a good representation of high magnitude events.

Wind was also in a direction approximately perpendicular to the sign face, which theoretically induces the greatest forces on the structure. The recorded maximum daily wind speed on September 4, 2017 was 46.8 mph. Most of the strain gauges, besides 1 and 5, also experienced maximums for the month on September 4.

Before covering the strains induced by wind gusts and speed, Figure 5.9 illustrates the wind speed distribution, the wind direction distribution, and a probability density visualization to observe the most likely combinations of loading.
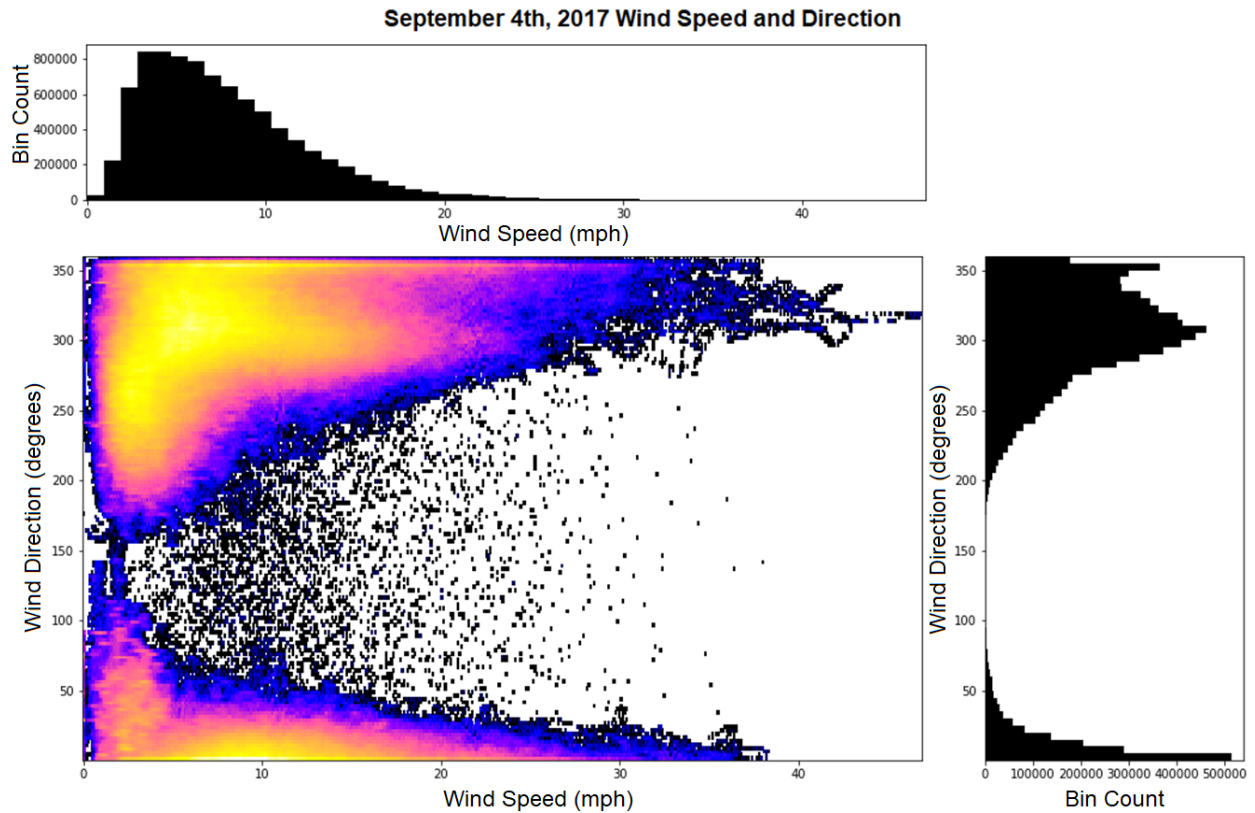
Figure 5.9. Wind characteristics for September 4, 2017

The wind speed in Figure 5.9 shows a fairly typical Weibull distribution with a peak probability in the 3.5 mph to 4 mph bin. Wind direction had peaks at 300 degrees and 0 degrees, with the maximum wind gust occurring at 320 degrees, or from a northwest wind direction. The distribution also indicates that the stress readings in approximately the 100 to 200 degree range may not represent the true behavior of the structure due to the limited number of data points.

Figure 5.10 shows the wind speed, direction, and force distribution of the gauges on September 4, 2017.

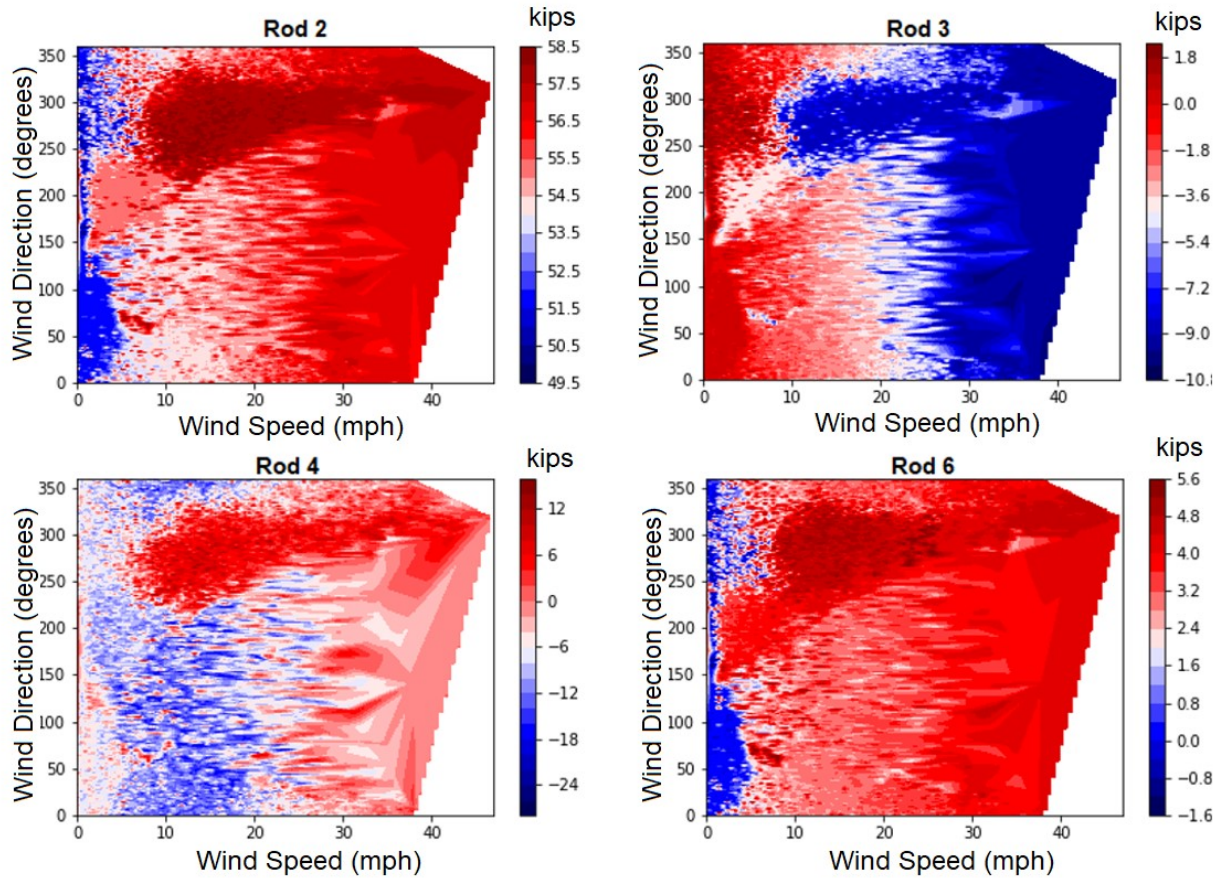**September 4th, 2017 Anchor Rod Responses to Wind Loading**

Figure 5.10. Anchor rod response to wind loading

On the four subplots in Figure 5.10, the x axis is wind speed, the y axis is wind direction, and the induced forces, in kips, are shaded corresponding to the keys to the right of each plot. Darker red colors indicate larger relative tensile forces and darker blue colors indicate larger relative compressive forces. White indicates the approximate middle of the loading values for the day. Note that the shading is determined by triangulation of the data points, so areas with decreased point density, as shown in the previous Figure 5.9, are less reliable. Additionally, it is important to consider that the recorded forces are over an entire day and include temperature changes, which increase the error in these data.

Of all the anchor rods, rod 3 was the only middle anchor rod instrumented and the rest were corner anchor rods. The sign post was instrumented before laboratory testing results indicated greater forces on middle anchor rods in square groupings, so the instrumentation was designed assuming a uniform strain distribution in the baseplate. Rod 5 is not shown on the plots because it exhibited sensitivity errors shortly after installation. The magnitudes observed in rod 4 were also deemed excessive after investigating the short-term dynamic response, and the rod likely experienced a sensitivity failure before the average daily values could detect it.

Of rods 2, 3, and 6, rod 3 experienced the greatest differential force of 12.6 kips, followed by rod 2 with 9 kips and rod 6 with a 7.2 kip difference. This distribution matches with laboratory observations of the greatest stresses occurring in the middle rods of square anchor rod patterns.

Although the maximum wind speed recording occurred at 320 degrees, there was also a large peak in the stress for lower wind speeds around 10 to 20 mph out of the west, or approximately 250 to 300 degrees. The west direction was parallel to the sign face, so there may have been a resonant vibration condition induced by southwesterly winds.

The relative response of the anchor rods is also interesting, since the middle anchor rod, 3, responded approximately inversely to wind loading compared to the corner anchor rods, which may have been due to the non-uniform baseplate stiffness. On all anchor rods, for wind velocities under 10 mph, forces tended to be inverse to that of higher wind speeds, which may be attributed to consistent forces from vehicle gusts.

Figure 5.11 is similar to Figure 5.10, but covers the strains induced in the post structure by different wind speeds and directions.

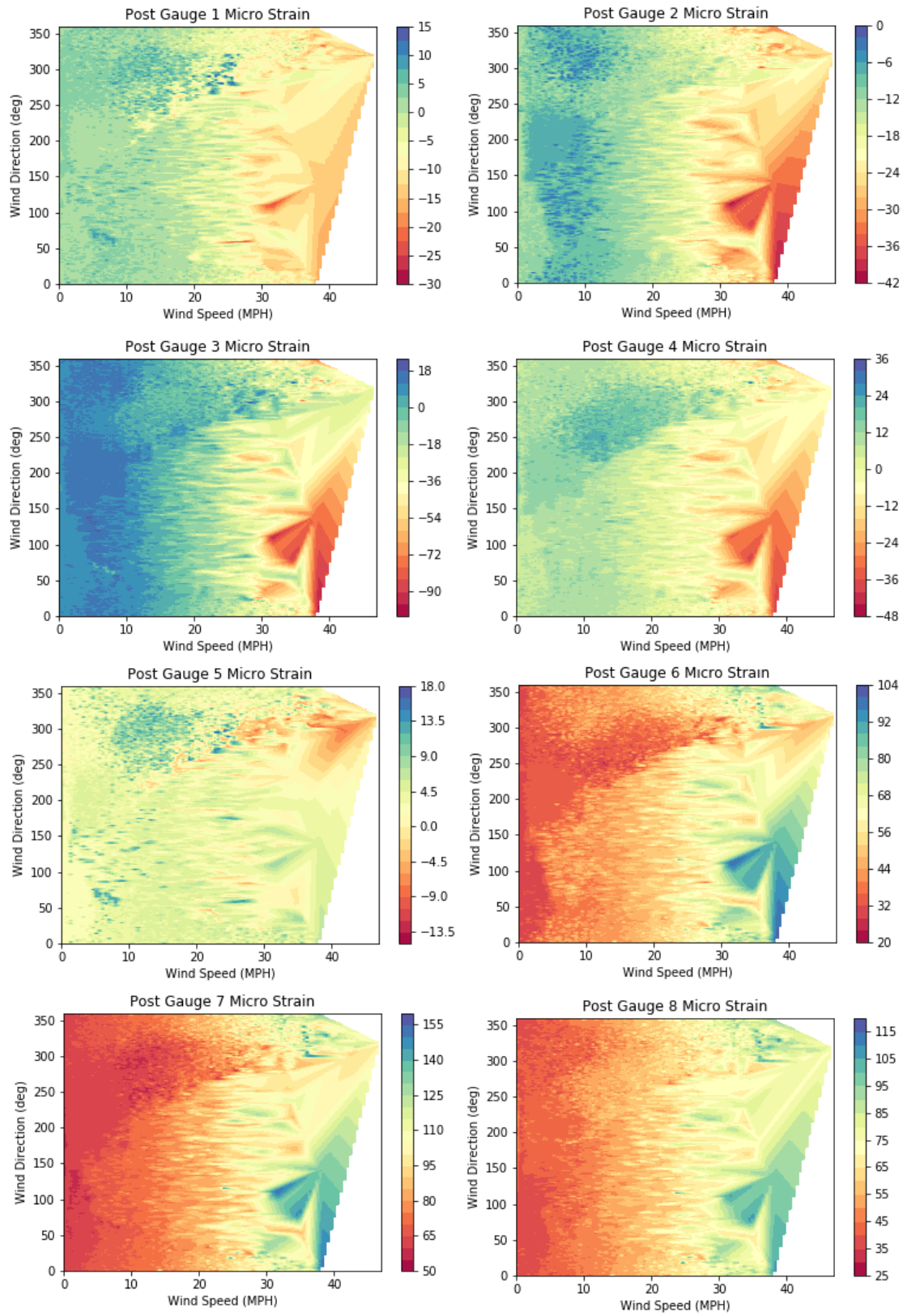# September 4th, 2017 Post Gauge Responses

Figure 5.11. Post strains induced by applied loading

In Figure 5.11, each of the opposite fixed strain gauges exhibit inverse behavior, which validates that the gauges are performing as expected. Unlike the anchor rod gauges, the post gauges do not have inverse behavior under 10 mph wind speeds. Gauges 1 and 5 experienced the lowest total strain ranges of 45 με and 32με, respectively, throughout the day, which was expected since the gauges' locations were parallel to the sign post. Gauges 3 and 7 experienced the greatest strain ranges of 108 με and 105με, respectively. These maximum field strains are less than the stresses induced in the laboratory, indicating that the laboratory testing procedure likely replicated a conservative case for anchor rod loosening.

5.2.3 Validation of Laboratory Testing and Dynamic Properties

In addition to the gross wind data for September 4, 2017, a short gust period of 250 seconds, including the maximum wind gust of 46.7 mph along with several other large wind gust events above 35 mph were investigated. The wind direction was primarily out of the northwest during the 250-second window. Figure 5.12 illustrates the wind speed over the selected timeframe for comparison to both the anchor rod and post strain gauge responses.
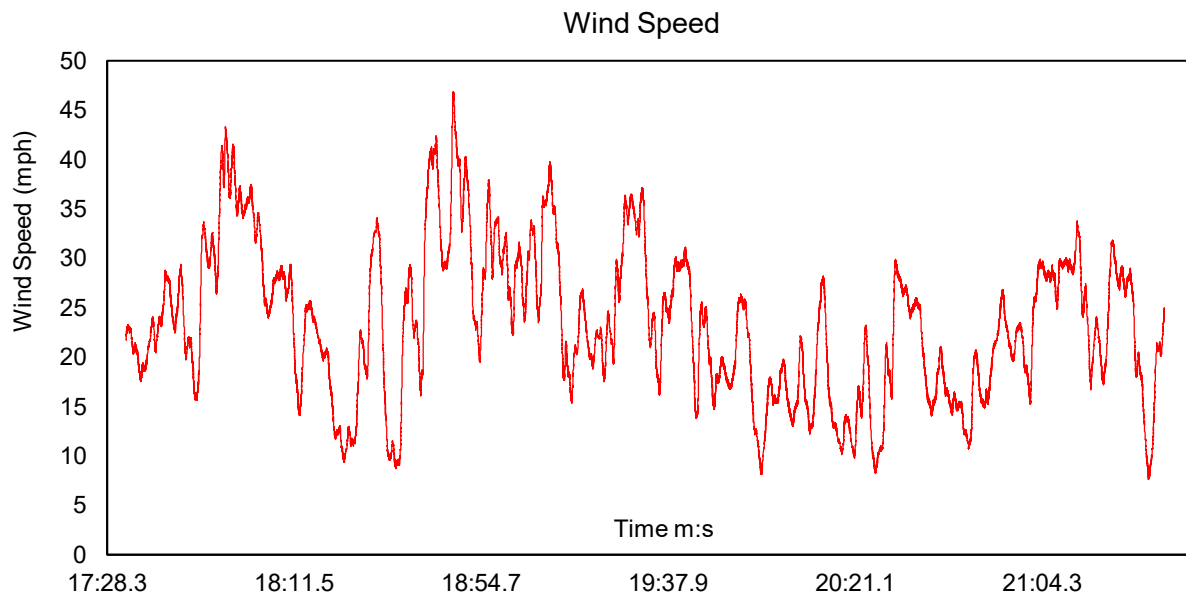

Figure 5.12. Wind loading over selected 250-second timeframe

Most of the highest peaks in the wind loading have a frequency of 1 to 5 seconds.

Figures 5.13 through 5.16 show the anchor rod responses to the selected wind loading.

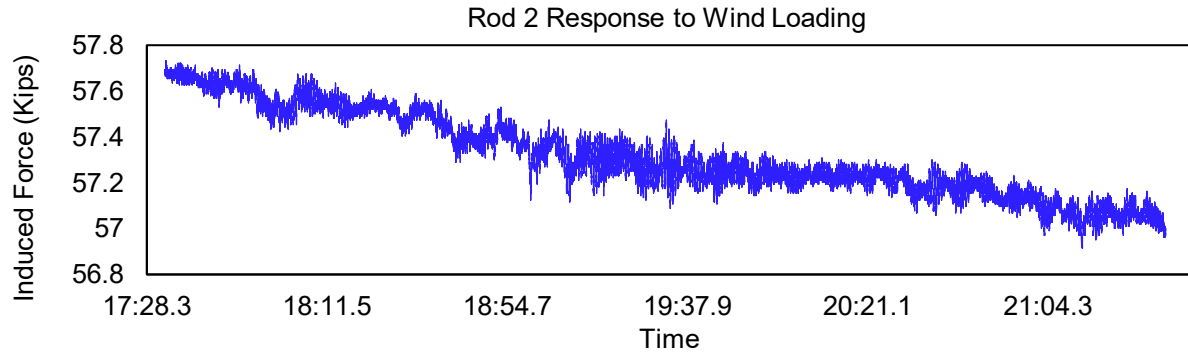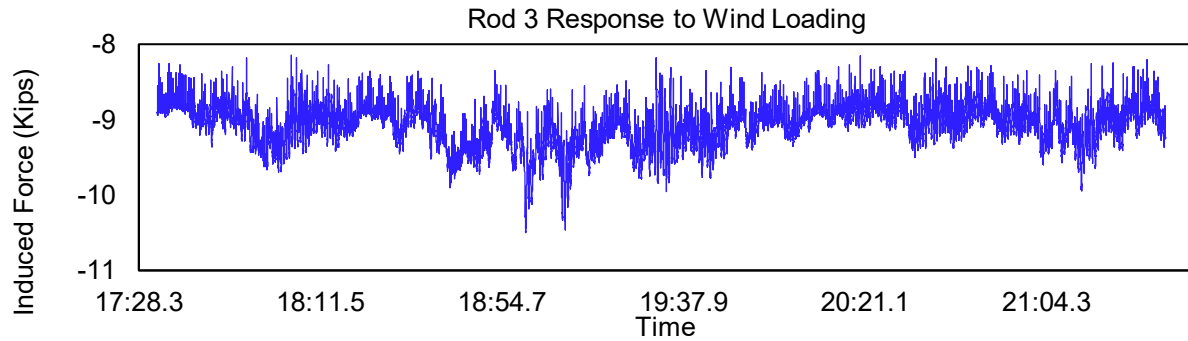**Figure 5.13. Rod 2 response to wind loading**

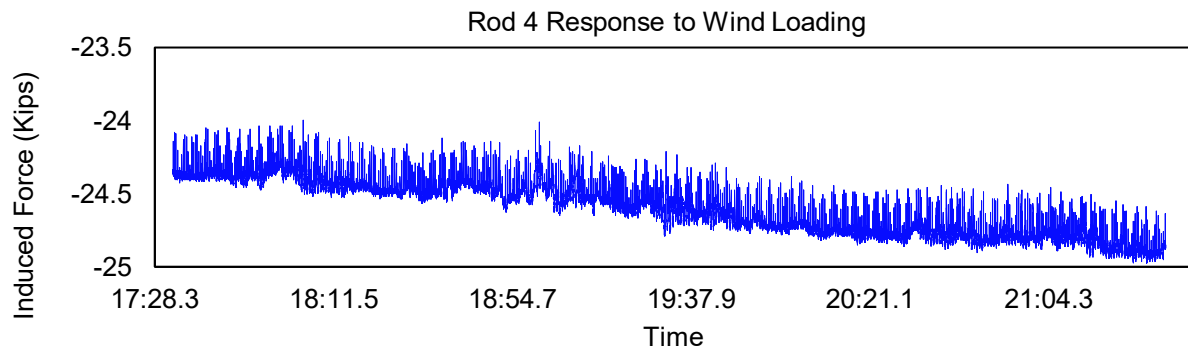**Figure 5.14. Rod 3 response to wind loading**

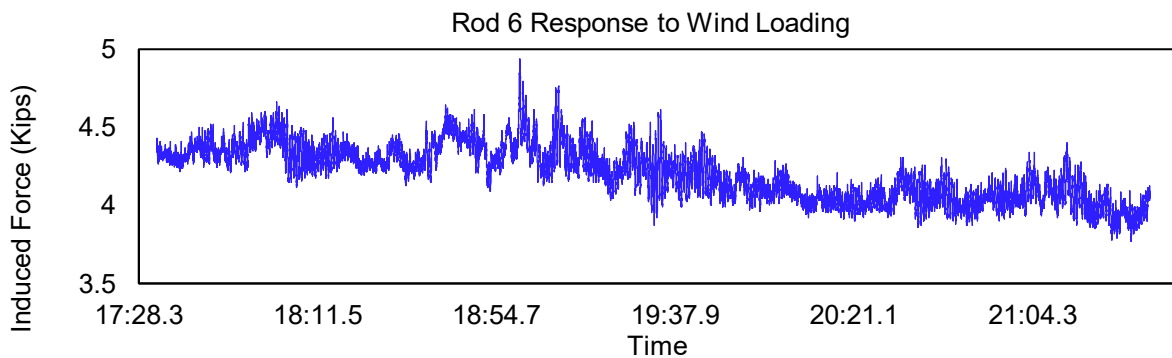**Figure 5.15. Rod 4 response to wind loading**

Figure 5.16. Rod 6 response to wind loading

Over a shorter timeframe, the stress increase on the middle anchor rod becomes more noticeable. Rods 2 and 4 show about 1 kip of drift over the measurement timeframe. Data from rod 4 also appeared to

have a stability issue and may not be completely reliable. Rod 3 experienced a 2.14 kip force range after the peak wind loading, whereas rods 2, 4, and 6 had a 0.36 kip, 0.62kip, and 0.76 kip force range, respectively.

These observations validated the overall behavior observed in the laboratory that middle anchor rods, in stiffer areas of the baseplate, will take more of the applied loading than corner anchor rods. Additionally, the design procedures recommended by AASHTO should likely not be used with square anchor rod distributions due to the non-uniform baseplate stiffness.

The maximum stress range of 0.86 ksi for anchor rod 3 validated that the fatigue procedure used during laboratory testing was likely conservative, since the test to the full fatigue life of the sign was completed at a stress range of 2.2 ksi for the anchor rod grip lengths with negligible pre-tension loss observed. Temperature may govern the recorded anchor rod forces, since, compared to the overall daily force change, anchor rods experienced much lower stress ranges under peak wind loading.

Figures 5.17 through 5.20 show the post gauge responses to the selected wind loading.
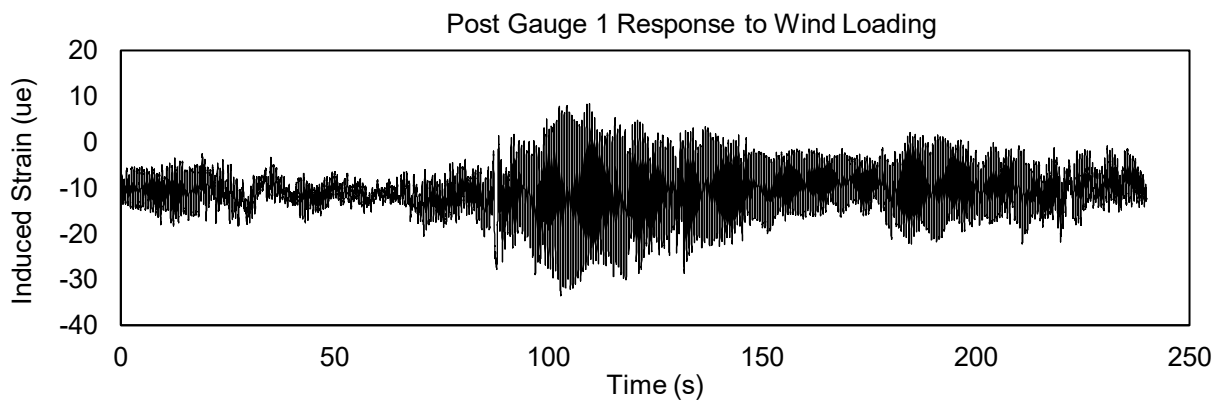

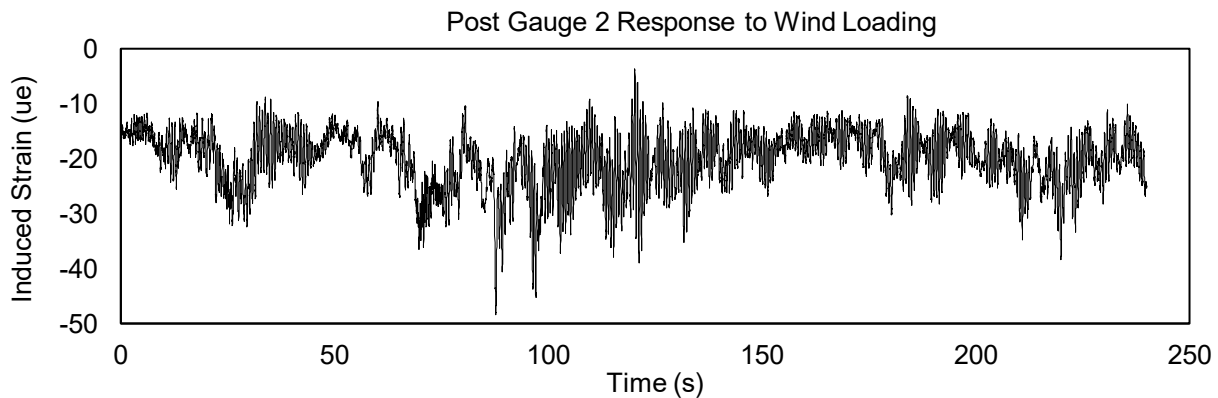**Figure 5.17. Post gauge 1 response to wind loading**

Figure 5.18. Post gauge 2 response to wind loading
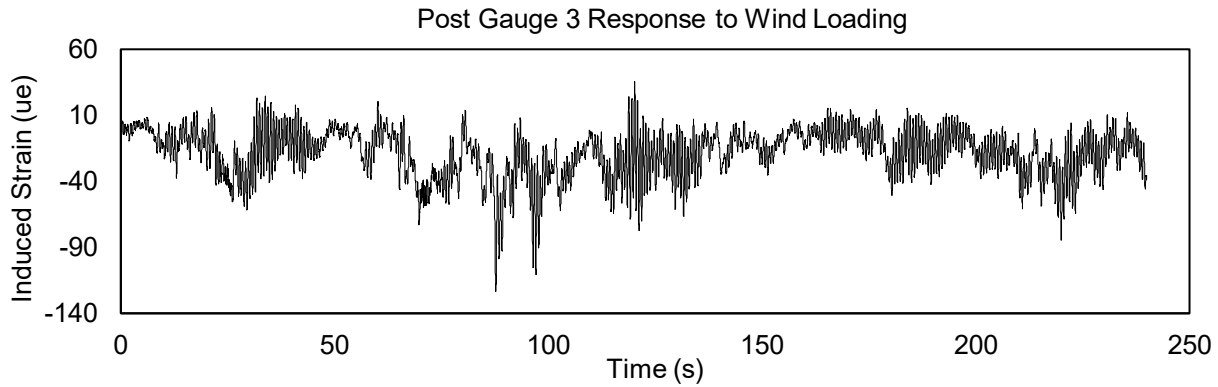
Figure 5.19. Post gauge 3 response to wind loading
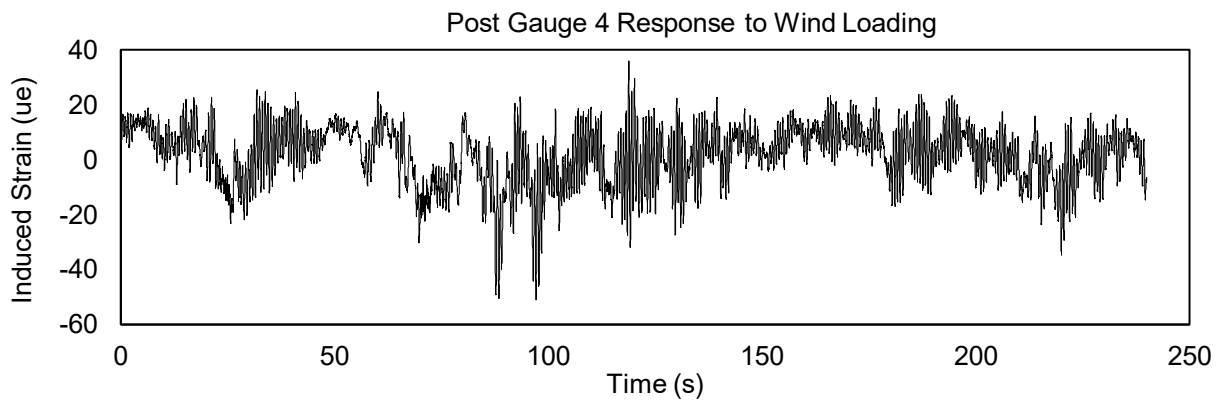
Figure 5.20. Post gauge 4 response to wind loading

Only gauges 1 through 4 are discussed given the opposite matching gauges consistently exhibited the same behavior with mirrored tension and compression forces. Much like the total daily data, post gauges 1 and 5 had the lowest strain range, while gauges 3 and 7 had the greatest strain range. As with the anchor rods, the greatest strain range of 154 με was lower than that used in laboratory testing for the AASHTO limit of the post structure.

Finally, all of the gauges exhibited approximately the same dynamic response to wind loading other than the outer gauges 1 and 5. Given these gauges were parallel to the overhead sign, the responses appear to have a higher frequency and lower amplitude than the other post gauges.

After observing the time domain of the strain responses of the sign post, the data were changed into the frequency domain and visualized with a power spectral density plot to better understand the natural frequencies and vibrational modes of the overhead sign structure. Python code developed from Welch's average periodogram method (Bendat and Piersol 2010) was utilized for the plotting and an estimation of the spectral density plot.

The wind speed power spectral density plot shown in Figure 5.21 is governed by excitation frequencies under 1 Hz.
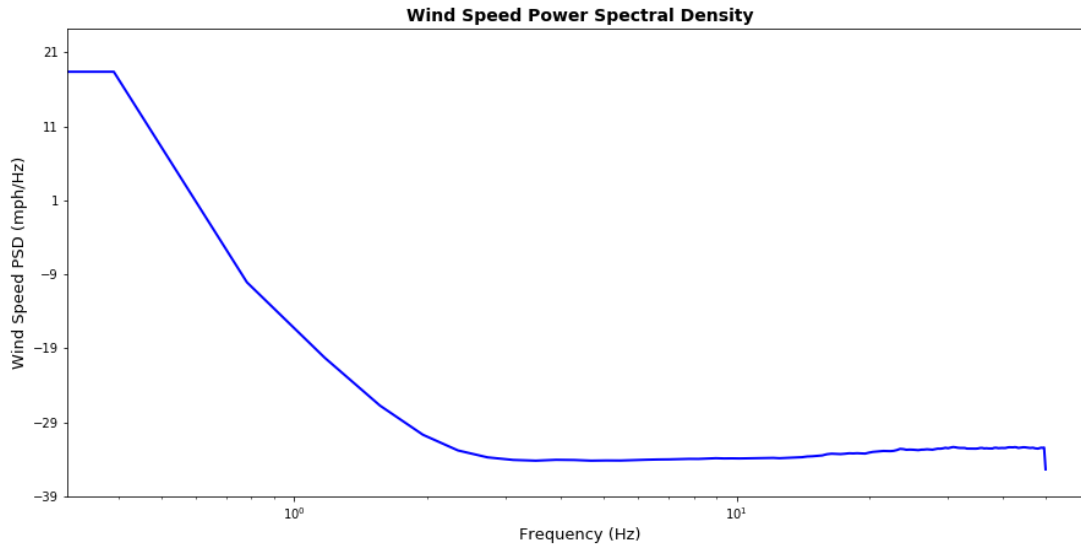
Figure 5.21. Wind speed power spectral density

Considering the gusts observed in time domain plots and literature, this behavior matches expectations given that most of the higher speed wind gusts will be a lower frequency (Harris 1996, AASHTO 2015, Hosch 2015).

Figure 5.22 shows the power spectral density (PSD) of the post gauges, which has the same broad banded peak under 1 Hz as the wind PSD plot indicates, but with additional peaks indicating different vibrational modes of the structure.
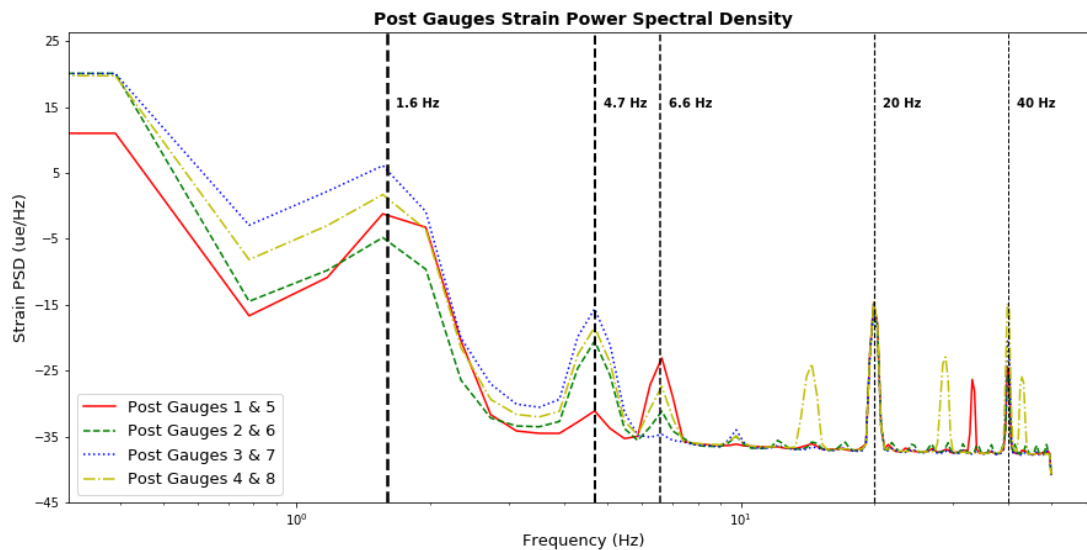
Figure 5.22. Post gauge power spectral density

The large peak under 1 Hz is likely due to wind turbulence impacts as noted in NCHRP Report 469 (Dexter and Ricker 2002). The first three vibrational modes of the structure are likely 1.6 Hz, 4.7 Hz, and 6.6 Hz. Although there are also peaks at 20 Hz and 40 Hz, these peaks have some uncertainty since data were collected at 100 Hz (so the resolution was limited on higher frequency peaks).

The first mode of 1.6 Hz matches Hosch's (2015) observations on a similar structure. Peaks in the previous Figure 5.21 also match the time domain graphs. Considering the second and third modes, gauges 1 and 5 are governed by their third, higher frequency mode, while all the other gauges experience higher responses in their second mode. Finally, the field-observed vibrational modes match the excitation frequencies used during the laboratory testing between 1 Hz and 5 Hz, so the anchor rods were effectively tested at the frequencies that likely would take place in the field.

Figure 5.23 shows the PSD developed for the anchor grip lengths.
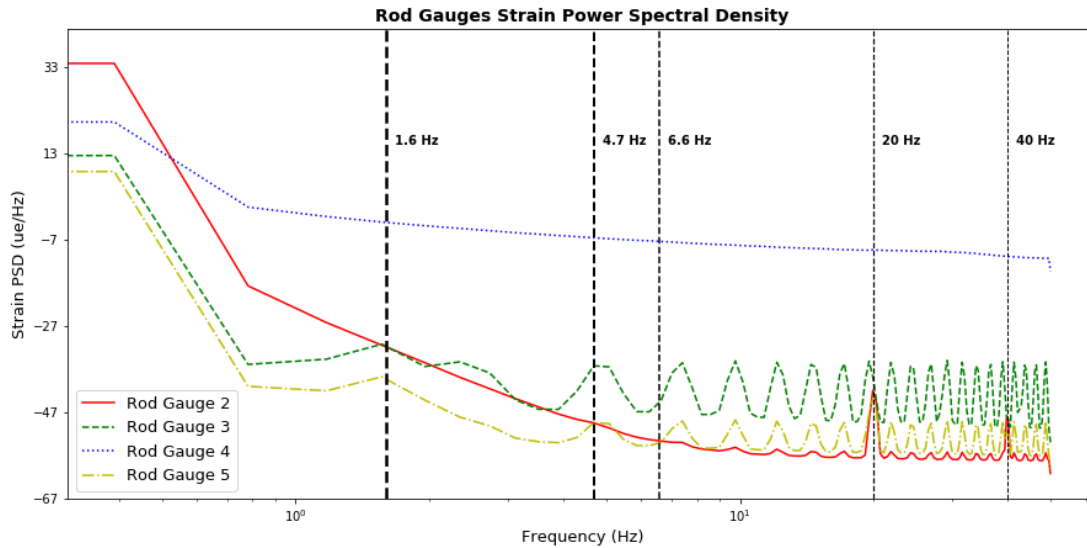
Figure 5.23. Anchor rod power spectral densities

All strain gauges in the anchor rods showed approximately the same overall behavior as the wind loading PSD. Unlike the post gauges, the vibrational modes of the structure are not observable in the anchor rods, which could be due to the sensitivity of the anchor rod gauges. It is also possible that the pre-tension in the double nut connection somewhat decreases the forces in the anchor rod grip lengths, which was also observed with calculations and during the laboratory testing.

5.3 CONCLUDING POINTS

- The middle anchor rod of the monitoring sign-post structure experienced greater forces than the corner anchor rods, which matched laboratory test results.
- Both the loading frequencies and amplitudes used during laboratory testing match observations in the field-monitored post.
- Loading amplitudes used in the laboratory present a conservative condition for forces applied to the anchor rods as observed in the field, likely validating the conclusions made in the laboratory testing results.

CHAPTER 6: **CONCLUSIONS AND RECOMMENDED CHANGES TO PROCEDURES**

6.1 CONCLUSIONS

After reviewing the literature, previous laboratory testing, results from implementation, and the field sign-post monitoring data, it is likely that the majority of issues with anchor rod pre-tension loss is related to installation procedures. For connections to retain pre-tension, tensioning procedures need to be effective, constructible, and verifiable.

6.2 RECOMMEND CHANGES TO MNDOT TIGHTENING PROCEDURES

6.2.1 Specification Clarity

6.2.1.1 Separation of Overhead Sign and Lighting/Traffic Signal Specifications

Because of the inherent differences in bases of overhead signs and traffic signal/lighting structures, it would likely be beneficial to separate the specifications for these two classes of structures. Separation of the specifications would increase the clarity of each and allow contractors to focus on some of the more specific aspects of each structure type.

For overhead signs, turn-of-nut specifications and torque could be used as a double verification as intended by the first phase recommended procedures. In the pre-tensioning steps for lighting and traffic signal structures, the specifications could focus on clearance issues and the quality of torque control. In addition, the contractors for each type of structure vary, and many lighting structures may be installed by an electrical contractor that may not have the same structural experience as an overhead sign contractor.

6.2.1.2 Create Maintenance Procedures

In addition to separating the specifications, it would likely be beneficial to create maintenance procedures for both overhead signs and traffic signal/lighting structures. Since maintenance procedures differ greatly from installation, it would likely benefit MnDOT maintenance personnel to have a set of procedures to which they could refer. Special care must also be taken during maintenance to ensure that the structure remains stable while anchor rods are serviced.

6.2.1.3 Verify Lubrication Areas

With both overhead sign and light pole installations, contractors expressed uncertainty concerning the exact areas to lubricate besides the anchor rods. Contractors often needed specific instructions on what areas needed to be lubricated on the nuts and washers. The current language in the installation record form does not clearly state the surfaces needing lubrication. In addition, a graphic should be created to illustrate proper lubrication areas.

6.2.1.4 Specify Steps in Logical Manner

Each required step should likely be laid out as an individual torque, so steps can be logically followed one at a time without having to go back and forth with half torques. It also may be beneficial to add some descriptions to the steps to explain why they are important for contractors to follow.

6.2.2 Error Minimization/Control

6.2.2.1 48-Hour Re-Tightening Torque

Currently, one of the AASHTO-recommended procedures is to retighten connections after 48 hours to 110% of verification torque. This retightening is supposed to account for creep in the galvanizing and minimize initial relaxation losses. The 48-hour retightening was first proposed in *NCHRP Report 469* (Dexter and Ricker 2002) without noted references or reasoning for the specified timeframe.

It is suspected that the current specification arose from Fisher's and Struik's 1974 text (second edition from Kulak et al. 2001) that states "90% of [the] loss occurs during the first day," and "the relaxation characteristics of assemblies of galvanized plates," and "bolts were found to be twice as great as plain… materials" (Kulak et al. 2001). The specification also may have been influenced by Yang's 1999 research in galvanized structural bolting relaxation but is not noted in the references for *NCHRP Report 469* (Dexter and Ricker 2002).

In practice, the 48-hour retightening torque is likely seldomly followed, was not recorded on any of the installation structures, and not used during maintenance due to the resources required. Although the 48-hour retightening is difficult to perform, the concerns about losses are still valid (Bickford 1995, Fisher and Struik 1974, Yang and Dewolf 1999, Nijgh 2016). Laboratory testing and literature indicated that the retightening torque could likely be applied approximately 10 minutes after the initial tightening with the same relaxation performance improvement.

It is recommended that another pass of the final 100% torque is performed at least 10 minutes after the initial pre-tensioning. This process should both ensure that the retightening torque is performed and limit the lifespan relaxation losses to approximately 25% to 10% of the applied pre-tension.

6.2.2.2 Lubrication

Throughout implementation, the specified MnDOT bridge grease was generally not used on installations. The majority of lubricants were a sort of anti-seize compound though. Review of various literature suggests that the nut factors of many of the used greases are comparable to the specified grease, but verification for specific cases was required. In addition, the AASHTO-derived nut factor was found using stick wax by Till and Lefke (1994), which was compared.

In laboratory testing, it was found that most anti-seize lubricants have a nut factor of approximately 0.11, which is 8% lower than that specified by AASHTO. This is likely because the nut factor derived in AASHTO was manually read off a gauge and would include the 5% to 10% immediate losses, whereas the laboratory-tested nut factors were read directly from the instruments by a data collection system. It is

recommended that the AASHTO 0.12 nut factor is used, though, so immediate relaxation can be automatically accounted.

6.2.2.3 Specification Simplification

Fewer steps could likely be used than currently specified. In all of the maintenance and most of the installations, steps were skipped when bringing nuts to snug-tight and with the verification torque. The reasoning for the steps is to prevent differential stresses in the rods; however, doing two steps at snug and two steps at verification may not be proportional enough to cause major differentials in rod stresses compared to taking rods from snug to fully tightened. Contractors and maintenance workers also expressed that there could be confusion over the snug-tight term, as many field personnel connotated it to be hand-tight, or an approximation.

Changing the specification to four torque steps of: 20%, 60%, 100%, and 100% (repeated) of the required tightening torque is recommended. A minimum 10-minute relaxation period between the repeated 100% torques would be ideal, although the precise timing could be researched in more depth to determine a more accurate retightening timeframe.

Required torque can be calculated with the current equation in AASHTO (2015), shown below, where T is the required torque, F is the desired pre-tension force, and D is the anchor rod diameter.

$$T = 0.12FD$$

All applications of pre-tensioning should be applied in a star pattern/sequence.

Turn-based pre-tensioning is not recommended due to the high sensitivity of elastic displacement-controlled pre-tensioning with small grip lengths, accuracy challenges from a constructibility standpoint, and variability of base designs. If AASHTO desires to specify a turn specification and keep connections in the elastic region, accurate snug-tight values must be defined given they are the basis for displacement-controlled pre-tensioning. In addition, grip length and connection stiffness must be taken into account.

For some conditions, particularly in maintenance, a turn specification may be the only option. In this case, it is recommended that snug-tight be specified as 0.1 Fy, as recommended from the previous study (Chen et al. 2018), and that requires a calibrated torque wrench to be used to achieve the specification. The nut factor must be adjusted accordingly from the literature for structures installed or maintained without lubricant or an anti-seize type of grease.

6.2.2.4 Existing HMLT Installation and Maintenance

With the revised design clearances, the HYTORC low profile Stealth series hydraulic torque wrench, or similar wrenches, should work on new HMLT installations. The wrench was very close to fitting on the newer base design at the Maple Grove, Minnesota, site (A14E 4). With the stack socket attachment, the wrench nearly worked on the older base design and was far easier to place. Contractors may want to consider using the stack socket attachment during installations for easier placement and removal of the hydraulic torque wrench.

On in-place HMLT structures, though, the only feasible retightening option is likely a slugging-type wrench given significant difficulties were encountered with both hydraulic wrench options. For in-place retightening procedures on MnDOT HMLT structures, an approximate turn procedure will need to be used.

From the results, 1/12 of a turn or refusal from a slugging wrench, whichever comes first, is recommended for legacy design structures. The required snug-tight force is 26.25 kips, which corresponds to a snugging torque of 1,100 ft-lbs if the anchor rods are unlubricated, using an approximate nut factor of 0.25. This may be able to be achieved with a 10-ft cheater bar attachment to an open-ended wrench, since the average person can apply 100 lbs of force without slipping in the field. There will naturally be a high degree of error with this method, but for maintenance of these particular existing structures, it is likely the most feasible option. The required force to rupture the anchor rods is not achievable manually, so the anchor rods will not be in danger of failing with this method.

6.2.2.5 Pre-Tensioning with Direct Tension Indicators

If a calibrated wrench is not used for pre-tensioning, DTIs are recommended for installation. DTIs will also likely result in greater pre-tension accuracy than torque-controlled pre-tensioning given they directly measure the clamping force in a connection. DTIs also enable inspection after installation since the DTI gap can be measured with a feeler gauge. However, DTIs may require more skill during installation to correctly check if the gap is adequate and may be difficult to observe in enclosed bases.

The relaxation of connections with DTIs has been researched on structural bolts with inconclusive results (Reuther et al. 2014). These findings may not extrapolate well to anchor rods with galvanized DTIs, and additional research needs to be pursued on the subject. Moreover, since the DTIs are plastically deformed, they cannot indicate pre-tension loss or relaxation.

Any installations using DTIs should adhere to ASTM F2437, Style 2, and either grade 55 or 105. For this specification, the DTIs are calibrated to 60% of the rod yield strength. It is also permitted to pre-tension to a different force, if desired, but the DTI gap must be calibrated with a bolt tension calibrator (ASTM 2017). AASHTO and manufacturers recommend that DTI washers be used on the top of the leveling nuts so that the complete clamping force in the connection can be measured and to further prevent the nut from turning on the DTI. If the structure was being pre-tensioned from the leveling nuts, the opposite would be true, and the DTI would be placed under the top nut.

6.2.3 Quantifiable Verification

In interviews and during site inspections, MnDOT inspectors noted it would be helpful to have an inspection method after installation since observing every structure installation is burdensome on resources.

If DTIs are not used for installation, torque, supplemented with a check for lubricant type, could be substituted to approximate a minimum pre-tension in the anchor rods. While this is an approximation, it could ensure that the connections are pre-tensionied to approximately the correct value. A negative, or

loosening, nut factor of 0.7 is recommended for an inspection reverse torque as determined using the following equation.

$$T_{insp} = 0.5T$$

The 0.7 nut factor was simplified to half of the installation torque to account for relaxation and error, so it is outside the 95% confidence interval for all loosening torques.

For the inspection torque to be valid, the lubrication type also must be verified during the inspection, so the nut factor is consistent. If the nut on a pre-tensioned connection turns off with the prescribed inspection torque, it is highly probable that the connection was under pre-tensioned during installation.

Naturally, one of the downsides to inspecting connections after installation is that exact following of the procedure cannot be checked, such as tightening in a star pattern, thorough lubrication, tightening the leveling nuts, and use of the proper number of steps. This may result in greater error in the final pre-tensions; however, the savings in inspection after installation may justify the limitations.

6.2.4 Final Recommended Installation Steps

After Phase II, it was found that the anchor rod pre-tensioning procedures could be simplified down to a 7-step process for all structures. The 7 steps are as follows:

1. Verify the installation
2. Level leveling nuts and place post
3. Lubrication
4. Bring top nuts to hand tight and tighten the leveling nuts with an open-ended wrench in a cross-tightening pattern
5. Torque top nuts in steps of 20%, 60%, and 100%, each individually in a cross-tightening pattern
6. Allow rods to relax for 10 minutes
7. Re-tighten to 100% torque

Results from Phase II suggests that, though fewer steps are used than in the current AASHTO LRFD – SLTS procedures, these procedures will likely result in greater accuracy for final connection pre-tension across a wide spectrum of SLTS structures, increase efficiency in the field, and communicate better with filed workers.

6.3 FURTHER TESTING RECOMMENDATIONS

As with many testing regimens, many questions were raised throughout the testing and data processing. Recommended areas for further investigation that could be pursued to improve the performance of double nut connections on SLTS structures follow.

- **Relaxation Loss of Connections**
  This study could compare the relaxation of different sized connections with retightening torques applied at different time periods after tightening. In addition, the impact of DTI washers and surface

coating could be investigated to better quantify the time for the retightening torque. The statistics of the relaxations could also be used to better estimate final pre-tension values.

- **Force Distribution of Square Anchor Rod Groups with More than Four Rods**
  Laboratory testing indicated that the linear strain distribution used to estimate design forces significantly underestimates forces in center anchor rods for square anchor rod groups. Because this effect is affected by the stiffness of the baseplate, MnDOT may want to reevaluate its design procedures, lengthen the corner pole to baseplate stiffeners, or change to a circular anchor rod group to better ensure a uniform baseplate stiffness.

- **Further Field Implementation**
  While the revised procedures are backed up by laboratory studies, there still may be areas to improve in the field or possible unforeseen installation difficulties, so the procedures may benefit from another implementation investigation. In addition, in-field DTI procedures were not attempted in this study and may present difficulties considering the variety of SLTS structure bases and required operator training.

REFERENCES

AASHTO. 2015. *LRFD Specifications for Structural Supports for Highway Signs, Luminaires, and Traffic Signals* (First edition). American Association of State Highway and Transportation Officials, Washington, DC.

ASME. 2005. *Unified Inch Screw Threads: UN and UNR Thread Form*. American Society of Mechanical Engineers, New York, NY.

ASME. 2010. *Nuts for General Applications: Machine Screw Nuts, Hex, Square, Hex Flange, and Coupling Nuts* (Inch series). American Society of Mechanical Engineers, New York, NY.

ASTM. 2020. *ASTM A194/A194M-20: Standard Specification for Carbon and Alloy Steel Nuts for Bolts for High Pressure or High Temperature Service, or Both*. ASTM International, West Conshohocken, PA.

ASTM. 2020. *ASTM F1554-14: Standard Specification for Anchor Bolts , Steel , 36 , 55 , and 105-Ksi Yield Strength, 1–10*. ASTM International, West Conshohocken, PA.

ASTM. 2015. *ASTM A563-15: Standard Specification for Carbon and Alloy Steel Nuts*. ASTM International, West Conshohocken, PA.

ASTM. 2017. *ASTM F2437/2437M: Standard Specification for Carbon and Alloy Steel Compressible-Washer-Type Direct Tension Indicators for Use with Cap Screws, Bolts, Anchors, and Studs*. ASTM International, West Conshohocken, PA.

Bendat, J. S., and Piersol, A. G. 2010. *Random Data: Analysis and Measurement Procedures* (Fourth edition). Wiley, Hoboken, NJ.

Bickford, J. 1995. *An Introduction to the Design and Behavior of Bolted Joints* (Third edition). Marcel Dekker, New York, NY.

CEN. 2018. *EN 1090-2: Technical Requirements for the Execution of Steel Structures*. European Committee for Standardization, Brussels, Belgium.

Chen, A., Schaeffer, C., Zhang, Y., Phares, B., Shafi, B., Yang, M., Lin, Z., and Paudel, S. 2018. *Re-Tightening the Large Anchor Bolts of Support Structures for Signs and Luminaires.* Minnesota Department of Transportation, St. Paul, MN.

Christopher, R. J., and Fisher, J. W. 1964. *Calibration of Alloy Steel Bolts*. Fritz Engineering Laboratory, Lehigh University, Bethlehem, PA.

Dally, J. W., and Riley, W. F. 2005. *Experimental Stress Analysis* (Fourth edition). College House Enterprises, Knoxville, TN.

Dexter, R. J., and Ricker, M. J. 2002. *NCHRP Report 469: Fatigue-Resistant Design of Cantilevered Signal, Sign, and Light Supports*. National Cooperative Highway Research Program, Washington, DC.

Fisher, J. M., and Kloiber, L. A. 2006. *Design Guide 1: Base Plate and Anchor Rod Design* (Second edition). American Institute for Steel Construction, Chicago, IL.

Fisher, J. W., and Struik, J. H. A. 1974. *Guide to Design Criteria for Bolted and Riveted Joints*. John Wiley and Sons, New York, NY.

Fukuoka, T., and Takaki, T. 2003. Elastic Plastic Finite Element Analysis of Bolted Joint during Tightening Process. *Journal of Mechanical Design*, *125*(4), 823–830.

Harris, C. M. 1996. *Shock and Vibration Handbook* (Fourth edition). McGraw-Hill, New York, NY.

Hoisington, D., and Hamel, S. 2014. I*nvestigation of Anchor Nut Loosening in High-Mast Light Poles Using Field Monitoring and Finite Element Analysis*. Pacific Northwest Transportation Consortium, University of Washington, Seattle, WA.

Hosch, I. E. 2015. Experimental Validation of the AASHTO Natural Wind Fatigue Design Specifications for Cantilevered Sign Support Structure Anchor Bolts. *Practice Periodical on Structural Design and Construction*, *20*(1), 1–8.

James, R. W., Keating, P. B., Bolton, R. W., Benson, F. C., Bray, D. E., Abraham, R. C., and Hodge, J. B. 1997. *Tightening Procedures for Large-Diameter Anchor Bolts*. Texas Transportation Institute, Texas A&M University System, College Station, TX.

Jiang, Y., Zhang, M., and Lee, C.-H. 2003. A Study of Early Stage Self-Loosening of Bolted Joints. *Journal of Mechanical Design, 125*(3), 518–526.

Kulak, G. 2002. *Steel Design Guide 17: High Strength Bolts – A Primer for Structural Engineers*. American Institute for Steel Construction, Chicago, IL.

Kulak, G. L., Fisher, J. W., and Struik, J. H. A. 2001. *Guide to Design Criteria for Bolted and Riveted Joints*. Second edition. American Institute for Steel Construction, Chicago, IL.

Lassen, T., and Recho, N. 2006. *Fatigue Life Analyses of Welded Structures* (Second edition). ISTE USA, Newport Beach, CA.

Miner, M. A. 1945. Cumulative Damage in Fatigue. *Journal of Applied Mechanics, 12*(3), A159–A164.

MnDOT. 2015. *Standard Overhead Sign Supports Interim Design B* (Design drawing). Minnesota Department of Transportation, St. Paul, MN.

MnDOT. 2018. *Standard Specifications for Construction*. 2018 edition. Minnesota Department of Transportation, St. Paul, MN.

MnDOT. 2019. *MnDOT Standard Plan Transmittal No. 19-01* (Design drawing). Minnesota Department of Transportation, Minneapolis, MN.

Nijgh, M. P. 2016. Loss of Preload in Pre-tensioned Bolts (Minor thesis). Delft University of Technology, Delft, Netherlands.

Phares, B., Dietrich, Z., Chen, A., Zhang, H., and Miller, E. 2020. *Implementation of New Guidelines for Tightening Large Anchor Rods of Support Structures for Signs and Luminaires.* Minnesota Department of Transportation, St. Paul, MN.

RCSC. 2015. *Specification for Structural Joints Using High-Strength Bolts*. Research Council on Structural Connections, Chicago, IL.

Reuther, D., Baker, I., Yetka, A., Cleary, D. B., and Riddell, W. 2014. Relaxation of ASTM A325 Bolted Assemblies. *Journal of Structural Engineering*, *140*(9), 1–7

Schaeffer, C. 2018. *Tightening the Large Diameter Anchor Bolts of Sign, Signal, and Luminaire Structures*. MS thesis. Civil Engineering, Iowa State University, Ames, IA.

Till, R. D., and Lefke, N. A. 1994. *The Relationship between Torque, Tension, and Nut Rotation of Large Diameter Anchor Bolts*. Michigan Department of Transportation, Materials and Technology Division, Research and Technology Section, Lansing, MI.

Tokyo Measuring Instruments Laboratory Co., Ltd. 2020. *Precise and Flexible Strain Gauges*. Tokyo Measuring Instruments Laboratory Co., Ltd., Tokyo, Japan.

Yang, J. and Dewolf, J. T. 1999. Mathematical Model for Relaxation in High-Strength Bolted Connections. *Journal of Structural Engineering*, *125*(8), 803–809.

Yokoyama, T., Olsson, M., Izumi, S., and Sakai, S. 2012. Investigation into the Self-Loosening Behavior of Bolted Joint Subjected to Rotational Loading. *Engineering Failure Analysis*, *23*, 35–43.

Zhang, M., Jiang, Y., and Lee, C.-H. 2007. Finite Element Modeling of Self-Loosening of Bolted Joints. *Journal of Mechanical Design*, *129*(2), 218–226.